EVALUATION OF SUSPENDED SEDIMENT TRANSPORT IN THE RIVER MALEWA BASIN USING THE SWAT MODEL AND FIELD DIGITAL TURBIDITY SENSOR DATA

WILLIAM MAKAU
March 2018

SUPERVISORS:
Dr.ir. C.M.M. Mannaerts
Dr.ir. S. Salama (Suhyb)
ADVISOR
Yasser Abbasi-Ph.D. Candidate

EVALUATION OF SUSPENDED SEDIMENT TRANSPORT IN THE RIVER MALEWA BASIN USING THE SWAT MODEL AND FIELD DIGITAL TURBIDITY SENSOR DATA

WILLIAM MAKAU
Enschede, The Netherlands, March, 2018

Thesis submitted to the Faculty of Geo-Information Science and Earth Observation of the University of Twente in partial fulfillment of the requirements for the degree of Master of Science in Geo-Information Science and Earth Observation.
Specialization: Water Resources and Environmental Management

SUPERVISORS:
dr.ir. C.M.M. Mannaerts
dr.ir. S. Salama (Suhyb)

ADVISOR
Yasser Abbasi-Ph.D Candidate

THESIS ASSESSMENT BOARD:
Dr. M.W. Lubczynski (Maciek) - Chair
Dr. Hamideh Nouri (University of Twente - ET-WEMWM)

DISCLAIMER

This document describes work undertaken as part of a programme of study at the Faculty of Geo-Information Science and Earth Observation of the University of Twente. All views and opinions expressed therein remain the sole responsibility of the author and do not necessarily represent those of the Faculty.

ABSTRACT

The problem of sedimentation and nutrient enrichment in the L.Naivasha has been an issue of environmental concern in the last decade. The loss of aquatic life and the decreasing lake depths have led to a lot of environmental entities raising the red flag. This has led to several studies being done to quantify and qualify the inflows into the lake in terms of sediments and nutrients. In this study, the employment of the SWAT model in the quantification of the sediment fluxes in the River Malewa (The main river into L. Naivasha) Basin gave the estimates of the sediments that flow into the Lake from the Basin into the Lake. The objective was to evaluate the transport of suspended sediment transport in the River Malewa basin and its calibration using observation data from a digital turbidity sensor installed at the 2GB04 Gauging station. The SWAT model is an appropriate tool to model these scenarios. It was built using input files (LULC, Soils, Precipitation and DEM) for the Naivasha area.

The runoff measurements from the Gauging stations 2GB05 were used for hydrological calibration and validation since runoff is the vehicle to sediment transport. The Calibration period was from 2004-2010 with a 3yr warm-up period while the Validation was from 2010-2013. The hydrological calibration was done monthly. The most sensitive parameters (CN2, GWQMN, GW_REVAP, REVAPMN, SOL_AWC, ALPHA_BF) were identified and adjusted until the simulated results match the observed values. The calibration of the sediment was done for the period April-Sep 2017 using the turbidity sensor data from The DTS installed at the 2GB04 Gauging station. The sensitive parameters in sediment calibration were SPCON, CH_COV, CH_EROD, and USLE_P. The production and distribution of the sediment per sub-basin were simulated using the sediment calibrated model to ascertain the areas with maximum production rates and their respective amounts.

The results of the model simulations were evaluated for performance using the various statistical measures (R^2, PBIAS, NSE, and RSR). The hydrological calibration was evaluated and found to be good with NSE=0.625, PBIAS=0.216 and R^2=0.75 The hydrological validation of the results was also evaluated and proved to be good also with NSE=0.40, PBIAS=-0.39, RSR= 1.19 and R^2=0.67. The sediment calibration was performed and the results evaluated using the same statistical measures as the hydrological results. The results were: PBIAS=0.2705, NSE=0.651 and R^2=0.786.

Using the calibrated model, a simulation was done for sediment production expected in the catchment. It was deduced that Sub basins 13, 14 and 22 produced the most sediments (8115.4, 11779.2, 13953.9 tones) respectively while Sub basins 14,15, 18 and 20 had the highest sediment production rates (0.165, 0.158, 0.165 and 0.0.152tones/ha) respectively. Factors that led to the different production amounts and rates were found to be Precipitation amounts, slope, soil type and soil Land use/land cover. These factors could be addressed in efforts to conserve the L.Naivasha basin and therefore curb the sedimentation menace in the Lake as earlier mentioned.

Keywords: SWAT, R. Malewa, L. Naivasha, Sediment yield, sub basin, Turbidity, MUSCLE, Simulation, watershed delineation, Runoff, Enrichment ratio, Digital Turbidity Sensor, NSE, PBIAS, RSR, Discharge, Calibration and validation.

ACKNOWLEDGEMENTS

First and foremost, my gratitude to the Government of The Netherlands for providing the much needed funding for my studies here in the Netherlands through their fellowship programme (NFP).

I also wish to express my sincere gratitude to my first supervisor Dr.ir. C.M.M. Mannaerts for his continued support and for believing in me throughout the process. The guidance and help that he gave me is very much appreciated and acknowledged with the strongest terms.

To my second supervisor Dr.ir. S. Salama (Suhyb). His encouragement and wise counsel during the whole Thesis writing period cannot go unappreciated. Thank you so much.

My Sincere gratitude to the Course Director, Ir. Arno van Lieshout for the support, care, advice and guidance during my stay at the ITC WREM Department. His professional guidance and understanding is unmatched. Thank you very much.

To my Advisor, Mr Yasser Abbasi. Without his assistance and guidance, this dream would have been very hard to achieve. His patience with me even when it was hard for him and his commitment to see me through. Thank you so much and God bless.

To the WRMA fraternity, my fieldwork would have been almost impossible without them. I really appreciate the efforts that you made to make data for my research available to me in time.

To my fellow Kenyans. The most awesome lot I have ever been around. A family away from home. A loving, caring and always resourceful lot. For all the fun moments, the not so fun and the memories we made together. Many Thanks to the my Kenyan WREM colleagues (Peter Muiruri, Samuel Kipyegon, and Irene Kathambi). Together we made it. God bless you abundantly.

Finally, my Parents: Mr and Mrs Jackson Makau. The support they accorded me was overwhelming. In them I knew I had a source of hope. It felt like I was never away. To my Siblings (Benjamin, Rose and Freddie) thanks so much for the love and support. Finally, to my beloved Niece, Linet; The world is yours to conquer. Whatever your mind can conceive, you can achieve. Dare to dream.

TABLE OF CONTENTS

List of figures

List of tables

List of appendices

ACRONYMNS

SWAT	Soil and Water Assessment Tool
SWATCUP	Soil Water Tool Calibration Uncertainty Programme
SUFI	Sequential Uncertainty fitting
DO	District office
ET	Evapotranspiration
HRU	Hydrological response unit
KMD	Kenya Meteorological Department
KSS	Kenya Soil Survey
LH_OAT	Latin Hypercube one factor at a time
PBIAS	Percentage BIAS
RMSE	Root mean square error
NSE	Nash-Sutcliff efficiency
RSR	Relative standard deviation ratio
PET	Potential evapotranspiration
RGS	Rainfall gauging station
RVE	Relative volumetric error
SCMP	Sub-catchment management plan
UTM	Universal Transverse Mercator
WRMA	Water Resources Management Authority
WRUA	Water Resource users association
AGRC	Wheat agricultural land
AGRR	Maize agricultural land
AGRL	Irrigated agricultural land
URHD	Urban high density
URLD	Urban low density
URMD	Urban medium density
FRSE	Forest
RNGE	Rangeland
WATR	Water
WETL	Wetlands
USLE_C	Crop cover management factor
USLE_P	Soil management factor
IRRL	Irrigated land
PAST	Pasture
POTA	Potato
ORCD	Orchard
SOL_ALB	Soil albedo
SOL_AWC	Soil available water content
SOL_K	Soil hydraulic conductivity
GWQMN	Threshold depth of water in shallow aquifer required for return flow to occur
ALPHA_BF	Base flow alpha factor
GW_REVAP	Groundwater revap coefficient
SLOPE	Average slope steepness (m/m)
SLUBBSN	Average slope length
BIOMIX	Biological mixing efficiency

1. INTRODUCTION

Water is essential for human activities and in the preservation of the natural environment (benedini & tsakiris, 2013). The rise in the world population, intensified agricultural activities, industrialization and urbanization have caused the scarcity of the resource in many parts of the globe. The quality of the available water has also deteriorated, and many people are today faced with the problem of unsafe water for human consumption. This has led to a gradual decrease in the food production, increased disease prevalence and eventual rise in poverty levels(benedini, marcello, tsakiris, 2013).

Sediment deposition is an issue of concern in the management of the quality of water in any watershed. The deposition of sediments and sediment adsorbed pollutants deteriorate the quality of fresh water bodies in various regions in the world. The turbidity, light penetration, water temperature and dissolved oxygen are largely affected by sediments. They also carry with them adsorbed pollutants into the water bodies (Vigiak et al., 2017a). Quantification of the sediment loading into the water resources can be helpful in the adoption of the best management practices (BMPs) for the improvement of the quality of water(Liu, Yang, Yu, Lung, & Gharabaghi, 2015a). However, estimates of soil erosion in the catchment and sediments resulting from it are not achievable through measurements (Odongo, Onyando, Mutua, van Oel, & Becht, 2013). The estimation of the sediment loading into a water resource can also be helpful in many other applications such as structural designs, protection of aquatic life habitats, etc. This exercise can be very complex if the proper tools are not used. The SWAT model is one of the tools that has proven reliable in the accurate prediction of the sediment loads in catchment system (Liu et al., 2015a)

The L. Naivasha is located in the Rift valley of Kenya and serves as a source of fresh water for domestic and agricultural use in the surrounding areas. It also provides the water that is used in horticultural farming and recreational activities in the area. Unfortunately, the lake Naivasha is slowly filling up with sediments from the Basin and has seen the depth of the lake decrease in the recent past. The dregs cause pollution of the water directly or indirectly by acting as modes of transport for pesticides and other agrochemicals (Tiruneh B.A, 2004).

The sources of pollution are both point and non-point which makes it hard to propose mitigation measures. Sustained contamination of the lake by sediment related pollutants has led to the detriment of aquatic life due to the enrichment of the aquatic system by minerals and chemical compounds which increase the turbidity of the water (Kitaka, Harper, Mavuti, & Pacini, 2002). Quantifying suspended sediment load washed into the Malewa river and eventually into L. Naivasha is crucial in mitigating soil erosion and formulating better management practices to lower stream sediment and by association the adsorbed pollutants. This will help in improving the quality of the water that flows into L. Naivasha.

Several approaches have been used previously to qualify and quantify the pollutants that are loaded into the L. Naivasha basin through the rivers over a temporal span. One of the common methods used was the longitudinal study design which involved laboratory investigations of collected samples of water from the basin for physicochemical parameters and the mineral residue concentrations in the water (Kaoga, Ouma, & Abuom, 2013a). These methods gave good results but could not be relied upon for analysis of the whole catchment due to its vastness and the ever-changing agricultural patterns in the region. Other methods include: the modified Universal Soil Loss Equation (MUSCLE) the key equation in cooperated into the SWAT algorithm that was used to estimate the sediment yields in the upper Malewa catchment (Odongo, Onyando, Mutua, van OEL, & Becht, 2013). This was for calibration and validation of the SWAT model and the use of the two stream remote sensing model for water quality mapping; which tries to measure the

water quality by trying to quantify the sediment concentration by interpretation of the backscattering of incident light on the water(Salama & Verhoef, 2015).

The Soil and Water Assessment Tool (SWAT) is a catchment simulation model developed for simulation of the effects of practices carried on land in vast, heterogeneous watersheds. It is a physically based semi-distributed model integrated into the Arc GIS and allows for the prediction of the impacts of on land tilling practices on water, sediment and agrochemical productions in watersheds with diverse soil types and varying land use and management conditions (Caitlin Scopel, 2012). In this study, the SWAT was identified as an appropriate tool to use for simulating the suspended sediment transport and deposition into L. Naivasha.

This research was aimed at evaluating the feasibility and reliability of the SWAT model in the determination of the suspended load in Malewa River and into the L. Naivasha. It was also used to predict the extend of pollution of the water resource by agrochemicals and pesticides carried by the suspended sediments. The results of the model were validated using measurements recorded using in situ digital turbidity sensors (DTS) and other relevant data collected during fieldwork.

1.1. Problem Statement

Sediments contribute to the pollution of the L. Naivasha by degrading its water quality. It also fills up the lake and thus threatens aquatic life in the Lake. Sediments also provide a means by which pollutants are transported into the Lake by adsorption. The L. Naivasha basin is an agricultural hub, and therefore considerable amounts of sediment are generated after each rain event. These sediments have however not been quantified, and no study up to date has been successfully done to quantify the fluxes of the sediments into the lake.

Previous attempts to quantify the sediments have not been able to address the areal vastness of the catchment and thus could not be relied on. The application of the SWAT model has however been proven as a reliable tool for estimating sediment load fluxes in a watershed (Vigiak et al., 2017) and has been applied in quantifying sediment loads in various watersheds across the world. Liu et al., 2015 applied the model to quantify the sediment flux in the South Tobacco Creek (Basin) in Canada. Michael et al. (2005) used the SWAT model to assess the effects of different tilling orientations in lowering erosion in the Lake Creek watershed, South-western Oklahoma, USA. Odongo et al., 2013 validated the MUSCLE equation in cooperated into the SWAT model and came to conclusions that the model was fit for adoption as a sediment quantification tool. Thus, this model was applied in this project to quantify the volumes of sediment resulting from the Malewa River Basin and finding its way into the L. Naivasha aquatic system since there is no record of any study that has successfully quantified the sediment fluxes into the Lake.

The Digital Turbidity Sensor data has not been used in any study in the validation of any hydrological model for the modeling of sediment fluxes in any watershed. In this study, the DTS data was used in the validation of the model results and hence give a clear impression of the sediment potential sediment loads into the Lake Naivasha from the various sub-basins.

1.2. Research objectives

1.2.1. Main Objective

- To quantify the sediment flux of the R.Malewa catchment into the L. Naivasha

1.2.2. Specific Objectives

- To Evaluate the reliability of the SWAT in Quantifying the sediment fluxes into L. Naivasha
- To Calibrate and Validate the SWAT model using the Insitu data.

1.3. Research questions

- How much sediment is transported from the upper catchment into L.Naivasha from the R. Malewa catchment?
- What are the factors that influence sediment production in the Watershed?
- How reliable is the SWAT model for quantifying sediment fluxes from Malewa River catchment into L. Naivasha?

1.4. Hypothesis

- The SWAT model is a reliable tool for modeling and quantifying the sediment loads in R. Malewa catchment that finds its way into the L. Naivasha

1.5. Relevance of the study

L. Naivasha serves as a source of fresh water for most of the farms around the area. It also provides fresh water for domestic consumption and supports a variety of wildlife around the Lake (Harper et al., 2011). These activities rake in a lot of income for the local people and the Kenyan Government at large. The continued sedimentation of the lake, therefore, poses a danger to the ecosystem and threatens the livelihood of the local people. Pollution by Agrochemicals, for instance, causes the death of aquatic life which is a means of livelihood for many fishermen living in the area.

Intensive and extensive Agricultural activities have been identified as the main contributor to sediment generation in the L. Naivasha catchment(Harper et al., 2011). The sediments carry within themselves dissolved agrochemicals which are released upon arrival into the lake thus causing a health hazard to both aquatic and human lives.

The study, therefore, was aimed at quantifying the of sediment flux that is generated in the catchment due to the various land uses and is transported into the L. Naivasha by the River Malewa water. This will by extension inform proper management decisions that need to be adopted to curb the pollution of the lake and to save the natural ecosystem of the lake. It will also help in determining the pollution extend caused by agrochemicals and other chemical substances dissolved in the sediment.

1.6. Study area.

Lake Naivasha is a fresh water lake located in the Eastern Rift valley of Kenya located at 00° 46' to 36 15 to 36 25 longitudes and is located in zone 37 UTM. It is situated 90Km to the Northwest of Nairobi and has an altitude of between 1900 to 3200masl (Tiruneh B.A, 2004). Its basin is closed and has no identifiable outlet(Tang Zhen Xu, 1999). The catchment is bound by the Aberdare Mountains (4000msl) and the Mau Escarpment (3048msl) to the East and West respectively. The Eburu hills (2800msl) cut between the catchment from the Elementaita. The Basin is administratively located within eight districts (Naivasha, Narok north, Gilgil, Mirangini, Kipipiri, Kinangop, Nyandarua central and Nyandarua South). The catchment has an area of 3400km^2 and is dominated by the L. Naivasha which covers an area of 150km^2 and has an average depth of 4.7m(Everard, Vale, Harper, & Tarras-Wahlberg, 2002). The main sources of water for the lake are rivers Malewa and GilGil that enter the lake from the Northern side. The source of the rivers are the highlands in the basin.

The L. Naivasha Basin supports a wide spread scope of social and economic activities. Agricultural activities such as Horticulture, Animal keeping and Fishing are just but a few of the economic activities carried out in the catchment. Tourist hotels and camping sites are also prevalent in the region. Figure 1 below shows the map of the study area.

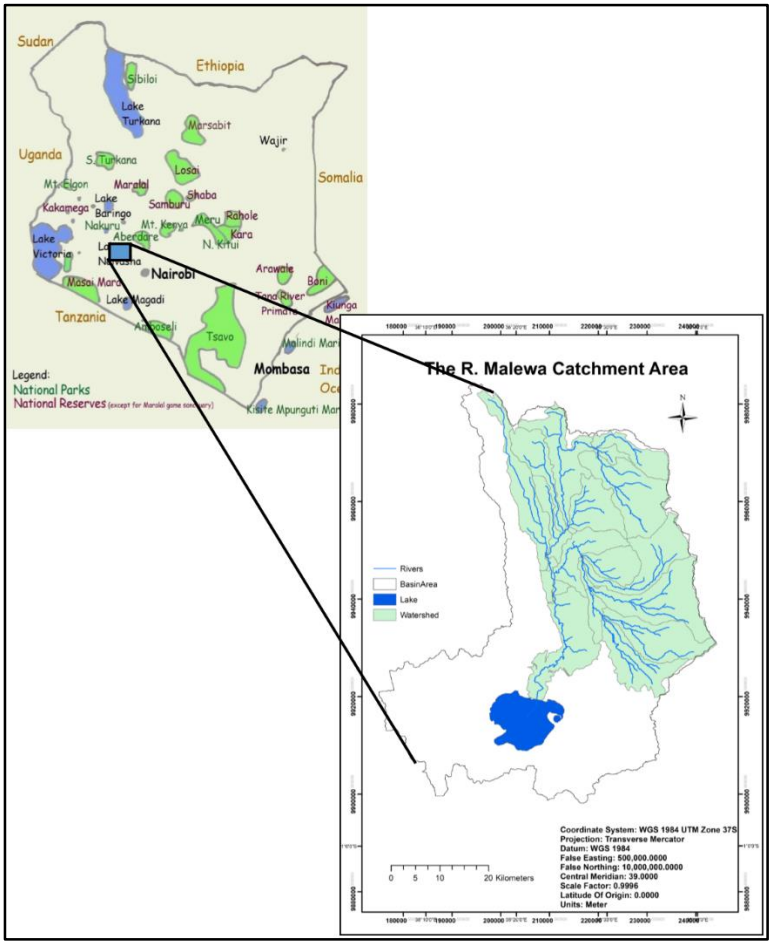

Figure 1: Study area map showing the Malewa river basin (inset a map of Kenya)

1.6.1. Climate

1.6.1.1. Temperatures

The catchment is semi-arid with the mean monthly temperatures varying from 15.9 to 17.8 ^{0}c. The highest mean temperatures range from 24.6^{0}c to 28.3^{0}c. The highest temperatures are recorded in January and February. The minimum mean temperatures range from 6.8^{0}c to8.0^{0}c. The coldest months are July and August(Tang Zhen Xu, 1999). The temp lapse rate is estimated to be 0.56^{0}c for every 100m increase in elevation(Tiruneh B.A, 2004).

1.6.1.2. Rainfall

The rainfall regime in the area is mainly affected by the rain shadow effect from the neighboring Nyandarua and Mau ranges. There are two distinct rainy seasons (Bi-modal). Rains start from March to May for the long season and the short rains are experienced in October through November to early December. The rainfall pattern is also subject to relief with higher altitudes receiving slightly higher rainfall than the lower altitudes. The average rainfall is received in the area is about 610mm with the high-altitude areas receiving rainfalls as high as 1525mm. The evaporation estimates for the lake are about 1360mm per year(Md. Azizul Haque podder, 1998). The rainfall seasons are succeeded by dry months that span from December to February and again from July through to September. The relationship between the rainfall and the altitude for is shown in

Figure 2. This was based on the stations located at various points in the water shed for the simulation duration (2004-2017)

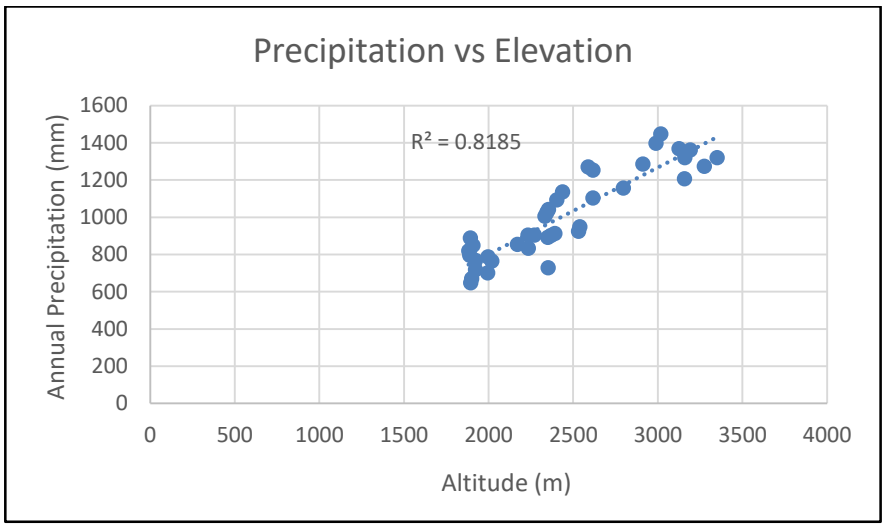

Figure 2: Plot of rainfall vs altitude

1.6.2. Hydrology

The Lake Naivasha Basin is rich with rivers and tributaries that crisscross the watershed from the uplands into the Lake. The Major rivers in the Basin are the Malewa River, The Gilgil river and the Karati rivers. The Malewa river is the dominant inflow into the Lake being responsible for up to 90% of the total inflow into the lake(Tiruneh B.A, 2004). It has its origin in the Kinangop plateaus. The river Malewa basin is approximately 1600km^2.

The Lake Naivasha does not have a surface outlet. It, however, has been argued that the Lake leaks to several underground aquifers to its North and South (Meins, 2013). Evaporation also plays a major role in the water balance of the Lake system with the area experiencing high evaporation and evapotranspiration rates.

Previous studies suggest that 80% of the water flowing into the lake is form surface flow while the rest (20%) comes from subsurface flow. This is however not verifiable as data is not available to support the same. It has also been suggested that there is significant percolation into the deep aquifers from the water resources in the basin.
The soils in the Basin are predominantly of volcanic origin due to the faulting activity during the formation of the Rift valley. These soils are highly permeable and do not have high water retention capacity. Rain water and irrigation water, therefore, finds its way into the deep aquifers easily (Becht & Harper, 2002)

1.6.3. Water Use

The dominant water use in the R.Malewa basin is irrigation. The most pronounced activities are near and around the lake where flower farming is fully fledged. This accounts to 2/3 of the water abstracted from the Lake. On the upper catchment, water use is minimal with most farming activities being rain fed. The water requirements/consumption in the watershed was investigated by Musota, 2008 using the preliminary assessment of the Water Resources Assessment programme data to come up with the water demand for the basin as is shown in Table 1-1

Table 1-1: Water use in the Basin

Demand	Quantity	Units	Quantity Required (Mm^3/Yr)	Representative %
Irrigation	5897	Hectares	56.6	71.7
Livestock	32005	Livestock Units	0.5	0.6
Wildlife	29013	Livestock Units	0.9	1.1
Domestic	812389	People	17.1	21.7
Industry			3.8	4.8
Total			78.9	100

1.6.4. Land use

The L. Naivasha basin supports various land use activities both economic and social. The major portion of the basin is used for agriculture (Both irrigated and rain-fed). There is also a big portion of the basin under natural vegetation (shrubs, grasses and forests). A small portion is covered by water bodies (L.Naivasha and Rivers). The main agricultural activities in the Basin are cattle rearing and small-scale crop growing mostly for subsistence use. There is also some commercialized vegetable growing in the lower parts of the watershed as one nears the lake. The upper part of the basin has been intensively cultivated with commercial crops like pyrethrum, wheat, onions and potatoes. A considerable portion of the basin has also been put under pasture whereby livestock rearing is practiced both intensively and extensively. The central part of the basin is composed of natural vegetation and bush where there is no significant human activity undertaken. Wildlife preservation is however undertaken in these areas.

2. LITERATURE REVIEW

Prediction of the amount of sediments resulting from soil erosion plays an important role in the assessment of water quality management practices. Research shows that soil and river channel erosion increase in certain climates and land use practices (Ouyang, Skidmore, Hao, & Wang, 2010). Excessive sediments in water reduce the quality of water by increasing its turbidity and providing a means for sediment-adsorbed pollutants to be transported. The understanding of the source of sediments and their quantification can be of importance in the adoption of best management practices (BMPs) for water quality safeguarding at both field and watershed scales. The erosion and sediment creation dynamics can be understood through Field monitoring. However, the process is expensive and spatially limited. This led to the adoption and use of mathematical modeling techniques in large catchment areas. The SWAT is one of the models that has been employed to simulate the erosion process in the watershed scale and to analyze the sediment transport and deposition dynamics and processes in the catchment.

2.1. Related Studies

The SWAT Model has been applied previously in the L. Naivasha watershed for several studies. The studies mainly were looking into the quality of the water resources in the area and into the lake in relation to the agricultural activities dominant in the area.

(Odongo, Onyando, Mutua, van Oel, et al., 2013) Looked at the feasibility of adopting the MUSLE algorithm as used in the SWAT in the simulation of sediment transport. They performed sensitivity analysis on the model using the Sobol sensitivity analysis method. They also evaluated the sensitivity of the model using the Nash-Sutcliffe(NSE) and the modified Nash-Sutcliffe efficiency by choosing the objective functions and robustness of the outcome of the model with the sediment measurements values that were acquired for the Malewa catchment. The conceptual factors for the MUSLE model were found to be the most sensitive with a contribution of 66% of the sediment yield variability. The use of the NSE to validate the use of the MUSLE model for the upper Malewa was also successful and hence the conclusion that the MUSLE model could be used satisfactorily in the simulation of the sediment yields in the catchment.

Tiruneh B.A, (2004) Used the SWAT model to model the nutrient fluxes in the watershed and consequently quantify the nutrient loads into L. Naivasha. He also sought to model the transport processes of both P and N using the model under four different scenarios of land management. The calibration of the nutrients and the sediments was done using the gauge data from the streams and from laboratory analysis of the collected water samples. He found out that the coeficient for Nitrogen percolation (NPERCO), Phosphorus percolation coefficient (PPERCO), The soil portioning coefficient for Phosphorus (PHOSKD), Slope, Slope length, The Biological mixing efficiency (BIOMIX), the support practice factor (USCLE_P) and the Curve Number (CN) were some of the most sensitive parameters of the model. The most sensitive was the curve number whose increase in 26% resulted in 269.77% and 51.61% increase in the yields of NO_3 and P respectively. This he attributed to increased surface runoff.

He also tested the model by running different scenarios of management practices. One was with the application of fertilizers and grazing activities, and the other was without. The overall deduction from the above scenarios was that there were increased NO_3 and P fluxes into the Malewa river in the presence of the above activities while in the absence of the activities, reduced nutrients were output by the model.

Another study that was performed in the L. Naivasha was by (Kaoga, Ouma, & Abuom, 2013b). It was aimed at investigating the effects of the increased horticultural activities qualitatively on the water in the lake. He tested the presence of Organochlorine and Organophosphates in the water and their respective concentrations. Using the Gas-liquid chromatography technique and subjecting the results to statistical

analysis, he was able to conclude that the lake water did not contain alarming amounts of the Organochlorides and Organophosphates and that the water quality was within the recommended WHO levels.

A remote sensing approach was adopted in the study of the sedimentation process by (R.A.P. Rupasingha, 2002) to investigate the sedimentation rate of the Lake. The study applied Bathymetry techniques, suspended sediment surveys and core sampling as well as analysis suspended sediment in river inflows. He carried out an exploratory analysis using models and correlated the incoming sediment fluxes to the lake sedimentation rates. He was able to predict and quantify the sedimentation rates for the duration 1932-11990 and analyze its spatial distribution on the Lake bed. Using the results, he was able to predict the period which it would take for the Lake to be at a threatening level due to sedimentation.

2.2. Overview of the SWAT Model

The SWAT was developed for use in catchments and sub-catchments extending from several hundred to a few thousand square kilometres in area. It takes into consideration the soil type, the land use, and the slope. All these, when combined, represent a similar agro-hydrologic response unit.(Zettam et al., 2017). The point weather data is also used as an input to the model. The daily precipitation, net solar radiation and the maximum and minimum average temperature extremes per day are also used as inputs to the model.

The SWAT model was developed to estimate the impacts caused by various land management activities on the quality and quantity of water over a span of time. It is executed at a daily temporal scale but can also be simulated on half day temporal scale depending on the intended output(Teshager, Gassman, Secchi, Schoof, & Misgna, 2016). Weather, land management use, and cover, Topography, vegetation and Soil properties are some of the inputs that are the main data inputs into the model. The model however simulates prolonged rain events and therefore cannot be used to simulate the effects of a single rain event(Liu, Yang, Yu, Lung, & Gharabaghi, 2015b). The ArcSWAT interface is the GIS-based graphical input interface that will be used in the configuration of the model to the GIS environment.

The SWAT model makes use of the Hydrological response units (HRUs) and the sub-catchments during its simulation. The HRU is defined as a unit of uniform hydrological response and environmental properties in terms of land use, Soils and Topography. A sub-basin is defined as an area that is composed of several Hydrological response units (HRUs) (Neitsch, Arnold, Kiniry, & Williams, 2011)

The model delineates the watershed into several sub-watersheds and HRUs based on the working combination among the data fed into the model, i.e. Land use map, Soil map, and DEM. In the Hydrological Response Units, water inflows and outflows and the sediment yields are computed at daily intervals.

The considerations taken for the water balance are: the precipitation, evapotranspiration, Quick runoff, irrigation, infiltration rates and lateral flow (Neitsch et al., 2011). The hydrological component of the model at each HRU simulates the hydrological balance using the relation:

$$SWt = SWo + \sum_{t=1}^{t}(Rday - Qsurf - Ea - Wseep - Qgw) \quad \text{.....Equation 1}$$

Where:

SW_t = Final soil moisture content (mm)
SW_0 =Initial water content on day i (mm)
t = Time in days
Rday =Precipitation on day i (mm)

Qsurf = Surface runoff on day i (mm)
Ea = Evapotranspiration on day i (mm)
Wseep = Amount of water seeping into the soil profile on day i (mm)
Qgw = Amount of return flow on day i (mm).

The rates of Evapotranspiration, surface runoff, seepage and channel routing within the catchment and the HRUs are simulated within the model by the inbuilt statistical tools. The hydrological variables of each HRU are computed by the Model using The Curve number method. These parameters are but not limited to: Initial Abstraction, retention parameter and peak runoff.(Gessesse, Bewket, & Bräuning, 2015)

The Modified Universal Soil Loss Equation (MUSLE) is applied by the model for the calculation of the rates of erosion and resultant sediment yield. However, the MUSLE based model simulates sediment generated in one single storm, and this can be translated to the output coming out of the watershed depending on the HRUs. The MUSCLE equation was investigated and validated for use in sediment simulation in SWAT by (Odongo, Onyando, Mutua, van Oel, et al., 2013). The latest version of the equation which was modified by Vigiak et al., (2015) to minimize the effects of HRU coverage on the generation of yields in big HRUs. The equation developed by Vigiak et al., (2015) is as follows

$$s_y = [11.8(QqlA_{min})^{0.56}(CPKLSF_{CRFG})]\left(\frac{A}{A_{min}}\right) \quad \text{..Equation 2}$$

Where:
Q= Daily volumes of run off(mm)
ql= Peak run off discharge volume (m^3/s)
$ql=q_p(A_{min}/A)$ and q_p = HRU Runoff peak discharge (m^3/s)
Amin=min (A, A_t) the minimum between the HRU area A[ha] and the user-defined threshold area, A_t[ha]
C= crop cover for the HRU
P=Soil protection factor
K= Soil erodibility factor
LS= Topography factor
F_{CRFG}= Soil stoniness factor

The MUSCLE equation primarily is applied to an area of size A_{min} (ha) then multiplying the results by the number of A_{min} units making up the whole HRU (A/A_{min}). The A_{min} is the largest hydrologically isolated unit within the HRU (Mccool et al., n.d.).
The HRUs daily outputs are transported through the stream channels in the stream phase. The routing mainly affects the streamflow, the suspended sediments, and other materials and occurs in the dropping sequence of the single sub-catchments. The sediment yield is determined by the streams capacity to transport it and the amount of sediment input from the upstream of the sub-catchment and from the individual HRUs. The maximum sediment load that can be transported is estimated using the modified Bagnold's stream power equation (Vigiak et al., 2017a).

$$C_{max} = C_{sp}\left(\frac{prfq_{ch}}{A_{ch}}\right)^{esp} \quad \text{.....Equation 3}$$

Where
$(prf q_{ch}/A_{ch})^{exp}$= Peak channel speed (m/s) as a function of q_{ch}
q_{ch}= Sub-catchment peak flow rate (m^3)
A_{ch}= Area of Channel cross-section (m^2)
P_{rf}= factor for Sediment peak rate adjustment.
C_{sp} and e_{sp} are used to regulate the relationship between the power of the stream and the peak velocity of the stream. They are also used as calibration parameters.

Deposition of sediments occurs when the incoming sediment concentration exceeds C_{max}. The excess sediment is deposited in the reach. On the other hand, if the concentration of the sediment is below the carrying capacity of the stream, channel and bank erosion will occur (Vigiak et al., 2017a).

2.3. Factors that control the Generation of Suspended sediment

The factors that influence the generation of sediments in a watershed are diverse. They include: Runoff amounts, the rock formation of the watershed, Topography, Land use, relief etc.

2.3.1. Rainfall

The amount of rainfall that falls in a watershed is the main source of runoff. The resultant discharge is the main soil particle detaching medium. The detached particles eventually find their way into the river channels and are transported to different areas in the watershed.

2.3.2. Basin Area

The influence of the size of a watershed in the generation of sediments was investigated by Miliman and Syvitski (1992). He found out that the smaller watersheds (Sub basins) tend to produce more residue compared to the larger watersheds.

2.3.3. Mean Elevation and Relief.

According to a study by Pinet and Souriau (1998), sediment production tends to be correlated with the average relief of a basin. The study was based on large world rivers, and he developed an equation to support his findings.

$$R^{3/2}A^{1/2}E^{kt} = q_s \quad \text{.....Equation 4}$$

Where:
Qs= Amount of sediment produced
R= The relief of the watershed defined by the difference between the highest point and the sediment measuring station
A = Basin Area (Km^2)
E= Elevation mean
T = The temperature of the Basin (Surface)
K and a = Constants ($2*10^{-5}$ and 0.1331)
The study also found out that under natural conditions, the sediment production in mountainous regions was 28 times higher than that in lower regions. The rate of mechanical erosion changes based on the altitude and the relief.

Spatial and Temporal Variability in Sediment Production

The spatial and temporal characteristics of sediment production in a watershed have been studied in several studies. The overall findings in most of these studies are that, the temporal and spatial changes in the watershed can have a direct impact on the production of sediments in the watershed. Golosov et al., 2017 experimented on spatial and temporal aspects of sediment production in Sichuan Basin in China. He concluded that the variability of rainfall and slope coupled with human management activities are the major factors playing a big role in sediment transfers.

2.4. The Soil Erodibility Factor

The erodibility factor of soil is caused by its properties. It refers to its rate of loss of soil per erosion index unit measured on a unit area (Neitsch et al., 2011). The erodibility factor indicates how easily soil particles detach and are transported by rainfall runoff. For any soil type, the erodibility factor is determined by the rate of erosion index from a standard area plot. The plot is 22.1m with a slope of 9%. And is continuous fallow and is tilled (Kept without vegetation for over 2years) both up and down. The soil becomes resistant to erosion when the amount of silt in it decreases but does not matter if the sand and clay fractions in it increases or decreases. The erodibility factor can be measured when fine sand and silt content of the soil make up below 70% of the distribution of the soil particles size distribution. The equation below is used.

$$K_{USLE} = \frac{0.00021.M^{1.14}.(12-OM)+3.25.(C_{soilstr}-2)+2.5.(C_{perm}-3)}{100} \quad \text{.....Equation 5}$$

Where:
K_{USLE}= Soil erodibility factor
M= Soil particle size parameter
OM= % soil organic matter content
$C_{soilstr}$= Soil structure code as used in soil classification
C_{perm} =Permeability class of the soil

The erodibility factor shows the ease of erosion by different soils when other factors are kept constant (The rate of infiltration, AWC, Rainfall intensity, Dispersion). The soil texture is a major contributor to the erodibility factor with others like organic matter content and structure also playing major roles. Soil erodibility factor ranges are 0.02 to 0.69 (Imani, Ghasemieh, & Mirzavand, 2014)

2.5. Transport Of Adsorbed Pesticides

Surface runoff transports runoff adsorbed in the sediments into the main channels. The more the sediment, the more the pesticides transported and consequent pollution. The sediment adsorbed pesticide loads can be calculated by the equation formulated by McElroy et al. (1976) and later improved by Williams and Hann (1978)

$$Pst_{sed} = 0.001\frac{C_{solidphase}*sed}{Area_{hru}*\varepsilon_{pstsed}} \quad \text{.....Equation 6}$$

Where:
Pst_{sed} = Sediment sorbed pesticide in the main channel (Kg pst/ha)
$C_{solidphase}$ = Concentration of sediment on the top soil layer (10mm) in gpst/metric ton soil
Sed = Daily sediment yield (metric tonnes)
$area_{hru}$ = Area of the HRU (ha)
$\mathcal{E}_{pstsed}$ = Enrichment ratio of the sediment
The total amount of pesticides is calculated by summing up the adsorbed and the dissolved amounts

$$Pst_{sly}\left(C_{solution} * SAT_{ly} + C_{solidphase} * O_b * depth_{ly}\right) \quad \text{Equation 7}$$

Where:
$Pst_{s,ly}$ = Pesticide amount in the soil layer (kg pst/ha)
$C_{solution}$ = Concentration of the pesticide in solution (mg/l)
SAT_{ly} = Soil water at saturation point (mm H_2o)
$C_{solidphase}$ = Pesticide concentration in the solid phase (mg/kg, g/ton)
ϱ_b = Soil layer bulk density (mg/m^3)
$depth_{ly}$ = Soil layer depth (mm)

2.6. Enrichment Ratio

This is the amount of the adsorbed pesticide concentration in the residue to the pesticide concentration in the soil layer (Neitsch et al., 2011). SWAT uses the enrichment ratio for the individual HRUs for a time series of events to determine the overall enrichment ratio for the whole storm. The relationship used by SWAT was outlined by Menzel (1980). In this, ratio is related to the concentration of the sediments in a logarithmic manner. The enrichment ratio for a storm event is calculated using the equation

$$\varepsilon_{pstsed} = 0.78\left(Conc_{sed,surq}\right)^{-0.2468} \quad \text{Equation 8}$$

Where:
$Conc_{sed,surq}$ = Sediment concentration in surface runoff (mg sed/m^3 H_2o)

Sediment concentration in the quick runoff is determined using the equation

$$Conc_{sed,surq} = \frac{Sed}{10 * area_{hru} * Q_{surf}} \quad \text{Equation 9}$$

Where:
Sed = Sediment yield (Metric tonnes)
$area_{hru}$ = HRU area (ha)
Q_{surf} = Surface runoff in a day (mm H_2o)

2.7. Turbidity Measurements

2.7.1. The Digital Turbidity Sensors

These are devices used to measure the turbidity of liquids depending on the suspended solids in it. They use the principle of the optical backscatter by employing a detector at 90 degrees to the incident beam. The device emits light to the liquid and records the amount of reflection coming from the suspended solids. The latest technology in terms of micropower, infrared laser technology, and solid state is used to achieve the desired results. Modulation of the laser light output and synchronization detection is done to minimize the effects of the ambient light conditions. The DTS-12 measurement range is 0 to 1500 NTU (Nephelometric Turbidity Unit), thus is an ideal choice for stream and river applications (FTS, 2016).

The DTS-12 has the capability of reducing silt build up and biological fouling by use of an inbuilt sensor. This makes sure that the sensor optics are not affected and that the sensor functions well at all times. The DTS-12 has been programmed with turbidity calibration coefficients. Using the coefficients, the microcontroller uses the raw measurements to compute the maximum, minimum, mean, median, variance and Best Easy Systematic estimator (BESE). The results are returned in NTUs. The control and measurement functions are initiated by sending an SDI-12 (Serial Digital interface at 1200baud) An asynchronous serial communications protocol for intelligent sensors for the monitoring of environment data) command to the DTS-12

2.7.2. Turbidity Measurements

The data logger sends an appropriate SDI command to the DTS-12 to initiate the measurement process. This is followed by a cycle of measurements that follow a series of steps as below

- The sensor head powers up
- The analog circuitry is calibrated to the digital one
- The water temp is read
- Wiping
- Acquisition of 100 samples at a speed of 20 samples per second
- Calculation of required statistics

This is followed by retrieval of measurements by the data logger by issuing of a SDI "DO" command. This process takes 10 to 20 seconds depending on the type of measurement required.

2.7.3. DTS-12 Calculations

The calculations carried out by the DTS-12 on the samples are as in the equations below

Mean = Total Sum of measurements/100 = $\frac{1}{100} + \sum_{i=1}^{100}(x_i)$……*Equation 10*

Variance = $\frac{1}{99}\sum_{i=1}^{100}(x_i - mean)^2$……*Equation 11*

Median = $\frac{X50+X51}{2}$……*Equation 12*

BES = $\frac{X25+X50+X51+X76}{4}$……*Equation 13*

Minimum = Min (100 readings) = $\text{Min}_{i=1}^{100}$

Maximum = Maximum of all readings = $\max_{i=1}^{100} X_i = X_{100}$

X_i = Measurement 'I' in the sorted list

2.7.4. Calibration of the DTS-12

The DTS is usually returned to the manufacturer for calibration on Annual basis

2.7.5. The US DH-48 Depth Integrating Suspended Hand Line Sampler

This is a depth integrating sampler that can be used in shallow wadable streams to collect samples. The isokinetic principle allows water and sediment to enter the nozzle at the same velocity as the stream thus taking a representative sample. The Commonly used is the ½ inch (Diameter) wading rod. Extensions can be added to it to sample deeper stream portions. The Sampler can be used to take samples in streams having velocities from 1.5 to 8.9 ft/sec.

A Digital Turbidity sensor is shown in Figure 3

Figure 3: The FTS Digital Turbidity Sensor as used at 2GB04 station

3. DATA COLLECTION AND PREPARATION

3.1. TSS and Turbidity measurements.

A field survey campaign was carried out during the first week of the field work (19th- 22nd Sep) to familiarize with the Malewa basin and identify appropriate sites for sampling for the measurement of the TSS and TDS in the WRMA lab. Three sites were chosen based on their location in the basin to have a representation of the whole basin. The gauge stations 2GB04,2GB01 and 2GB02 were selected as they represent the upper, middle and lower catchment respectively. Taking samples from these points would be appropriate for the determination of the sediment flux changes from the upper watershed to the lake.

3.1.1. Sampling

The samples were taken for the Three weeks of the fieldwork expedition. The handheld sampler was used to obtain the grab samples from the flowing river sections at a uniform depth of 0.5m. The samples were later analysed for TSS and TDS and the results recorded.

3.1.2. TSS Measurements

This was done in the WRMA lab using the automatic UV-VIS spectrophotometer. 25mm water samples from the various sampling sites were put into a test tube and placed into the spectrophotometer. Running the machine for a few minutes gave the value of the concentration of the TSS. The readings were then recorded as the values of TSS in the river sections.

3.1.3. TDS Measurements

The samples taken from the sites mentioned above were analyzed using the Turbidity meter in the WRA lab. The respective readings of the TDS measurements were recorded.
This process was repeated for three consecutive weeks, and the results were as tabulated in Table 3-1 (More sample results are shown in the appendix)

Table 3-1: Water samples Analysis Results

Station	Elevation (masl)	Co-ordinates (UTM)		Week 1		Week 2		Week 3	
		X	Y	TSS (mg/L)	TDS (NTU)	TSS (mg/L)	TDS (NTU)	TSS (mg/L)	TDS (NTU)
2GB04	2356	219808.8	9969175.2	40	15.2	36	32.5	11.0	16.33
2GB01	1948	210908.0	9938530.8	35	32.3	23	53.1	23.0	39.2
2GB02	1928	209311.88	9926149.6	78	86.5	72	80.3	43.0	56.6

More measurements made by Yasser Abbasi in his field expedition in April were also acquired. The measurements would be used in the conversion of the field data from the station from NTU units to mg/l

3.1.4. DTS Data

A DTS installed at the 2GB04 in April was also used to collect TDS data in the Wanjohi stream (A tributary of R. Malewa).
The turbidity measurements were downloaded from the logger using a flash drive. The measurements were in 15min time steps for a period of 4 months spanning from 16th April to 27th Sep 2017. The data was analysed and converted to daily time steps for easier consumption in the validation of the in-situ measurements. The data was as shown in Figure 4

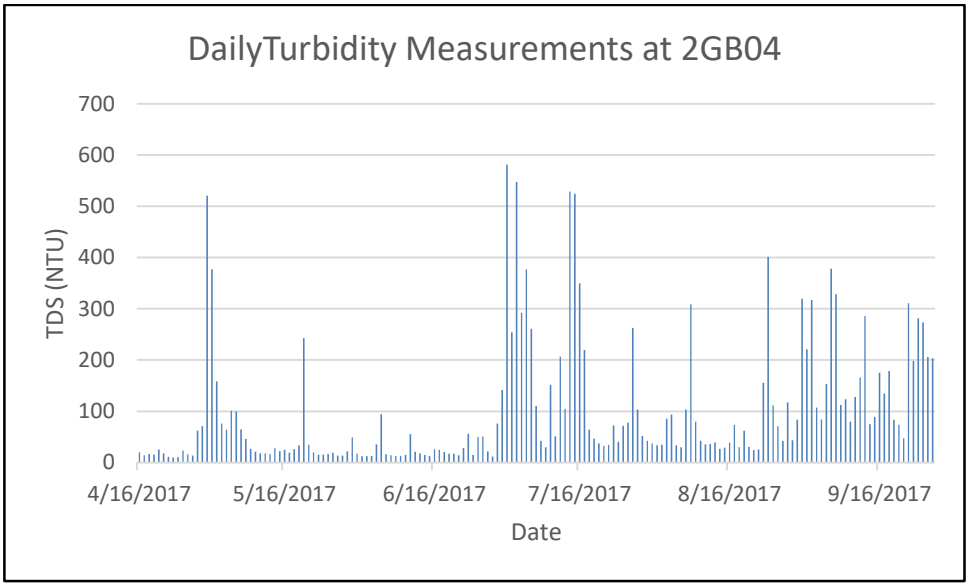

Figure 4: Turbidity measurements as made by the TDS at the 2GB04 station

3.2. The Digital Elevation Model

The Digital elevation model is essential for the provision of Topographic information in the basin. The DEM was acquired from the ITC data archives that had been prepared by Lukman (2003). It has a resolution of 20m. A previously masked DEM for the Lake Naivasha Basin was available and was used. The elevation accuracies of the DEM range from 10 to 20m RMSE (ASTER GDEM Validation Team 2011)

A stream network for the Malewa basin was also acquired from the ITC data archives and was used to check for the correctness of the DEM by visual inspection. It was found that the river and stream networks of the basin match correctly with DEM. The network as such would be used where the GDEM does not provide sufficient detail for the delineation of the streams properly. The DEM properties were as in Table 3-2

Table 3-2: DEM Properties

Projection	Universal Transverse Mercator
Spheroid	WGS_1984
Datum	WGS_1984
Zone	37S
Central Meridian	39
Reference Latitude	0
Northing	10000000
Easting	500000
Scale factor	0.9996

3.3. Land Use/Landcover Map

The land use/ Land cover map is a major input component of the SWAT model as it is used in the delineation of the basin and the creation of the HRUs. The characteristics of the various vegetation and land cover dictate the responses of the hydrology of the area. On the basis of the characteristics of the land cover and use, SWAT is able to compute the canopy storage and the ease at which soil is going to be eroded into the streams (Meins, 2013).

A LULC map released by the Copernicus Global Land Services through the Geo-Wiki.org website was downloaded. The Sentinel-2A map has a pixel resolution of 20m and covers the whole of Africa. It was released on 3/10/2017 (Copernicus Global Land services 2017)and contains a modified Copernicus LULC data for the period Dec 2015-Dec 2016 for the entire African Continent. It has been processed using 180,000 Copernicus Sentinel-2A images by land cover cci, ESA. The LULC map has 11 general classes that cut across the whole continent(Copernicus Global Land services 2017). Closer visual inspection proved that 10 of the 11 classes were represented to a fair proportion in the Naivasha Basin area.

3.3.1. Processing

The LULC Map was downloaded to a hard drive. Using the sentinel processing software SNAP, a subset of the central Kenyan region was made. The subset was then saved imported into ArcGIS where a shapefile for the Lake Naivasha Basin was used to mask out the Basin area. The resultant LULC Map was inspected and compared with the 2012 LULC Map produced by Odongo et al. It was noted that there was no substantial change in Land use or Land cover during the period and that the two LULC Maps bore a lot of resemblance to each other. There is, however, a slight difference in the classes with the 2012 LULC map having eight classes as opposed to the 2016 one which has ten classes. The two LULC Maps were combined in ArcGIS software to come up with a more comprehensive, more inclusive map that would be used in the model. The various classes were then named as follows for adoption into the SWAT model. The respective areas covered by the different classes were as shown in the table

Table 3-3: LULC classes and codes for use in the model

Original LULC class	SWAT classification	SWAT Code
Water	Water	WATR
Trees cover areas	Forest	FRST
Shrubs Cover areas	Rangeland-bush	RNGB
Grassland	Range -grasses	RNGE
Cropland	Agricultural Land-Generic	AGRL
Aquatic vegetation (Regularly flooded)	Wetlands-mixed	WETL
Lichen Mosses/ Sparse Vegetation	Range-Grasses	RNGE
Bare areas	Range- Grasses	RNGE
Built-up areas	Urban-High density	URHD
Open water	Water	WATR

3.4. Soil Map

The soil map adopted for use in the SWAT simulation was acquired from ITC database. It was prepared by the Kenya Soil Survey. Different soil groups were identified from the map. The parameterization of the soil map is however different from the ones used in SWAT. A field expedition was made by Tiruneh (2003) to identify the parameters that were missing in the soil map. The hydraulic conductivity, bulk density and the percentages of sand, silt, clay and rock of the soil were some of the parameters identified during the field expedition(Tiruneh B.A, 2004)

The identified and measured parameters were translated into SWAT usable formats and stored in excel files for model input.

For the purposes of the maintaining the scale, the soil map was used for all the scales. This is because it is only the HRU composition that changes for the different scales and not the map itself (Meins, 2013). To connect the shapefile to the measured parameters, the parameter set was incorporated into the SWAT database file and a look-up table made which links the soil id in the shapefile to the corresponding name and properties in the SWAT database (User soils).

3.5. Weather/Climatic Data

Several weather attributes are required in SWAT simulation. The precipitation data, Solar radiation data, temperature records, relative humidity data and wind speed data. The latter two datasets are not required in the case that the Hargreaves method is employed in the determination of the potential evapotranspiration. Rainfall records for several stations within the catchment were acquired from the relevant offices and the rainfall was analysed. The other weather attributes were however not adequate to run the SWAT model since the stations were not measuring them. The lack of these other parameters was however solved by the use of the weather generator within the SWAT model to simulate temperatures and solar radiation. On the same note, due to the insufficiency of relative humidity and wind speed data, for the calculation of parameters for the weather generator, the Penman/Monteith method was adopted for the calculation of PET.

3.5.1.1. Missing Data

The rainfall records for the stations contained some major gaps in the data. These gaps are as a result of the malfunctioning of the rain gauges due to poor maintenance of the stations and vandalism. The rainfall data from the stations, therefore, required significant gap filling to be acceptable by the model. In this case, it was not possible to gap-fill the rainfall time series data due to the huge proportion of the unavailable data (Over 40%) in most stations

3.5.1.2. CHIRPS Data

The use of the Climate Hazards Group Infra-Red Precipitation with station data (CHIRPS) was adopted to solve the problem of missing data. The data is available online via the ISOD toolbox platform in ILWIS. The data was downloaded for the simulation period (2004-2017) for several stations within the catchment. The data was scrutinized for and compared with the available station data to establish the level of BIAS and hence check whether correction would be needed. After a thorough comparison, the Percentage BIAS was found to be low and hence, the Chirps data was not subjected to BIAS correction. The respective input text files were prepared and stored in a folder for the SWAT input.

3.6. Stream Flow Data

The River Malewa catchment has several gauging stations installed for periodic measurements of the flow for management purposes. The gauge stations are manned and managed by WRMA in association with the affiliate WRUAS in the region. The stream flows are measured by reading the staff levels that have been installed in the streams. The water levels were converted into flow volumes by use of the respective rating curves developed for the river section. During my fieldwork, I carried out some gauging exercise on several of the gauging stations to obtain the stream flows. These were not enough for the SWAT simulation. However, I managed to obtain up-to-date flow records for the catchment from the WRMA offices for most of the gauging stations. Conversion of the water levels into flow was done using the rating curves for the various river sections. The station's codes are 2GB which represent the Malewa and wanjohi river, 2GC which represent the Turasha river and 2GD located in the Karati river.
The gauging station characteristics are as in Table 3-4

Table 3-4: Gauging stations in Malewa River geo-information

Station	River	X-Coordinate	Y-Coordinate	Elevation
2GB01	Malewa	210908.0	9938530.8	1951
2GB03	Malewa	221632.3	9973620.2	2366
2GB04	Wanjohi	219808.8	9969175.2	2334
2GB05	Malewa	210688.5	9945446.0	1987
2GB07/08	Malewa	212081.6	9964640.5	2264
2GC04	Turasha	212451.6	9946983.4	2000
2GC05	Kitiri	228295.2	9939060.7	2408

The measurements are made on daily timescales. Conversion of the water levels to discharge is required for input into the model. This conversion was done using rating curves which define the relationship between the streamflow and the water levels. Studies have been done before to establish the rating curves for the various streams in the catchment (Md. Azizul Haque Podder, 1998) with most rating curves failing the accuracy test due to continued erosion and river changing dynamics. Therefore, new rating curves need to be generated by using the measurements of the stream at several points. The water levels are also measured and a fitting function is found for the points. The most used function is derived from the Chezy law for a rectangular cross section of a river. The formula is written as

$Q=C(H-H_0)^n$ if $H>H_0$……..…….*Equation 14*

$Q=0$ if $H \leq H_0$

Where
Q= Streamflow (m^3/s)
H= Measured water depth (m)
Ho = Depth at which water starts flowing (m)
C, n =Coefficients
The rating curves for the different streams as generated by Meins, 2013 were adopted for the conversion of the water levels into flow. The least square method was used as an objective function in optimizing the coefficients of the rating curve.

$\text{Min}\sum_{t=1}^{T}(Q_{obs},t-Q_{calc},t)^2$……..……..*Equation 15*

Where
$Q_{obs,}t$ = Measured discharge at a moment t
$Q_{calc,}t$ = Calculated discharge using the measured water level at time t.
T = Number of observations

To test the goodness of fit for the resultant rating curves, the R^2 was calculated for the stations and the stations with high values of R^2 were as listed in Table 3-5

Table 3-5: Channel constants for the rating curves for the different gauging stations in the watershed

Station	Coefficient a	Coefficient b	Coefficient c
2GB01	28.26	0.00	1.77
2GB03	5.16	0.00	2.23
2GB04	7.9	0.0	1.67
2GB05	7.62	0.29	1.70
2GB08	9.82	0.00	2.52
2GC04	13.55	0.00	2.16
2GC05	4.47	0.00	1.52

Source (Meins, 2013)

4. METHODOLOGY

The approach and methodology adopted in the research was divided into the following stages

- **Pre-fieldwork**- This stage entailed desktop study and literature review of the study area as it pertains the Topic of research. It also helped in identifying the research problem, formulation of the objectives of the research, Identification and collection of available data, Identification of the suitable sites for the placement of the Digital Turbidity Sensors and General preparation for the fieldwork.
- **Fieldwork**- During this phase, Visual confirmation of the LULC was done at the site for any required reclassification, Reading and recording of the Turbidity Sensor readings, Collection of climate data from the various weather stations, Discharge measurements for the Malewa River,
- **Post-fieldwork-** At this stage, the collected data was processed and analyzed. The model input data was organized and uploaded to the model. The model settings which are American by default were adjusted to suit the area of study (Naivasha) and all other settings checked. The model was then run. Sensitivity analysis was conducted to establish the most responsive parameters of the model and determine their effects on the simulation outputs. Calibration of the was done to optimize the model parameters. Finally, the model was validated using the In-situ turbidity measurements and the discharge measurements to access the best of fit between the modeled and the observed parameters. The Nash-Sutcliff efficiency NSE, PBIAS, and R^2 were calculated to determine the model reliability in simulating the sediment yield. Results analysis and conclusions were finally drawn from the results of the model simulation.

The adopted chronology of steps that were undertaken in the study is as summarized in the flow chart in Figure 5

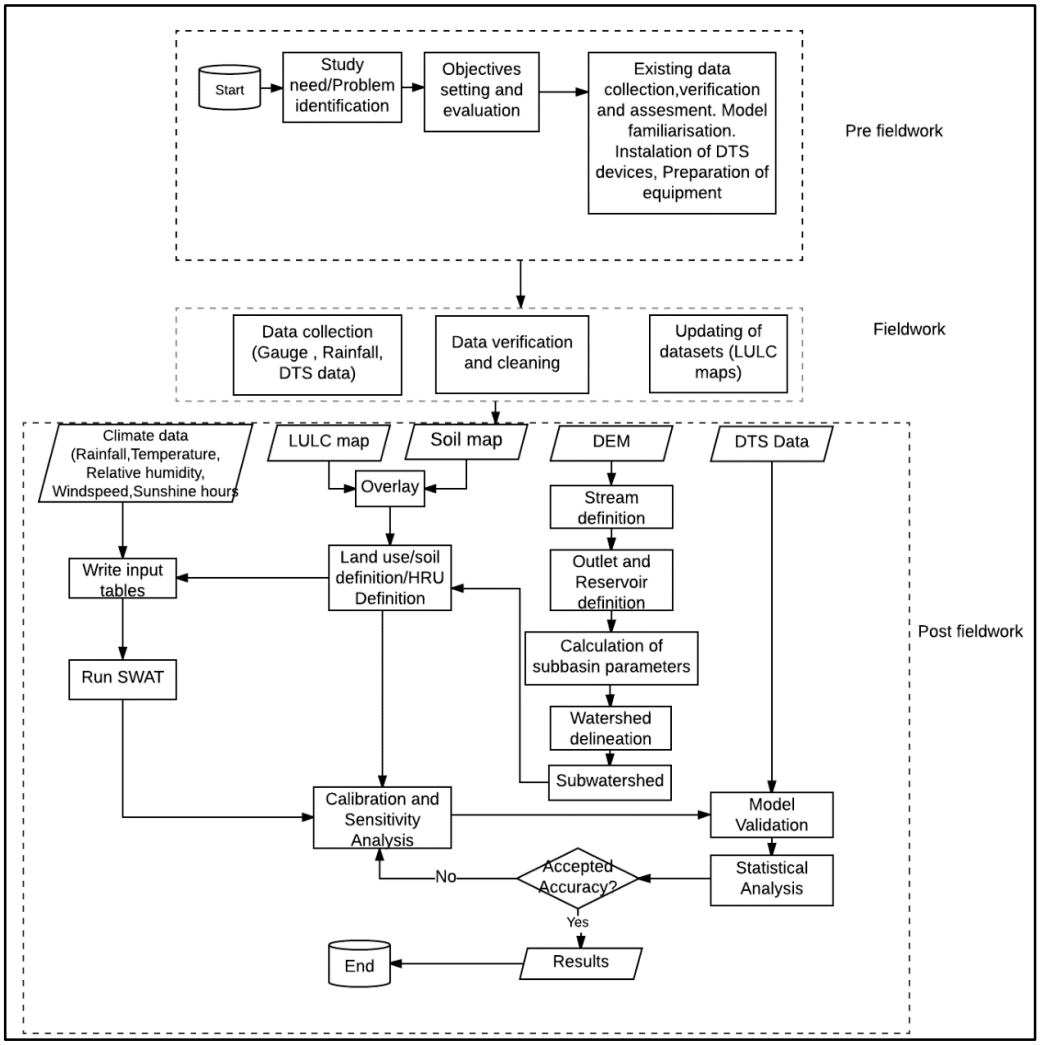

Figure 5: Workflow of the adopted methodology for the simulation

4.1. Model Set Up

The model set up process is a crucial step in making sure that the model has all the requisite inputs for the sediment simulation process. The already prepared data was organized into several stages that are interlinked. The steps are

- Watershed/Basin Delineation
- Land use, Soil characterization, and slope definition
- Climate data definition
- Editing of input files and information
- Running the simulation.

4.1.1. Basin/Watershed Delineation

This step is dictated by the DEM. It provides the required topographical information that would be adopted by the model. The 20m resolution DEM was loaded into the model in a grid format. It was then projected to UTM projection and all properties defined as in Figure 6. The burn in function was used to import the river network for the watershed and therefore create the basin.

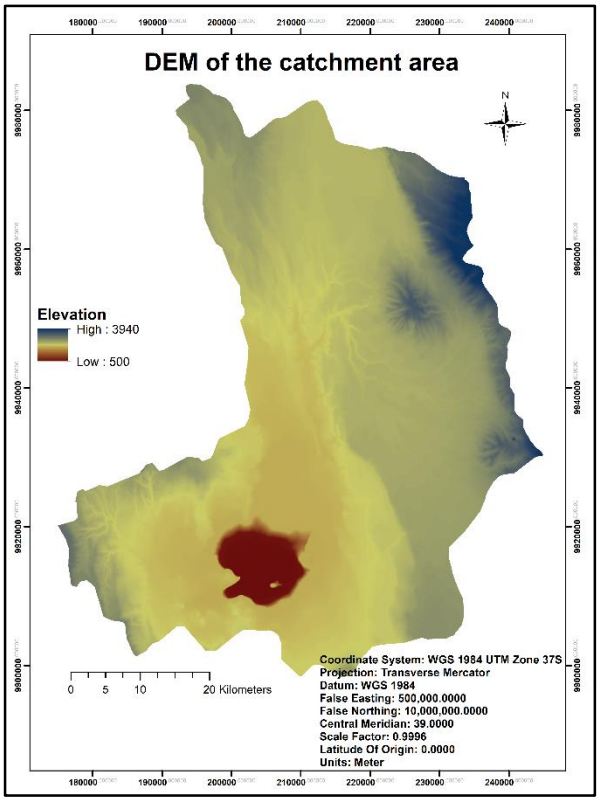

Figure 6: DEM of the L. Naivasha Basin

4.1.2. Outlet definition

Outlet points for the various streams in the watershed were defined and marked. These points would be used in the comparison of the sediment fluxes in the stream system. They would also be used to locate the sediment flux measurement points. The most downstream outlet point was selected so that the sediment flux would be monitored to totality. This point was identified and marked just before the River enters the Lake. The setting of this point provided the needed information for SWAT to delineate the watershed and create the HRUs and sub-basins. The other two outlets were marked at stations 2GB04 and 2GB01.

However, because the Digital turbidity sensor had been installed at the 2GB04 station (Wanjohi), the station was later adopted for the calibration of the sediment fluxes.

4.1.3. Land Use, Soil Parameterization, Slope definition and Overlay

The movement of water in a watershed depends mainly on the combination of the slope, the soil properties and the land use of the watershed. The LULC determine the amount of interception on the rainwater which falls on the basin. At the same time, vegetation cover mainly reduces the amount of erosion that takes place by reducing the force with which the raindrops hit the soil. A reduction of the vegetation cover, therefore, pays a very significant role in the increase of dredging activity in the watershed.

The properties of the soil on the other hand dictate the mobility of the water within the soil profile. The soil porosity, bulk density, texture among other factors influence the storage capacity, infiltration and many other elements of the soil, water interaction during the modeling process(Lukman A.p, 2003).

The slope (General orientation of the subbasin) dictates the direction of flow of the water after it rains. It dictates the speed of flow of water and hence the erosion rates of the soil. It also prescribes the soil type of the area and in extension, the kind of vegetation that grows in an area (Armesto & Martinez, 1978)

The watershed was divided into regions with unique soil and LULC and slope combination to enable the SWAT model to identify the variations in the hydrologic events and evapotranspiration for the various land cover, land use and soils(Neitsch, Arnold, Kiniry, Srinivasan, & Williams, 2002).

4.1.3.1. Land use

The land use map used in the simulation was prepared according to the ground truth as observed during the fieldwork and an earlier map that had been prepared by Tiruneh. The map contains 11 classes that were derived from an earlier version of 18 classes used by (Tiruneh B.A, 2004) in his Thesis

The reclassification of the map was done by using the combine operation in ArcGIS to combine the 2012 land cover map with the newly released Sentinel land cover map. The 2012 land cover map used previously had 16 classes. It was resampled to 20m resolution and then the classes were collapsed and joined with the 10 classes from the Sentinel image. The two maps were projected to the same coordinate system and then combined to attain common classes for all pixel values. The classes were then assigned depending on the dominant LULC to create a new map as shown in Figure 7

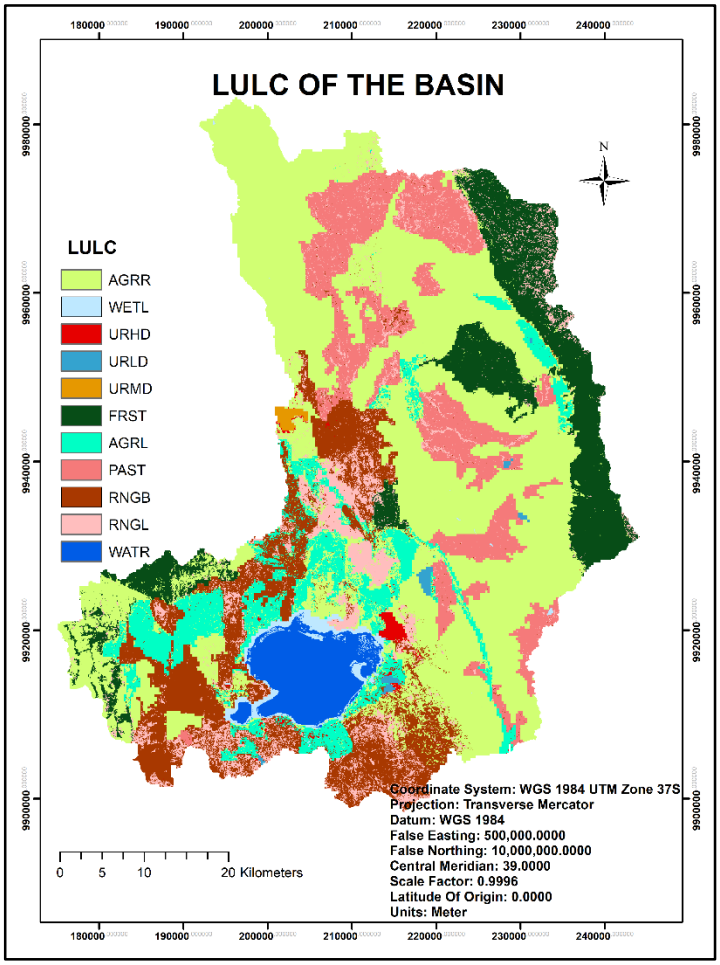

Figure 7: LULC Map of the catchment

The land use map was then uploaded to the SWAT model. The model trimmed the ma to the basin and the respective land use codes listed. The land use SWAT codes were then uploaded as a text file (file.txt) that was used to give the respective codes their land use meaning. Only ten land use classes were existent in the watershed and were used in the model. The classes were as shown in Table 4-1.

Table 4-1: Land use codes for the Model

Value	SWAT LULC Code
1	AGRL
2	WETL
3	URHD
4	URLD
6	FRST
7	AGRR
8	PAST
9	RNGB
10	RNGE
11	WATR

4.1.3.2. Soil

The soils description of the area was mainly clay loam as reported by Tiruneh B.A in his Thesis having done the field soil tests. The soil composition is as summarized in Table 4-2

Table 4-2: Soils compositions in the Basin

Coordinate (UTM)		**Clay(%)**	**Silt(%)**	**Sand(%)**	**Type**
X	Y				
222306	9948922	31	31	38	Clay loam
220183	9930610	63	20	16	Clay
212566	9951038	40	31	29	Clay/Loam
234398	9949936	39	55	6	Silt-Clay-Loam
221093	9930550	27	62	11	Silt-Loam
234431	9947088	62	35	3	Clay
234769	9949590	41	43	16	Silty-Clay
201706	9973046	5	40	6	Silty-Clay-Clay
231553	9953324	52	32	16	Silty-Clay
213811	9972396	51	44	5	Silty-Clay
234759	9949558	43	51	6	Silty-clay
221083	9930450	32	60	7	Silty-Clay-Loam
211244	9910256	17	43	40	Loam
210050	9906318	8	30	62	Sandy-Loam
213298	9917422	22	32	46	Loam

The soil map was loaded into the model, and the various soil classes were identified by the model. The classes that were present in the Malewa catchment area were as shown in Table 4-3

Table 4-3: Percentage coverage of Soils present in the Malewa sub catchment

Soil Name	Area (%)
Ux3	0.9
H9	6.6
L20	20.8
Pi11	5.0
Ux7	15.4
LU2	0.3
L22	2.7
S1	9.0
R1	12.3
F7	4.4
M2	20.4
M9	2.0

The soils distribution in the whole of the Lake Naivasha Basin was as shown in Figure 8 Soil map of the whole of L.Naivasha basiFigure 8 below

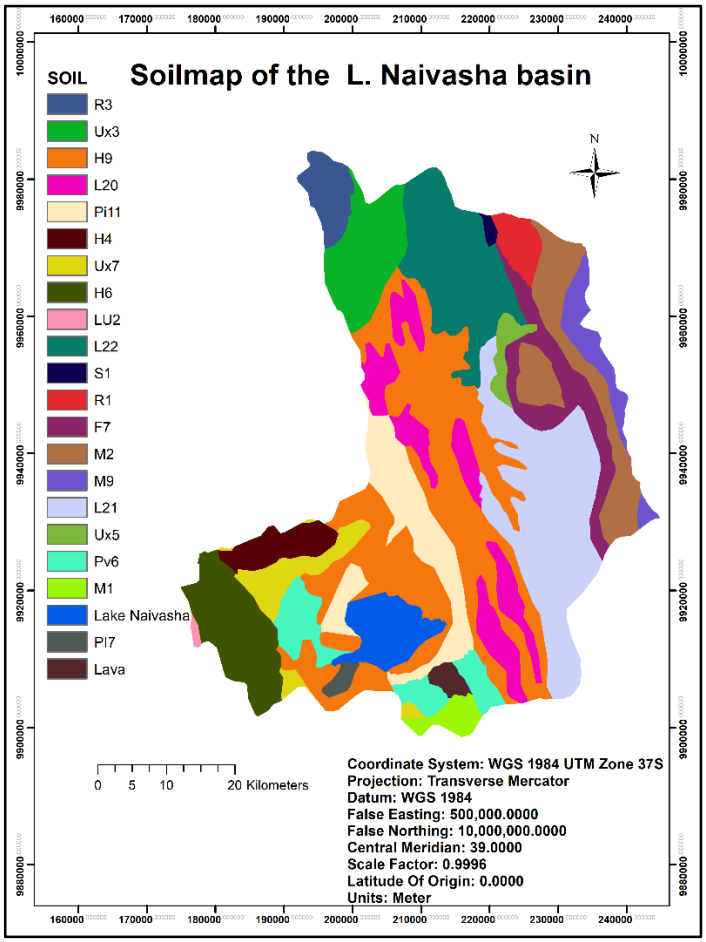

Figure 8 Soil map of the whole of L.Naivasha basin

4.1.4. HRU Definition

The composition of the various HRUs is dictated by the LULC, Soil, and slope that make up the HRU. This is used in the simulation of the hydrological conditions by the model. The model combined the 11 land use classes with the 12 soil classes and the 2% slope to create the HRUs. The sediment load predictions are more accurate If the HRUs consist of the various land use and soil classes in the watershed as these affect its generation. The total runoff is also a determinant of the amount of sediment loadings into the streams. A threshold for the land use, soils and slope were defined to increase the accuracy in the definition of the HRUs. The thresholds were 20%, 10% and 20% for land use, soil and slope respectively.

4.1.5. Climate Data

Due to the big gaps in the rain gauge measured rainfall data and lack of enough gauge data, CHIRPS Satellite rainfall data was used in this simulation. The min/max temperature, Relative humidity, Wind speed and net solar radiation were not fed into the model and thus were simulated using the SWAT inbuilt simulation mechanisms.

Chirps precipitation data for the stations that lie inside the basin were downloaded from the ISOD toolbox in the form of precipitation maps. The station pixel rainfall values were extracted in ILWIS and a comparison made with several neighboring pixels to make sure that the values were not erroneous. The average value for the 10 pixels was taken and applied for the station. Stations that lie within the catchment were identified and their precipitation values used. Rainfall estimates for the period (2004-Sep 2017) were retrieved and used for the simulation.

The stations used were as shown in Table 4-4 below

Table 4-4: Rainfall stations for the CHIRPS precipitation data

Station ID	Station Name	X Coordinate	Y Coordinate	Elevation (Msl)
ST02	North Kinangop Forest Station	236,356.606	9,935,754.941	2617
ST38	North Kinangop Mawingo scheme	223,656.581	9,945,068.293	2403
ST37	Olarangwai farm Naivasha	215,295.731	9,928,134.925	2019
ST09	Naivasha KCC Ltd	209,474.886	9,926,547.422	1900
ST47	Malewa Farmers Coop Society	216,036.565	9,959,990.822	2332
ST46	Wanjohi Chiefs Camp	223,127.413	9,962,530.827	2437
ST29	Geta Forest Station	233,287.433	9,948,349.132	2588
ST67	Laurel	220,058.240	9,969,833.342	2617

4.1.6. Building of Input Tables

After the gauge location file and the precipitation records are uploaded to the model and all settings defined, , the next step was to write the input tables. This process is meant to provide tables where the model output would be recorded when the model is run. The process is however repeated whenever one needs to reset the model to the default settings for a new run (During optimization of parameters)

4.1.7. Setting the model for a run

The model was set ready to be run after writing the input tables. The simulation was run for a calibration period of 7 years (2004-2010) with a 3 years warm up period (2004-2007) and a validation period of 3 years (2011-2013) at monthly time steps. However, several other settings had to be specified before the run as listed in Table 4-5

Table 4-5: Model settings

Component	Setting
Runoff generation method	CN method
Distribution of rainfall	Skewed Normal
Output time step	Monthly
Channel water routing	Variable-Storage method
PET	Penman/Monteith

4.2. Sensitivity analysis

Usually, the default run in SWAT using the default parameters does not give satisfactory results in relation to the model Inputs. This calls for the model to be calibrated to achieve parameter optimization for a better simulation. The calibration involves adjustment of parameters until the simulation results agree with the observed data. The identification of which parameters to manipulate is the sensitivity analysis. It aims at reducing the amount of time consumed in trying to adjust the parameters so that one does not waste time adjusting non responsive parameters.

The parameters that were identified in previous studies to be sensitive were 21 (Dutta & Sen, 2017). These included 15 for discharge and 6 for the sediment loads. The parameters were ranked by Dutta & Sen according to their sensitivity as in Table 4-6

Table 4-6: Sensitive parameters

Parameter	Range	Rank
CN2	35-98	1
SURLAG	0.05-24	2
CH_N	-0.01-0.3	3
ESCO	0.01-1	4
SLSUBBSN	10-150	5
GWQMN	0-5000	6
EPCO	0.01-1	7
GW_REVAP	0.02-2	8
SOL_AWC	0.5-1	9
SOL_ALB	0-0.25	10
GW_DELAY(DAYS)	0-500	11
ALPHA_BF(DAYS)	0.1-0.3	12
REVAPMN(MM)	0-500	13
SOL_K(MM/H)	0-2000	14
TLAPS(^{O}C/KM)	-10-10	15

For sediment load simulation, a number of parameters were found to be sensitive and are as in Table 4-7 below

Table 4-7: Sediment simulation sensitive parameters

Parameter	Range	Rank
USLE_P	0-1	1
USCLE_C	0.001-0.5	2
SPCON	0.0001-0.01	3
CH_COV	-0.001-0.6	4
CH_EROD	-0.05-0.6	5
SPEXP	1-1.5	6

4.3. Model calibration

Calibration is the adjustment of parameters until a good match between the measured real values and simulated values is obtained. This process could be very challenging owing to the numerous parameters involved and the uncertainties involved (Abbaspour et al., 2015). The uncertainties are as a result of errors in measurements, data filling, assumptions, processes occurring in the model but unknown to the modeler or cannot be accounted for due to data limitations. These calibration uncertainties can be overcome by using an appropriate calibration method (Uniyal, Jha, & Verma, 2015).
The model was first calibrated using the SWATCUP software using the SUFI-2 Algorithm. However, after several attempts to use the SWATCUP calibration software, the results were not forthcoming. Studies have been done to prove this point. They concluded that manual calibration outperforms the automatic algorithms in the simulation of the magnitude of flows and that the automatic calibration is not able to maintain the mass balance(Arnold et al., 2012.). Based on this reasoning, the manual calibration procedure (LH-OFAT) was adopted. This enables the user to choose the parameters to manipulate while observing the parameters change effects on the results of the model simulation. The method was successful and reasonable results were acquired.

4.4. Model validation

This was done after the calibration process to get the optimum parameters. Validation was performed using runoff data for the period 2011-2013 without further adjustments of the parameters. This was aimed at giving the best simulation results for the two chosen periods. This process is however dependent on the availability of observed data. Different time periods could be used for validation provided that the parameters are not adjusted during the process. The model could be run severally to get the optimal values of the input parameters. The results were then evaluated for correctness using the suitable model performance statistical measures as listed below

- The Pearsons correlation coefficient (r) Which is a measure of the degree of correlation between the observed and the simulated values and ranges from -1 to 1. R=0 shows no correlation while the values -1 and 1 indicate a negative and positive correlation respectively.

$$R = \frac{\sum_{i=1}^{n}(Y_i^{obs} - y_{mean}^{obs})(y_i^{sim} - y_{mean}^{sim})}{\sqrt{\sum_{i=1}^{n}(y_i^{obs} - y_{mean}^{obs})^2}.\sqrt{\sum_{i=1}^{n}(y_i^{sim} - y_{mean}^{sim})^2}} \quad \text{.....Equation 16}$$

Where

Y_i^{Obs} = ith value of observed data

Y_i^{sim} = ith value of simulated data,

Y_{mean}^{Obs} mean is mean value of the observed data

Y_{mean}^{Sim} = Mean value of the observed data

N= Number of observations.

- Standard deviation of Observations Ratio (RSR) which evaluates the ratio of the(RMSE) and the standard deviation of the observed data

$$RSR = \frac{RMSE}{STDEV_{Obs}} = \frac{\sqrt{\sum_{i=1}^{n}(y_i^{Obs} - y_i^{sim})2}}{\sqrt{\sum_{i=1}^{n}(y_i^{Obs} - y_{mean}^{Obs})2}} \quad \text{...Equation 17}$$

RSR has a range from 0 to positive values. The lower the RSR, the better the simulation and vice versa. The RSR in cooperates the error index benefits of error index that includes a standardisation factor hence can apply to many constituents. resulting statistic values can be applied to various constituents as it incorporates the advantages of an error index statistics by including a scaling or normalization factor (Moriasi et al. 2007)

- The Nash-Sutcliffe efficiency (NSE) which is an arithmetical indicator of the relative degree of the variance of the observed data compared to the variance of the measured data (Nash and Sutcliffe 1970)

$$NSE = 1 - \frac{\sum_{i=1}^{n}\left(y_i^{Obs} - y_i^{sim}\right)2}{\sum_{i=1}^{n}(y_i^{Obs} - y_{mean}^{Obs})2} \quad \text{...Equation 18}$$

The range of the NSE is from - ∞ to 1. Values of the NSE from 0 to 1 show a tolerable level of performance and values below zero are not acceptable.

It is worth mentioning the assumption made that there was no change of land use and the extent of land during the entire simulation period.

- PBIAS which is a measure of the average likelihood of the simulated data to deviate from the observed data (Moriasi et al., 2007) The values of PBIAS can range from positive to negative values with low magnitude values meaning that the model modelled results are in agreement with the measured values. A large PBIAS value indicates an underestimation by the model while a lower value of the PBIAS means that the model overestimates the real scenario

$$PBIAS = \frac{\sum_{i=1}^{n}(y_i^{obs} - y_i^{sim}) * 100}{\sum_{i=1}^{n}(y_i^{obs})} \quad \text{....Equation 19}$$

Where PBIAS is the abnormality of the simulated data equated to a fraction of the observed data

5. RESULTS ANALYSIS AND DISCUSSION

5.1. Results analysis

5.1.1. Model Sensitivity Analysis

The sensitivity analysis was performed in two phases. The first involved the analysis of the simulated discharge parameters sensitivity. It was followed by the sediment production responsible parameters. The first set was tested for the changes in the parameters that altered the water cycle. The LH-OFAT (Latin hypercube one factor at a time) method was adopted. A total of 15 factors identified in literature as the most sensitive were adjusted carefully and the resulting changes in the simulation values noted.

The parameters were classified into processes with which they are associated.

- Actual Evapotranspiration determination parameters (EPCO, ESCO, BLAI, CANMAX)
- Soil property parameters (SOL_Z, SOL_AWC, SOL_ALB, SOL_K, SOL_BD)
- Groundwater parameters (ALPHA_BF, GWQNM, REVAPMN, GW_DELAY)
- The soil surface Runoff (CN2, SLOPE, SLSUBSN, SURLAG)
- The channel processes parameters (CH_2, CH_N2)
- Crop parameters (BIOMIX, TLAPS)

Not all the above parameters were used in the sensitivity analysis as some of them were not sensitive to a noticeable extend. The outcome of the sensitivity analysis were as shown in Table 5-1

Table 5-1: Sensitivity of the model parameters

Parameter	**% Variation**	**% Change In Q (Cms)**
CN	±25	±21
ESCO	±25	±3.2
CH_N	±25	±0.04
SURLAG	±25	±0.05
SLSUBBSN	±25	±0.5
GWQMN	±25	±11.4
GW_REVAP	±25	±0.7
EPCO	±25	±1.36
SOL_AWC (MMH²O/MM SOIL)	±25	±0.2
SOL_ALB	±25	±0.1
GW_DELAY (DAYS)	±25	±0.1
ALPHA_BF (DAYS)	±25	±6.4
REVAPMN (MM)	±25	±0.44
SOL_K (MM/H)	±25	±0.2
TLAPS (°C/KM)	±25	0

The sediment load simulation parameters were also evaluated for their sensitivity, and the results were tabulated as shown in Table 5-2

Table 5-2: Sediment parameters sensitivity Analysis

Parameter	**% Variation**	**%Change in Sediment yield(Tonnes)**
USLE_P	±25	±40
SPCON	±25	±28.3
CH_COV	±25	±0.02
CH_EROD	±25	±48
SPEXP	±25	±40.6
USLE_C	±25	±12.4

The significance of the above parameters is as discussed below:
The surface runoff lag coefficient (SURLAG) is responsible for the control of the fraction of the total water that enters the reach in a day. The Manning's friction coefficient (n) affects the amount of peak discharge in the channel as it affects the time that is taken by concentration in the channel tributaries. ESCO and EPCO values are responsible for the amount of water that evaporates from the soil and that is taken up by plants respectively. The SLSUBBSN is the slope length and is responsible for adjustment of lateral flow. The flow of water through the soil is regulated by the hydraulic coefficient parameter (SOL_K) and GWQMN is the maximum depth of water that is needed for return flow to occur. GW_REVAP coefficient controls the movement of water from the shallow aquifer to the lower horizon of the unsaturated zone. The soil Albedo (SOL_ALB) controls the reflection of the amount of solar radiation by the water.

The groundwater delay period that is responsible for controlling the amount of time that the water takes to move from the vadose region to the deeper shallow aquifer is controlled by the GW_DELAY Parameter. The ALPHA_BF factor is responsible for making steeper or otherwise the discharge recession curve to correctly depict the drainage tendencies of the watershed. REVAPMN controls the threshold of water in the shallow aquifer to the unsaturated region by controlling the percolation of the water. The soil water available content (SOL_AWC) parameter controls the percolation of water through the soil profile. The temperature lapse rate (TLAPS) is an indicator of the variation of temperature within the watershed. An increase and decrease of the parameter indicates an increase and decrease in elevation respectively.

The support practice factor in the USLE equation (USLE_P) can be optimized depending on the LULC of the area. This parameter indicates the human interaction with the land and the crop management processes that take place in the catchment. The USLE_C factor controls the erosion process and the sediment forming process. SPCON and SPEXP are the parameters that are used in calculating the linear sediment that is restrained in channel sediment routing and exponent value for determining the sediment reins trained in the channel sediment routing respectively. The parameters for channel cover and erodibility (CH_COV and CH_EROD) influence the amount of sediment production due to soil loss from the channels. (Dutta & Sen, 2017). All these parameters were used to adjust the model and dictate the loads of sediment from the channels to the main streams. Their influence on the runoff, sediment and nutrient loss from the soil was therefore controlled during calibration

5.1.2. Model Hydrological Calibration

The calibration of was done manually by adjusting the various parameters of the model to achieve the optimum simulation values. The hydrological calibration was performed using the discharge data for the time period 2007-2010 and validated for the timespan 2011-2013 at the 2GB05 outlet. The parameters that were most sensitive in the calibration process were adjusted as in Table 5-3

Table 5-3: Hydrological calibration values

Parameter	Range	Calibration Value
CN2.mgt	35-98	66-82 (Depends on LULC)
SURLAG. bsn	0.05-24	4
CH_N. rte	-0.01-0.3	0.3
ESCO. hru	0.01-1	0.5
SLSUBBSN(m).hru	10-150	50(Varies with sub basin)
GWQMN (mm).gw	0-5000	195
EPCO. hru	0.01-1	0.6
GW_REVAP.gw	0.02-0.2	0.5 (Varies with LULC)
SOL_AWC (mm H^2O/mm soil).sol	0.5-1	0.3(Varies with soil)
SOL_ALB. sol	0-0.25	0.02
GW_DELAY (Days).gw	0-500	100
ALPHA BF (Days).gw	0.1-0.3	0.2
REVAPMN (mm).gw	0-500	200
SOL_K (mm/h).sol	0-2000	2.75(Varies with soil)
TLAPS ^{O}C/km).sub	-10-10	0

The resultant hydrological simulation was then plotted against the observed flow values to ascertain the performance of the model and determine the efficiency of the model in simulating the hydrological scenarios in the watershed. Manual techniques for evaluating the performance of the model were mostly based on the resultant hydrograph analysis. The monthly observed values of discharge at the outlet 2GB05 were plotted against the simulated discharge values. The monthly simulations were chosen as they give a clear visual impression of the simulation. The resultant plots are as shown in Figure 9 and Figure 10 for calibration and validation respectively.

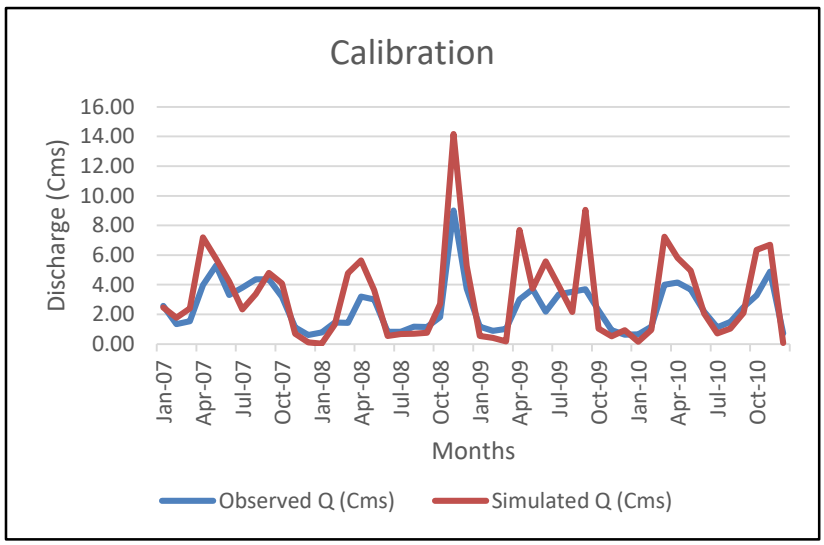

NSE=0.65
RMSE=1.83
PBIAS=-0.216
RSR=1.120

Figure 9: Calibration plot

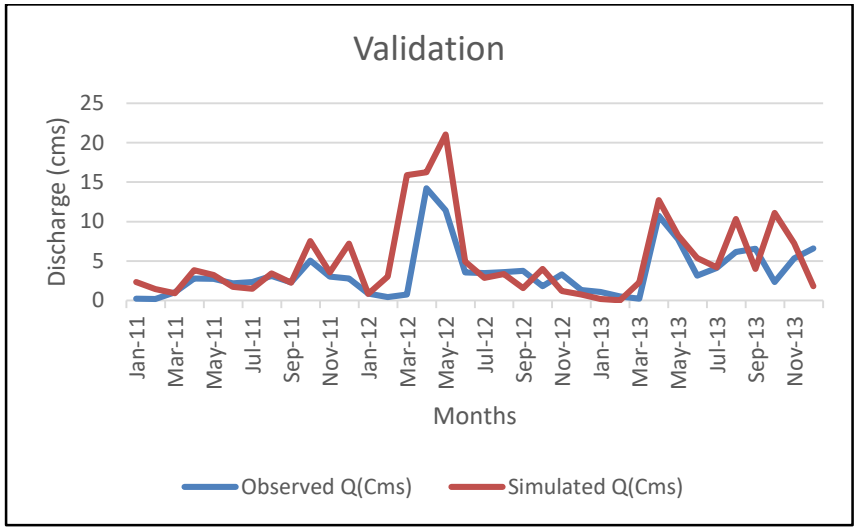

NSE=0.4
RMSE=3.82
PBIAS=-0.39
RSR=1.19

Figure 10: Validation Plot

The respective scatter plots were also generated to give a clear statistical impression of the R^2 value of the above calibration and validation hydrographs

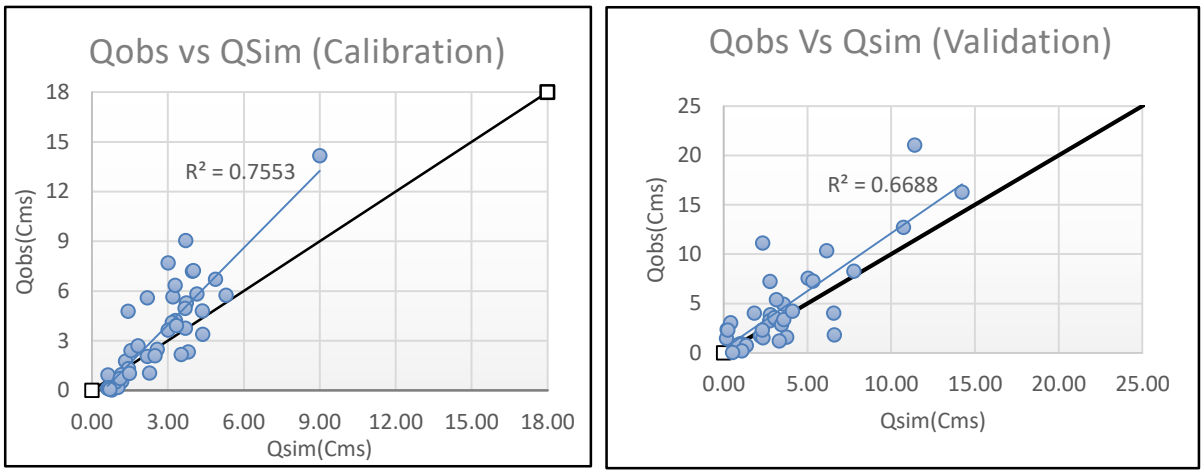

Figure 11: Calibration and Validation results for station 2GB05

The Precipitation for the entire period (Calibration and Validation) was also plotted against the discharge to enable easier comparison and interpretation of the results above. The resulting graph was as in Figure 12

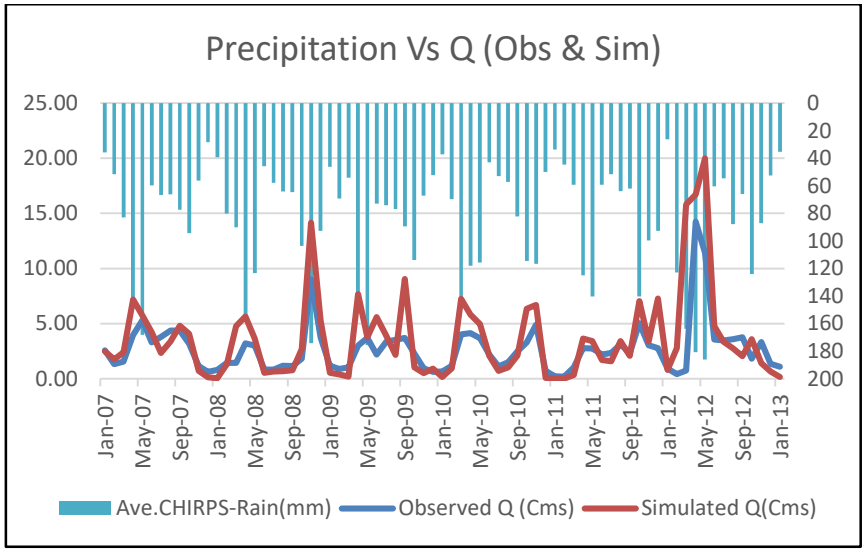

Figure 12: Precipitation vs Observed and simulated discharge

5.1.3. Model Sediment Calibration

After hydrological calibration, the model was further calibrated for sediments.
The calibration period covered five months for which the Digital Turbidity Sensor was operational. The DTS was installed in April 2017. It records turbidity measurements in quarter-hour intervals. A conversion of the TDS data (NTU) to TSS was done by relating the two using Lab measurements of Insitu grab samples acquired during the fieldwork expedition at the 2GB04 Gauging station. The measurements were recorded as in Table 5-4

Table 5-4: Insitu Turbidity and TSS measurements

Date	Turbidity (NTU)	TSS (Mg/L)
6/4/2017	6.32	5.17
	4.87	5.46
18/4/2017	16.45	9.23
	15.92	8.79
20/4/2017	12.75	6.66
	14.34	7.63
	11.51	6.06
25/4/2017	9.41	5.36
	9.14	5.31
	9.80	5.46
28/4/2017	11.38	6.00
	9.28	5.34
	10.79	5.77
	9.53	5.39
	10.71	5.74
	9.41	5.36
	11.21	5.93

	9.26	5.33
	11.08	5.88
	9.63	5.42
	11.97	6.26
	9.89	5.49
5/5/2017	83.82	69.00
	104.61	72.00

A linear relationship between the two parameters was established and was found to be of the form

TSS(Y)=0.7566TDS(X)-1.9194……..……*Equation 20*

Using the equation, the TDS (NTU) measured values were converted to TSS (mg/l) which made it easy to convert it to the sediment loads (Tonnes) by using the discharge data of the same station. The resultant monthly sediment loads were compared with the model simulated sediment loading for the same station (Sub-basin) to establish a good correlation. The model was calibrated for sediments until the relationship was acceptable. The parameters identified as the most sensitive by (Benaman, Shoemaker, & Ripley, 2016) were: USLE_P, USLE_C, SPCON, CH_COV, CH_EROD, and SPEXP. These factors were adjusted until a satisfactory match was found between the observed and simulated values. The results of the calibration were as in Table 5-5 below

Table 5-5: Sediment calibration values

Parameter	**Range**	**Calibrated Value**
USCLE_P. mgt	0-1	0.02
USCLE_C. crp	0.001-0.5	0.002 (Varies with crop)
SPCON. bsn	0.0001-0.01	0.0005
CH_COV. rte	-0.001-1	0.3
CH_EROD. rte	-0.05-0.6	0.6
SPEXP. bsn	1-1.5	0.9

The monthly simulation results for the sediments were plotted against the observed measurements, and the resultant plot was as in Figure 13.

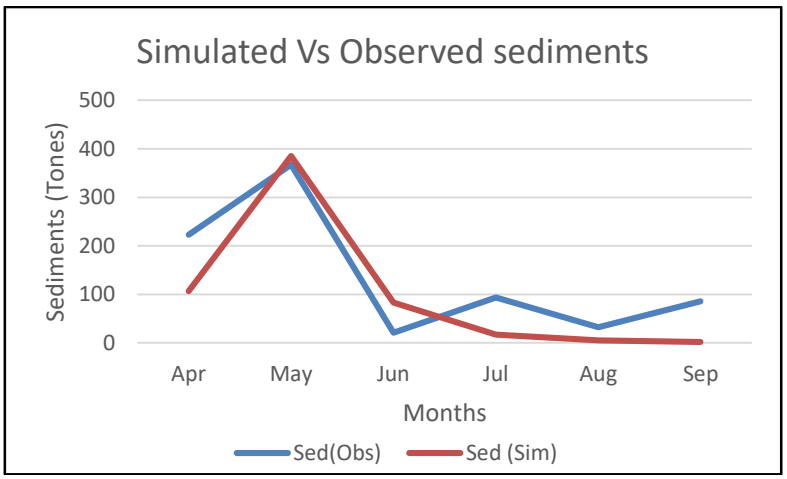

RMSE= 72.074
PBIAS=0.2705
NSE=0.651
RSR= 0.591

Figure 13: Observed vs. measured sediments at the 2GB04

A plot of the Average daily precipitation and the observed sediment at the 2GB04 station was made to visualize how the relationship between the two. The result was as in Figure 14

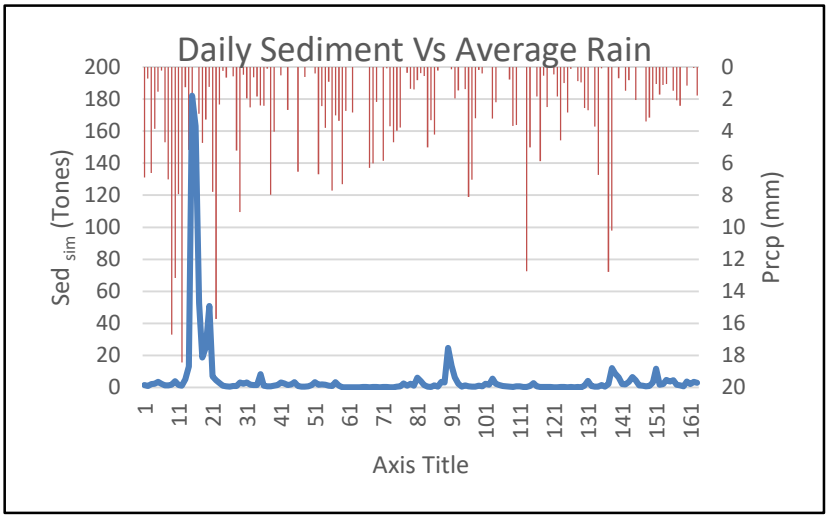

Figure 14: Average rain vs produced sediment at the 2GB04 station

As illustrated by Figure 14, the observed sediment produced from the sub-basins was at its maximum during the first 25 days. These days coincide with the wet season in the area (April-May) during which there was rainfall. As expected, the sediments in the river channels increased due to the increased discharge. The rain decreased from late May, and so did the observed sediment. Occasional small storms are observed in July and around Sep which may explain the reason for the slight rise in the observed sediments in the river channel at these particular times of the simulation.

5.2. Discussion of results

5.2.1. Evaluation of Runoff simulation

The values of the observed and the model simulated monthly discharge for the calibration period (2007-2010) as shown in Figure displayed a satisfactory statistical agreement by having acceptable values of R^2=0.7553, NSE=0.625, RMSE=1.83, PBIAS=0.216 and RSR=1.12**.** However, the model tended to overestimate the runoff over most of calibration period. Only in few instances did the observed runoff overshoot the simulated flow (June-Aug 2007, July-Sep 2008, Jan-March 2009 and June-Aug 2010). These are periods that mark the dry periods in the Naivasha Basin. Therefore, it can be argued that the model has a tendency to overestimate runoff during the wet season and underestimates it during periods of reduced precipitation. The rainfall peaks were also clearly simulated by the model indicating the rainy seasons.

The calibrated model was then simulated for the period 2011 -2013 to validate the model. The plots as shown in Figure 10 show an agreement with the calibration results with the model overestimating runoff in the wet seasons and underestimating it in the dry season. The statistical evaluation measures of the model were also acceptable (R^2**=**0.6688, NSE=0.4, RMSE= 3.82, PBIAS=- -0.39 and RSR= 1.19)

The reason as to why the dry seasons are underestimated by the model could be because the curve number method is not able to generate runoff accurately during prolonged dry periods even though there are independent rainfall events during that period (Qiu, Zheng, & Yin, 2012). These events influence the observed runoff while the model does not simulate any significant amounts of runoff. The SCS-CN method used determines the runoff in a day as a result of the sum of the individual storms during a day.

5.2.2. Evaluation of Sediment Simulation

The simulation of the Sediment production and transportation in the 2GB04 gauging station showed that most sediment is produced during events of high discharge. The calibration of the model for sediments was done for 5 months from April 2017 to Sep 2017 and captured at least the wet and dry season in the area. The simulation results plotted against the observed sediment loads confirm that there was more sediment production in April- June period with the maximum (peak) sediment production being in May (385.2 Tones) and receding from June onwards to a low of 1.928 Tones in Sep (Figure 13). The sediment production implies a declining trend onwards.

On the other hand, the Turbidity measurements by the DTS show an agreement with the model simulation trend for the first 4 months(April-July) with the maximum turbidity of 367 Tones being produced in May and the production declining through June.

A worth noting trend is however experienced from June onwards when the observed sediment amounts begin to rise. This is a peculiar trend as the area is known to be dry during this period and thus the production of sediment is not expected to be high as the rates of erosion from the basin are low. A possible explanation for the trend would be the occurrence of occasional sporadic rainfall events in the months of July and Sep which give rise to the higher amounts of sediment recorded in the 2GB04 gauging station. The model has a demerit in that it is not capable of detecting discharge (And in association sediments) produced by single storms in a day. It is more accurate in predicting sediments produced by a series of continuous rainfall events. Generally, the model tends to underestimate the sediment production for most of the simulation period except for the period May to mid-June when the simulation of sediments is higher than the observed measurements.

The comparison between the model simulated sediment load and the observed loads was tested with the various statistical measures to evaluate how good the performance of the model was. The values of NSE (0.651) and R^2 0.7866 showed that the model results were acceptable. Other statistical measures that were evaluated were the PBIAS (0.2705) and the Observed standard deviation ratio RSR (0.591) which were all within the recommended ranges.

The simulation of the sediment load depends on several factors in the watershed. These factors could be the physiographical, the contribution of the said watersheds to the stream flow that travels to the outlet, the quantity of the highest rate of runoff, The intensity of precipitation and concentration of the sediment(Dutta & Sen, 2017).

5.2.3. Sediment Production per Subbasin

The SWAT Model produces the sediment results per sub-basin which makes it possible to analyze it at the sub-basin level. The total production of the sediments per sub-basin was analysed and plotted to establish which subbasins produced more sediment and therefore inform the drawing of conclusions pertaining the same. Various statistics for the sediments generated for the four months were calculated and tabulated as in the Table 5-6

Table 5-6 : Sediment production in each subbasin

Subbasin	Subbasin Area (Ha)	Representative %	Total Sediment produced (Tones)	Sediment production rate (Tons/Ha)
1	6286	0.68	350.086	0.056
2	18110	1.96	432.232	0.024
3	16580	1.79	599.29	0.036
4	37160	4.02	709.521	0.019
5	9284	1.00	219.5216	0.024
6	7761	0.84	138.615363	0.018
7	46680	5.06	2202.081	0.047
8	12580	1.36	241.5164	0.019
9	58860	6.37	4534.5	0.077
10	6301	0.68	334.571	0.053
11	56710	6.14	2120.2	0.037
12	71950	7.79	1118.59	0.016
13	73220	7.93	8115.4	0.111
14	71490	7.74	11779.2	0.165
15	43980	4.76	6944.4	0.158
16	12660	1.37	1295.494	0.102
17	145600	15.77	5382.7	0.037
18	17070	1.84	2810.5	0.165
19	26060	2.82	2109.4	0.081
20	12520	1.35	1909.2	0.152
21	10890	1.18	233.5852	0.021
22	161400	17.48	13953.9	0.086
Totals	**923152**	**100**	**67534.50356**	**0.073**

The production of sediment was found to be more dependent on the amount of rainfall and the geographical characteristics of the area. It was also observed that the area of the subbasin also contributes to the amount of sediment produced with the sub-basins with the bigger area producing relatively larger amounts of sediment as compared to the smaller sub-basins. The comparison was plotted as in Figure 15

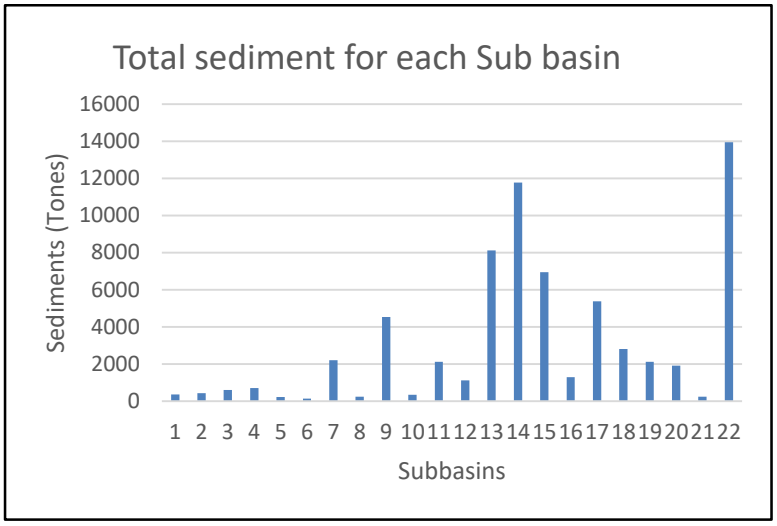

Figure 15: Total sediment production per sub basin

Figure 15 shows that there is more sediment production in sub-basins 13, 14,15 and 22 whose areas represent 7.93, 7.74,4.7 and17.48% of the total area of the catchment respectively.

5.2.4. Sediment Production Rates per Sub-basin

The different sub-basins in the catchment experienced different amounts of precipitation during the simulation period. The SWAT model uses the Thiessen polygon method to allocate the nearest station rainfall to a sub-basin. This could lead to different amounts of sediments being produced in each sub-basin. However, the variation of rainfall in the catchment was <5% thus cannot be attributed to the considerable differences in sediment production in the sub-basins. The average monthly sediment production rates (Figure 16) per sub-basin show that sub-basins 14,15, 18 and 20 have the highest rates of sediment production. Sub-basins 4, 6, 8 and 12 have the lowest sediment production ratios

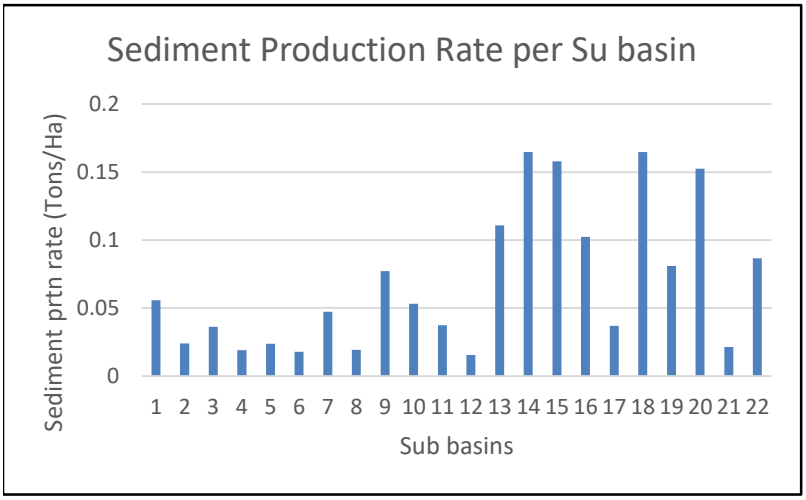

Figure 16: Sediment production rates per sub basin

The causes of the various results for the sediment production fluxes for the subbasins was investigated to ascertain the various factors other than the precipitation amounts and geographical factors that could influence the amount of sediment production rate in each sub-basin. The basins with the lowest and highest sediment production rates were investigated. A threshold was defined to classify the sediment production rates into Three Categories of High, Medium and low production as below:

- >0.10Tons/Ha= High
- >0.050<0.10Tons/Ha= Medium
- <0.05Tons/Ha=Low

A map representing the scenarios was also made. The result was as shown in Figure 17

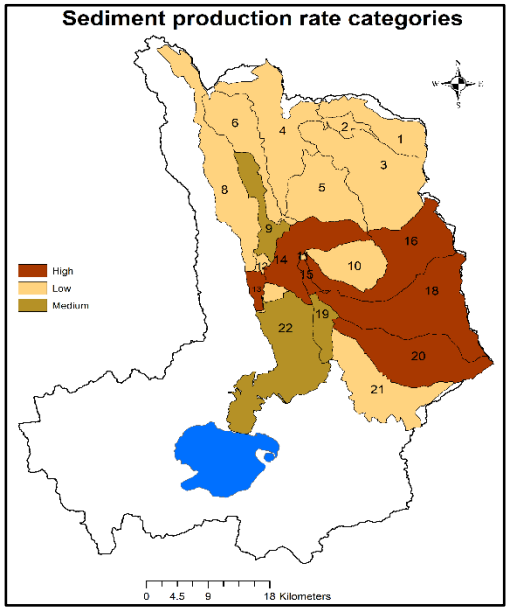

Figure 17: Sediment production rate categories in the basin

The sub-basins with the lowest and the highest production rates were also investigated to identify the factors leading to their sediment production.The findings were tabulated as in Table 5-7 and Table 5-8 respectively

Table 5-7: Sub basins with least sediment production rates

Sub basin	HRU	LULC	Soils	Slope	CN
4	22	AGRL	Ux7	0-5	77
	23	PAST	Ux7	0-5	69
6	32	AGRL	H9	0-5	83
	33	AGRL	H9	5-999	83
	34	PAST	H9	0-5	79
	35	PAST	H9	5-999	79
	36	PAST	L20	0-5	79
	37	PAST	L20	5-999	79
	38	PAST	Ux7	5-999	69
	39	PAST	Ux7	0-5	69

8	46	AGRL	H9	5-999	83
	47	AGRL	H9	0-5	83
	48	AGRL	L20	0-5	83
	49	AGRL	L20	5-999	83
	50	PAST	L20	0-5	79
	51	PAST	L20	5-999	79
	52	PAST	Pi11	0-5	69
	53	PAST	Pi11	5-999	69
12	72	AGRL	L20	5-999	83
	73	AGRL	L20	0-5	83
	74	PAST	L20	0-5	79
	75	RNGB	L20	5-999	74
	76	RNGB	L20	0-5	74

Table 5-8: Su basins with highest sediment production rates

Sub-basin	**HRU**	**LULC**	**Soils**	**Slope**	**CN**
14	83	AGRL	L20	0-5	83
	84	AGRL	L20	5-999	83
	85	FRST	M9	5-999	73
	86	FRST	R1	5-999	73
	87	FRST	S1	5-999	73
15	88	AGRL	L20	5-999	83
	89	AGRL	L20	0-5	83
	90	PAST	L20	0-5	79
	91	PAST	L20	5-999	79
18	108	AGRL	M2	5-999	83
	109	AGRL	M2	0-5	83
	110	FRST	R1	5-999	73
	111	FRST	S1	5-999	73
	112	PAST	L20	5-999	79
	113	PAST	L20	0-5	79
	114	PAST	M2	5-999	79
	115	PAST	M2	0-5	79
20	119	AGRL	M2	0-5	83
	120	AGRL	M2	5-999	83
	121	FRST	R1	5-999	73
	122	PAST	M2	0-5	79

From these tables, it was discovered that the Soils H9, Pi11 and Ux7 (Mostly silty clay) were not easily erodible and thus produced the less sediment compared to the rest. This is due to the soils low erodibility USLE_K factors (0.2, 0.3 and 0.25). The average slope of the sub-basins with the least sedimentation rates was also found to be low (65% of total HRUs in those sub-basins) This confirms the significance of slope in sediment production in the basin. A gentle slope encourages settling of the sediments in the river channels and hence reduction in the transportation power of the water and hence less amounts transported. It can also be observed that the presence of pastures is a major inhibiting factor to sediment generation. This can be attributed to the fact that the prevalence of grasses and shrubs as landcover slows down the water flowing

in the reaches before it gets to the channels. The reduced speeds inhibit erosion and thus lower sediment production. The roots of the pastures (Mostly grasses) also hold the soil particles together creating a stronger bond in the soil that the water cannot break easily as it passes. This, in the end, reduces the amounts of sediments generated in the sub-basins.

On the other hand, sub-basins that experienced high sedimentation rates were found to have specific common soil types (R1, M2, L20 and S1). However, the high rates of sediment production in these sub-basins can be attributed to the predominantly high slopes (5-999) in addition to the soil types. All categories of land use HRUs with steep slopes are found to have high sediment production rates irrespective of the soil type as shown in Table 5-8. The slope contributes to high rates of soil detachment by accelerating the runoff in the channels. Accelerated flow of runoff has increased energy and thus can easily carry away the soil particles resulting in the increase in the suspended sediment. The soils properties (Texture) could also be contributing factors to the production of the sediments. The soils in these sub-basins are mainly clay and clay loam which have a fine texture. The ease of erosion of fine-textured soils is higher than coarse-textured soils. This leads to more sediment production in these sub-basins.
The remaining sub-basins in the Naivasha Basin (1, 2, 3, 5, 7, 9, 10, 11, 13, 16, 17, 19, 21,22) have relatively low sediment yield rates. This is attributed to a variety of factors existent in those basins. The factors include: The soil properties, slope, vegetation cover, land management activities by humans among other factors. The sediment production in the watershed was also represented in a map
Further, the relationship between the amount of precipitation received in each sub-basin and the sediment production rates was investigated to establish the role of rainfall in the sediment production. The Average yearly precipitation in each sub-basin was calculated for the various rainfall stations in the basin. These were then used to make a rainfall distribution map which was used in comparison with the sediment production map created for the 22 sub-basins. The maps are as shown in Figure 18

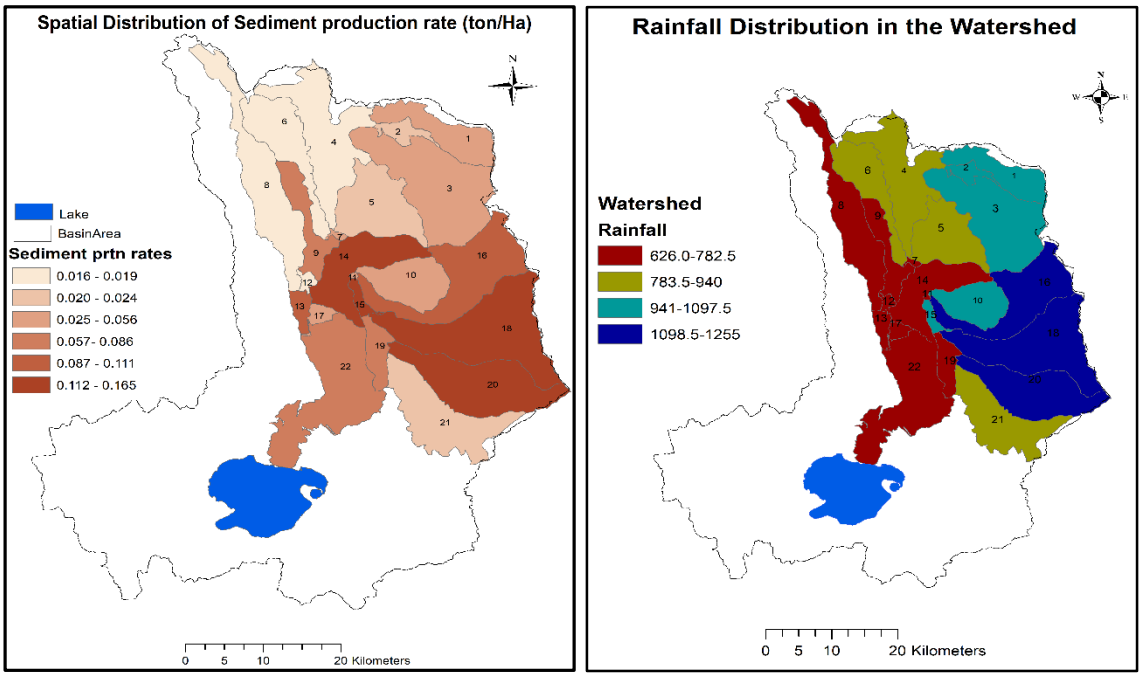

Figure 18: Sediment production and precipitation maps for the R. Malewa basin

Maps for the slope and land use were also made to make it easier to compare the sediment production with the different scenarios. The maps are as shown in Figure 19

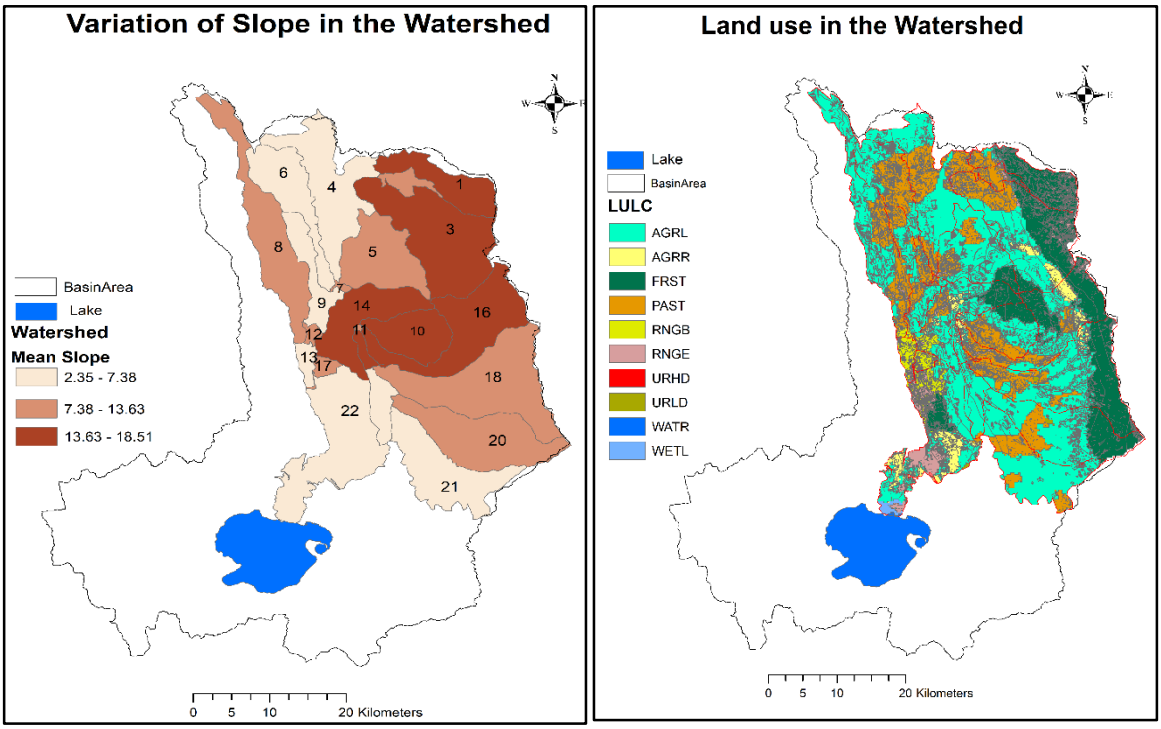

Figure 19: Slope and Land use maps for the R. Malewa basin

From the maps in Figure 18, it is observed that the sub-basins 1,2,3,10,15,16, 18 and 20 received a larger annual amount of rain during the simulation period (>940mm/year) as compared to the rest of the sub-basins. This coincides with the high sedimentation rates observed in the sub-basins 15,16, 18 and 20. The precipitation amounts dictate the amount of sediment produced in those sub-basins in that more precipitation leads to a larger discharge. The discharge is an agent for soil erosion which means that more soil will be eroded and thus raising the sediment amounts in the stream channels. This is in agreement to the findings of (Meqaunint Tenaw Asres1 & Seleshi B. Awulachew2, 2010) who in his research paper reported that precipitation is a key player in sediment yield in the Gumera watershed of Ethiopia

It is, however, worth noting that Sub-basin 14 has a large sedimentation rate (0.027ton/ha) despite it receiving a low amount of precipitation (626-782mm/year) on average for the simulation period. This is attributed to the high slope in the area (13.63-18.51%)(Figure 19). The steep slopes encourage accelerated soil erosion resulting in large amounts of sediment in the streams. (Zhang et al., 2015) did a research on the effects of slope and land use on the production of sediments in Southern China. His findings were that an increase in the slope will increase sediment production by a certain factor depending on the soil. He also found out that a transition of land use from farming to forest reduced sediment production by 61%. These findings are also in agreement with the above SWAT simulation which shows less sediment production in forested areas compared with the agricultural ones.

It is also evident from the maps Figure 19 that Sub basins that have more agricultural activity (AGRL, AGRR) experience a higher rate of sedimentation as opposed to sub-basins with less agricultural activity. The sub-basins with landcover RNGE, RNGB,PAST mostly lie on the low slopes of the watershed. The rates of sedimentation in these sub-basins is low (0-0.024 ton/Ha). This confirms that agricultural activities in the higher slopes of the sub-basin encourage soil erosion and hence sedimentation.

5.3. Conclusions

The employment of the SWAT model in evaluating the discharge and the resultant sediment production in the L. Naivasha Basin was successful to a large extent. The sediment produced in the area (Sub basins) was simulated successfully, and the DTS measurements were in agreement with the measured sediments (R^2=0.7866, NS= 0.651, PBIAS= 0.2705 and RSR=0.59). The hydrological simulation calibration and validation using the gauge measurements at the 2GB05 gauging station was also good with acceptable values of R^2 =0.75, NSE=0.625, PBIAS=0.216, RSR=1.12 and R^2=0.6688, NSE=0.4, PBIAS=-0.39, RSR=1.19 for calibration and validation respectively.

The sensitivity analysis on the model parameters helped in the identification of the most responsive parameters that would be mostly optimized in the calibration to achieve the optimum values of the said parameters and achieve the best results possible. The sediment simulation parameters that were sensitive included the SPCON, CH_EROD, CH_COV, and SPEXP. Hydrological simulation sensitive parameters were mostly groundwater parameters (GWQNM, GW_REVAP, and REVAPMN) and soil property parameters (Sol_AWC, SoL_K)

The calibration and validation results (Hydrological) and calibration (Sediment) gave good results that can be used in further study of the area for various applications. It is, however, important to note that the quality of the datasets used in this study was not good and hence in some instances, alternative sources of data were used to replace them, i.e. Use of Chips data instead of in-situ gauge data due to a large percentage of gaps in the data. The model results could have been better if the in-situ data was of better quality.

The sediment simulation and evaluation were also successful and meaningful deductions were made from the results. The sub-basins with low sediment production rates, i.e. 4, 6, 8 and 12 and those with high sediment production rates, i.e. 14,15, 18 and 20 were identified and an analysis made to ascertain the causes of the scenarios. The findings that the soils in the highly susceptible sub-basins are mostly clay or clay loam could be beneficial in the adaptation of Best management practices in those sub-basins to control the soil erosion and improve the crop production in those areas.

It was also deduced that the high slope sub-basins contributed to more sediment production and transportation to the streams regardless of the LULC. This information can be used to curb the erosion in those high slopes. This could be by adoption of terracing as a way of slowing down the runoff after a storm. Planting of cover crops could also help in reducing the impact of intense rainfall on the soil and also prevent detachment of soil particles. The plants also act as a means of binding the soil particles together thus preventing them from being washed away. Agricultural activities on high slope areas should also be minimized as they encourage soil erosion by making the soil loose and exposing it to runoff.

5.4. Recommendations

The results of this study have highlighted some important issues that need to be addressed for effective management and protection of the R. Malewa Basin and The L. Naivasha Basin as a whole. The sediment loads to the lake were found to be 67534.5 tones for the five months studied. This is quite a huge amount which can be attributed to the declining depths of the lake and possible aquatic life loss due to the reduction of dissolved oxygen as a result of increased temperatures of the water.
To reduce or curb the excessive sedimentation of the Lake, it would be important to implement the following control measures.

- Intensive farming on the high slopes should be discouraged to prevent excessive erosion from the farms. This will also encourage the growth of natural vegetation which prevents erosion by increasing interception by the canopy. Reduction of agricultural activities on the high slopes also increases the groundwater storage as less water evaporates from the soil and hence prolongs the river flow period after the rains.

- Soil preservation and conservation measures need to be undertaken to prevent the excessive erosion, especially on the high slope areas. The use of terracing as a means of reducing the quantity and speed of discharge as it flows downslope could help in combating erosion. Construction of gabions and small dikes across gullies could also help in the control of soil erosion. Planting of cover crops and pastures on bare parcels of land to reduce the impact of sheet erosion is another way that the erosion problem could be resolved.

- Intensive farming practices that require intensive use of machinery should be discouraged on farms that are on steep slopes or portions that have loose soils as the practice loosens the soil making it susceptible to erosion and increasing the sedimentation rates in those areas of the watershed. Use of minimum tillage practices could be used as an alternative to heavy machinery.

- It is also recommended that for future studies in the watershed, a data collection and storage strategy should be adopted by the relevant authorities. This will help in the provision of quality time series data that can be relied on for production of good results. These results will be used in the management of the water resources in the catchment for sustainability and environment conservation purposes.

REFERENCES

Abbaspour, K. C., Rouholahnejad, E., Vaghefi, S., Srinivasan, R., Yang, H., & Kløve, B. (2015). A continental-scale hydrology and water quality model for Europe: Calibration and uncertainty of a high-resolution large-scale SWAT model. *Journal of Hydrology*, *524*, 733–752. https://doi.org/10.1016/J.JHYDROL.2015.03.027

Armesto, J. J., & Martinez, J. A. (1978). Relations Between Vegetation Structure and Slope Aspect in the Mediterranean Region of Chile. *The Journal of Ecology*, *66*(3), 881. https://doi.org/10.2307/2259301

Arnold, J. G., Moriasi, D. N., Gassman, P. W., Abbaspour, K. C., White, M. J., Griensven, van, & Liew, V. (n.d.). SWAT: Model use, calibration, and validation. Retrieved from http://digitalcommons.unl.edu/biosysengfacpub

Becht, R., & Harper, D. M. (2002). Towards an understanding of human impact upon the hydrology of Lake Naivasha, Kenya. In *Lake Naivasha, Kenya* (pp. 1–11). Dordrecht: Springer Netherlands. https://doi.org/10.1007/978-94-017-2031-1_1

Benaman, J., Shoemaker, C., & Ripley, J. P. (n.d.). A Methodology For Sensitivity Analysis In Complex Distributed Watershed Models. Retrieved from http://citeseerx.ist.psu.edu/viewdoc/download?doi=10.1.1.126.8278&rep=rep1&type=pdf

Benedini, Marcello, Tsakiris, G. (2013). *Water Quality Modelling for Rivers and Streams*. Retrieved from http://ezproxy.utwente.nl:2201/(S(lmhsc5evh4ravffqcaubv4tv))/Reader.aspx?p=1083576&o=1200&u=QTjziN4g0zkNbuhhgqhoVw%3D%3D&t=1501060722&h=4FB5109071FFFCA5B842F61DD5BA78520814A172&s=60616338&ut=3997&pg=1&r=img&c=-1&pat=n&cms=-1&sd=2#

Benedini, M., & Tsakiris, G. (George). (2013). *Water quality modelling for rivers and streams* (1st ed.). Dordrecht: Springer. Retrieved from http://ezproxy.utwente.nl:2200/patron/FullRecord.aspx?p=1083576

Caitlin Scopel. (2012). SWAT: Soil & Water Assessment Tool | ArcGIS Blog. Retrieved May 31, 2017, from https://blogs.esri.com/esri/arcgis/2012/03/14/swat-soil-water-assessment-tool/

Dutta, S., & Sen, D. (n.d.). Application of SWAT model for predicting soil erosion and sediment yield. *Sustainable Water Resources Management*. https://doi.org/10.1007/s40899-017-0127-2

Dutta, S., & Sen, D. (2017). Application of SWAT model for predicting soil erosion and sediment yield. *Sustainable Water Resources Management*. https://doi.org/10.1007/s40899-017-0127-2

esa.Copenicus Global Land services 2017. (n.d.). Space in Images - 2017 - 10 - African land cover. Retrieved November 6, 2017, from http://www.esa.int/spaceinimages/Images/2017/10/African_land_cover

Everard, M., Vale, J. A., Harper, D. M., & Tarras-Wahlberg, H. (2002). The physical attributes of the Lake Naivasha catchment rivers. In *Lake Naivasha, Kenya* (pp. 13–25). Dordrecht: Springer Netherlands. https://doi.org/10.1007/978-94-017-2031-1_2

FTS. (2016). DTS-12.

Gessesse, B., Bewket, W., & Bräuning, A. (2015). Model-Based Characterization and Monitoring of Runoff and Soil Erosion in Response to Land Use/land Cover Changes in the Modjo Watershed, Ethiopia. *Land Degradation & Development*, *26*(7), 711–724. https://doi.org/10.1002/ldr.2276

Golosov, V., Collins, A. L., Tang, Q., Zhang, X., Zhou, P., He, X., & Wen, A. (2017). Sediment transfer at different spatial and temporal scales in the Sichuan Hilly Basin, China: Synthesizing data from multiple approaches and preliminary interpretation in the context of climatic and anthropogenic drivers. *Science of The Total Environment*, *598*, 319–329. https://doi.org/10.1016/J.SCITOTENV.2017.04.133

Harper, D. M., Morrison, E. H. J., Macharia, M. M., Mavuti, K. M., Upton, C., & Harper, D. M. (2011). Lake Naivasha, Kenya: ecology, society and future. *Freshwater Reviews*, *4*, 89–114. https://doi.org/10.1608/FRJ-4.2.419

Imani, R., Ghasemieh, H., & Mirzavand, M. (2014). Determining and Mapping Soil Erodibility Factor (Case Study: Yamchi Watershed in Northwest of Iran). *Open Journal of Soil Science*, *4*, 168–173. https://doi.org/10.4236/ojss.2014.45020

Kaoga, J., Ouma, G., & Abuom, P. (2013a). Effects of Farm Pesticides on Water Quality in Lake Naivasha, Kenya. *American Journal of Plant Physiology*, *8*(3), 105–113. https://doi.org/10.3923/ajpp.2013.105.113

Kaoga, J., Ouma, G., & Abuom, P. (2013b). Effects of Farm Pesticides on Water Quality in Lake Naivasha, Kenya. *American Journal of Plant Physiology*, *8*(3), 105–113. https://doi.org/10.3923/ajpp.2013.105.113

Kitaka, N., Harper, D. M., Mavuti, K. M., & Pacini, N. (2002). Chemical characteristics, with particular reference to phosphorus, of the rivers draining into Lake Naivasha, Kenya. *Hydrobiologia*, *488*(1/3), 57–71. https://doi.org/10.1023/A:1023353825462

Liu, Y., Yang, W., Yu, Z., Lung, I., & Gharabaghi, B. (2015a). Estimating Sediment Yield from Upland and Channel Erosion at A Watershed Scale Using SWAT. *Water Resources Management*, *29*(5), 1399–1412. https://doi.org/10.1007/s11269-014-0729-5

Liu, Y., Yang, W., Yu, Z., Lung, I., & Gharabaghi, B. (2015b). Estimating Sediment Yield from Upland and Channel Erosion at A Watershed Scale Using SWAT. *Water Resources Management*, *29*(5), 1399–1412. https://doi.org/10.1007/s11269-014-0729-5

Lukman A.p. (2003). *Regional impact of climate change and variability on water resources. Lake Naivasha Basin, Kenya*. Retrieved from https://www.imarisha.le.ac.uk/sites/default/files/Regional impact of climate change and variability on water resources. Lake Naivasha Basin%2C Kenya..pdf

Mccool, D. K., Director, G. R. F., Renard, K. G., Yoder, D. C., Weesies, G. A., Foster, G. R., & Weesies1, G. A. (n.d.). THE REVISED UNIVERSAL SOIL LOSS EQUATION. Retrieved from https://www.tucson.ars.ag.gov/unit/publications/PDFfiles/1132.pdf

Md. Azizul Haque podder. (1998). ESTIMATION OF LONG-TERM INFLOW INTO LAKE NAIVASHA FROM THE MALEWA CATCHMENT, KENYA. Retrieved from ftp://ftp.itc.nl/pub/naivasha/ITC/Podder1998.pdf

Md. Azizul Haque Podder. (1998). *Estimation of long term inflow into lake Naivasha from the Malewa catchment, Kenya*. Retrieved from ftp://ftp.itc.nl/pub/naivasha/ITC/Podder1998.pdf

Meins, F. M. (2013). Evaluation of spatial scale alternatives for hydrological modelling of the Lake Naivasha basin, Kenya, (April).

Meqaunint Tenaw Asres1, & Seleshi B. Awulachew2. (2010). SWAT based runoff and sediment yield modelling: a case study of the Gumera watershed in the Blue Nile basin. Retrieved from http://ezproxy.utwente.nl:2819/S1642359310701555/1-s2.0-S1642359310701555-main.pdf?_tid=d62d3e8e-7c33-11e7-8da5-00000aacb35d&acdnat=1502194953_2f7bd5418aaa43d9e1a15c32f37c45aa

Moriasi, D. N., Arnold, J. G., Liew, M. W. Van, Bingner, R. L., Harmel, R. D., Veith, T. L., … Moriasi, D. N. (n.d.). MODEL EVALUATION GUIDELINES FOR SYSTEMATIC QUANTIFICATION OF ACCURACY IN WATERSHED SIMULATIONS. *Transactions of the ASABE*, *50*(3), 885–900. Retrieved from http://citeseerx.ist.psu.edu/viewdoc/download?doi=10.1.1.532.2506&rep=rep1&type=pdf

Musota, R. (2008). USING WEAP AND SCENRIOS TO ASSESS SUSTAINABILITY OF WATER RESOURCES IN A BASIN. Case study for Lake Naivasha catchment-Kenya. Retrieved from https://www.imarisha.le.ac.uk/sites/default/files/document-upload-folder/Using weap and scenrios to assess sustainability water resources in a basin.case study for lake Naivasha catchment, Kenya..pdf

Neitsch, S. L., Arnold, J. G., Kiniry, J. R., Srinivasan, R., & Williams, J. R. (2002). Soil and Water Assessment Tool User's Manual. *TWRI Report TR-192*, 412. Retrieved from http://swat.tamu.edu/media/1294/swatuserman.pdf

Neitsch, S. L., Arnold, J. G., Kiniry, J. R., & Williams, J. R. (2011). *Soil and Water Assessment Tool Theoretical Documentation Version 2009 Texas Water Resources Institute*. Retrieved from http://swat.tamu.edu/media/99192/swat2009-theory.pdf

Odongo, V. O., Onyando, J. O., Mutua, B. M., van Oel, P. R., & Becht, R. (2013). Sensitivity analysis and calibration of the Modified Universal Soil Loss Equation (MUSLE) for the upper Malewa Catchment, Kenya. *International Journal of Sediment Research*, *28*(3), 368–383. https://doi.org/10.1016/S1001-6279(13)60047-5

Odongo, V. O., Onyando, J. O., Mutua, B. M., van OEL, P. R., & Becht, R. (2013). Sensitivity analysis and calibration of the Modified Universal Soil Loss Equation (MUSLE) for the upper Malewa Catchment, Kenya. *International Journal of Sediment Research*, *28*(3), 368–383. https://doi.org/10.1016/S1001-6279(13)60047-5

Ouyang, W., Skidmore, A. K., Hao, F., & Wang, T. (2010). Soil erosion dynamics response to landscape

pattern. *Science of The Total Environment*, *408*(6), 1358–1366. https://doi.org/10.1016/j.scitotenv.2009.10.062

Qiu, L.-J., Zheng, F.-L., & Yin, R.-S. (2012). SWAT-based runoff and sediment simulation in a small watershed, the loessial hilly-gullied region of China: capabilities and challenges. *International Journal of Sediment Research*, *27*(27), 226–234. https://doi.org/10.1016/S1001-6279(12)60030-4

R.A.P. Rupasingha. (2002). *USE OF GIS AND RS FOR ASSESSING LAKE SEDIMENTATION PROCESSES*. ITC, Enschede. Retrieved from ftp://ftp.itc.nl/pub/naivasha/ITC/Rupasingha2002.pdf

Salama, M. S., & Verhoef, W. (2015). Two-stream remote sensing model for water quality mapping: 2SeaColor. *Remote Sensing of Environment*, *157*, 111–122. https://doi.org/10.1016/j.rse.2014.07.022

Tang Zhen Xu. (1999). *Water Quality Assessment and Pesticide Fate Modeling in the Lake Naivasha area, Kenya*. ITC, The Netherlands. Retrieved from ftp://ftp.itc.nl/pub/naivasha/ITC/Xu1999.pdf

Teshager, A. D., Gassman, P. W., Secchi, S., Schoof, J. T., & Misgna, G. (2016). Modeling Agricultural Watersheds with the Soil and Water Assessment Tool (SWAT): Calibration and Validation with a Novel Procedure for Spatially Explicit HRUs. *Environmental Management*, *57*(4), 894–911. https://doi.org/10.1007/s00267-015-0636-4

Tiruneh B.A. (2004). *Modelling water quality using soil and water assesment tool (SWAT)*. ITC. Retrieved from http://www.itc.nl/library/papers_2004/msc/wrem/berihun_adamu_tiruneh.pdf

Uniyal, B., Jha, M. K., & Verma, A. K. (2015). Parameter identification and uncertainty analysis for simulating streamflow in a river basin of Eastern India. *Hydrological Processes*, *29*(17), 3744–3766. https://doi.org/10.1002/hyp.10446

Vigiak, O., Malagó, A., Bouraoui, F., Vanmaercke, M., Obreja, F., Poesen, J., … Grošelj, S. (2017a). Modelling sediment fluxes in the Danube River Basin with SWAT. *Science of the Total Environment*, *599*, 600–992. https://doi.org/10.1016/j.scitotenv.2017.04.236

Zettam, A., Taleb, A., Sauvage, S., Boithias, L., Belaidi, N., & Sánchez-Pérez, J. (2017). Modelling Hydrology and Sediment Transport in a Semi-Arid and Anthropized Catchment Using the SWAT Model: The Case of the Tafna River (Northwest Algeria). *Water*, *9*(3), 216. https://doi.org/10.3390/w9030216

Zhang, Z., Sheng, L., Yang, J., Chen, X. A., Kong, L., & Wagan, B. (2015). Effects of land use and slope gradient on soil erosion in a red soil hilly watershed of southern China. *Sustainability (Switzerland)*, *7*(10), 14309–14325. https://doi.org/10.3390/su71014309

APPENDICES

Appendix 1:.Lab measurements of TSS and Turbidity for the various stations

sampling Date:	4/4/2017	
analysis date:	6/4/2017	
subject:	TSS measuring	
sample name	Turbidity by manual	TSS (mg/l)
2GB2-1	10.70	5.74
2GB2-2	10.87	5.80
2GB2-3	8.08	5.16
2GB4-1	6.32	5.17
2GB4-2	4.87	5.46
2GB4-3	10.79	5.77
2GC5-1	4.08	5.71
2GC5-2	4.32	5.63
2GC5-3	4.61	5.53
sampling Date:	11/4/2017	
analysis date:	18/4/2017	
subject:	TSS measuring	
sample name	Turbidity by manual	TSS (mg/l)
2GB1-1	33.29	30.21
2GB1-2	29.21	24.33
2GB1-3	29.34	24.51
2GB4-1	16.45	9.23
2GB4-2	15.92	8.79
2GB4-3	19.64	12.25
sampling Date:	19/4/2017	
analysis date:	20/4/2017	
subject:	TSS measuring	
sample name	Turbidity by manual	TSS (mg/l)
2GB4-1	12.75	6.66
2GB4-2	14.34	7.63
2GB4-3	11.51	6.06
sampling Date:	24/4/2017	
analysis date:	25/4/2017	
subject:	TSS measuring	
sample name	Turbidity by manual	TSS (mg/l)
2GB1-1	10.99	5.84
2GB1-2	9.67	5.43
2GB1-3	10.26	5.59
2GB2-1	9.28	5.34
2GB2-2	9.92	5.49
2GB2-3	9.29	5.34

analysis date:	28/4/2017	
subject:	TSS measuring	
sample name	Turbidity by manual	TSS (mg/l)
2GB1-1	11.12	5.89
2GB1-2	11.49	6.05
2GB1-3	9.74	5.44
2GB1-4	10.50	5.67
2GB1-5	8.74	5.24
2GB1-6	10.05	5.53
2GB2-1	17.07	9.76
2GB2-2	16.58	9.34
2GB2-3	15.86	8.74
2GB4-1	11.38	6.00
2GB4-1-A-G	9.28	5.34
2GB4-2	10.79	5.77
2GB4-2-A-G	9.53	5.39
2GB4-3	10.71	5.74
2GB4-3-A-G	9.41	5.36
2GB4-4	11.21	5.93
2GB4-4-A-G	9.26	5.33
2GB4-5	11.08	5.88
2GB4-5-A-G	9.63	5.42
2GB4-6	11.97	6.26
2GB4-6-A-G	9.89	5.49
sampling Date:	3/5/2017	
analysis date:	5/5/2017	
subject:	TSS measuring	
sample name	Turbidity by manual	TSS (mg/l)
2GB1-1	55.13	62.00
2GB1-2	66.71	61.00
2GB1-3	59.21	63.00
2GB2-1	30.26	26.00
2GB4-1	83.82	69.00
2GB4-1-A-G	51.58	
2GB4-2	104.61	72.00
2GB4-2-A-G	50.79	
2GB4-3	104.47	
2GB4-3-A-G	51.71	
2GB4-1	9.41	5.36
2GB4-2	9.14	5.31
2GB4-3	9.80	5.46

Appendix 2: Model input parameter settings

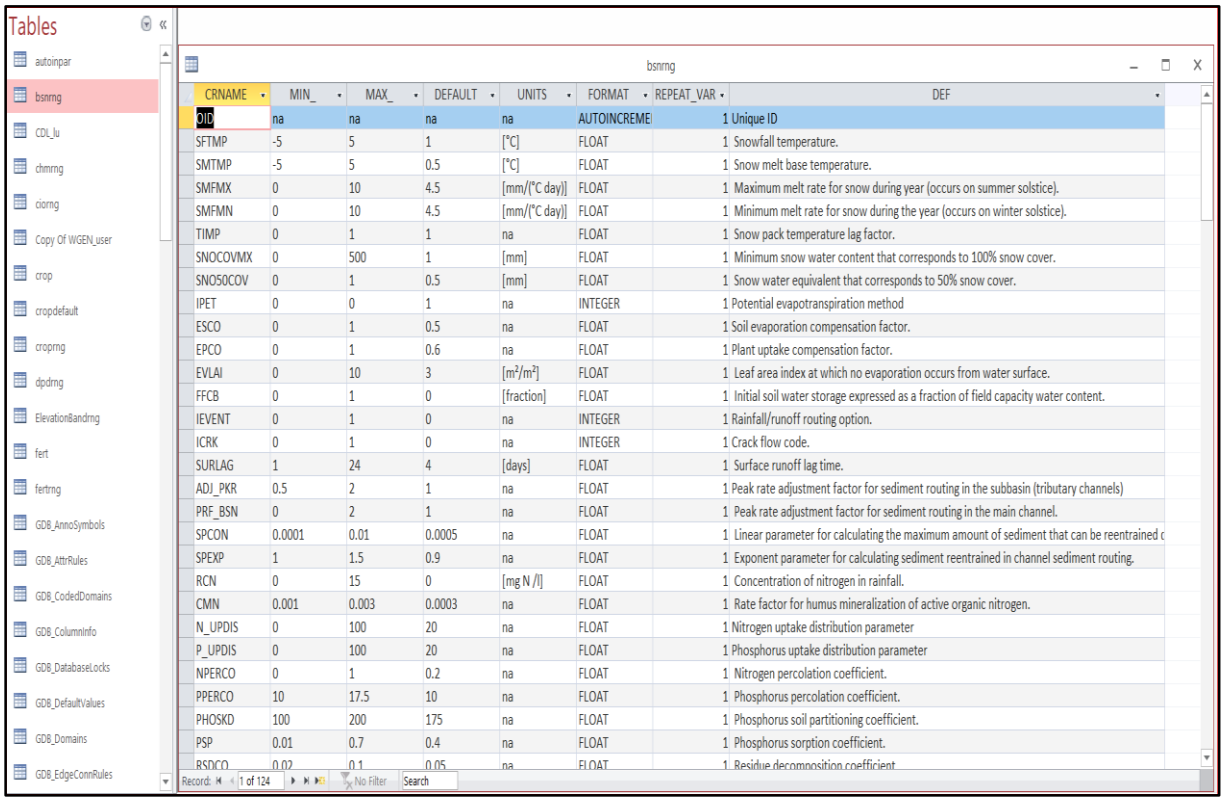

bsnrng

CRNAME	MIN_	MAX_	DEFAULT	UNITS	FORMAT	REPEAT_VAR	DEF
OID	na	na	na	na	AUTOINCREME	1	Unique ID
SFTMP	-5	5	1	[°C]	FLOAT	1	Snowfall temperature.
SMTMP	-5	5	0.5	[°C]	FLOAT	1	Snow melt base temperature.
SMFMX	0	10	4.5	[mm/(°C day)]	FLOAT	1	Maximum melt rate for snow during year (occurs on summer solstice).
SMFMN	0	10	4.5	[mm/(°C day)]	FLOAT	1	Minimum melt rate for snow during the year (occurs on winter solstice).
TIMP	0	1	1	na	FLOAT	1	Snow pack temperature lag factor.
SNOCOVMX	0	500	1	[mm]	FLOAT	1	Minimum snow water content that corresponds to 100% snow cover.
SNO50COV	0	1	0.5	[mm]	FLOAT	1	Snow water equivalent that corresponds to 50% snow cover.
IPET	0	0	1	na	INTEGER	1	Potential evapotranspiration method
ESCO	0	1	0.5	na	FLOAT	1	Soil evaporation compensation factor.
EPCO	0	1	0.6	na	FLOAT	1	Plant uptake compensation factor.
EVLAI	0	10	3	[m²/m²]	FLOAT	1	Leaf area index at which no evaporation occurs from water surface.
FFCB	0	1	0	[fraction]	FLOAT	1	Initial soil water storage expressed as a fraction of field capacity water content.
IEVENT	0	1	0	na	INTEGER	1	Rainfall/runoff routing option.
ICRK	0	1	0	na	INTEGER	1	Crack flow code.
SURLAG	1	24	4	[days]	FLOAT	1	Surface runoff lag time.
ADJ_PKR	0.5	2	1	na	FLOAT	1	Peak rate adjustment factor for sediment routing in the subbasin (tributary channels)
PRF_BSN	0	2	1	na	FLOAT	1	Peak rate adjustment factor for sediment routing in the main channel.
SPCON	0.0001	0.01	0.0005	na	FLOAT	1	Linear parameter for calculating the maximum amount of sediment that can be reentrained c
SPEXP	1	1.5	0.9	na	FLOAT	1	Exponent parameter for calculating sediment reentrained in channel sediment routing.
RCN	0	15	0	[mg N /l]	FLOAT	1	Concentration of nitrogen in rainfall.
CMN	0.001	0.003	0.0003	na	FLOAT	1	Rate factor for humus mineralization of active organic nitrogen.
N_UPDIS	0	100	20	na	FLOAT	1	Nitrogen uptake distribution parameter
P_UPDIS	0	100	20	na	FLOAT	1	Phosphorus uptake distribution parameter
NPERCO	0	1	0.2	na	FLOAT	1	Nitrogen percolation coefficient.
PPERCO	10	17.5	10	na	FLOAT	1	Phosphorus percolation coefficient.
PHOSKD	100	200	175	na	FLOAT	1	Phosphorus soil partitioning coefficient.
PSP	0.01	0.7	0.4	na	FLOAT	1	Phosphorus sorption coefficient.
BSDCO	0.02	0.1	0.05	na	FLOAT	1	Residue decomposition coefficient

Bsnrng

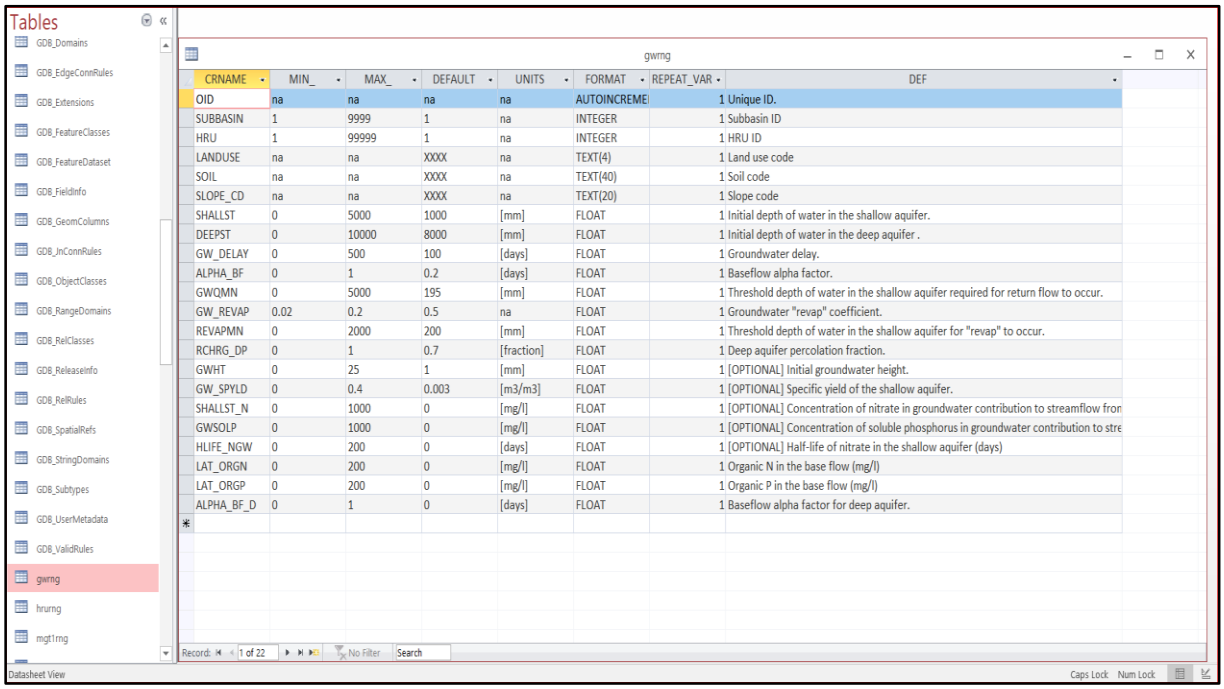

gwrng

CRNAME	MIN_	MAX_	DEFAULT	UNITS	FORMAT	REPEAT_VAR	DEF
OID	na	na	na	na	AUTOINCREME	1	Unique ID.
SUBBASIN	1	9999	1	na	INTEGER	1	Subbasin ID
HRU	1	99999	1	na	INTEGER	1	HRU ID
LANDUSE	na	na	XXXX	na	TEXT(4)	1	Land use code
SOIL	na	na	XXXX	na	TEXT(40)	1	Soil code
SLOPE_CD	na	na	XXXX	na	TEXT(20)	1	Slope code
SHALLST	0	5000	1000	[mm]	FLOAT	1	Initial depth of water in the shallow aquifer.
DEEPST	0	10000	8000	[mm]	FLOAT	1	Initial depth of water in the deep aquifer .
GW_DELAY	0	500	100	[days]	FLOAT	1	Groundwater delay.
ALPHA_BF	0	1	0.2	[days]	FLOAT	1	Baseflow alpha factor.
GWQMN	0	5000	195	[mm]	FLOAT	1	Threshold depth of water in the shallow aquifer required for return flow to occur.
GW_REVAP	0.02	0.2	0.5	na	FLOAT	1	Groundwater "revap" coefficient.
REVAPMN	0	2000	200	[mm]	FLOAT	1	Threshold depth of water in the shallow aquifer for "revap" to occur.
RCHRG_DP	0	1	0.7	[fraction]	FLOAT	1	Deep aquifer percolation fraction.
GWHT	0	25	1	[mm]	FLOAT	1	[OPTIONAL] Initial groundwater height.
GW_SPYLD	0	0.4	0.003	[m3/m3]	FLOAT	1	[OPTIONAL] Specific yield of the shallow aquifer.
SHALLST_N	0	1000	0	[mg/l]	FLOAT	1	[OPTIONAL] Concentration of nitrate in groundwater contribution to streamflow fron
GWSOLP	0	1000	0	[mg/l]	FLOAT	1	[OPTIONAL] Concentration of soluble phosphorus in groundwater contribution to stre
HLIFE_NGW	0	200	0	[days]	FLOAT	1	[OPTIONAL] Half-life of nitrate in the shallow aquifer (days)
LAT_ORGN	0	200	0	[mg/l]	FLOAT	1	Organic N in the base flow (mg/l)
LAT_ORGP	0	200	0	[mg/l]	FLOAT	1	Organic P in the base flow (mg/l)
ALPHA_BF_D	0	1	0	[days]	FLOAT	1	Baseflow alpha factor for deep aquifer.

gwrng

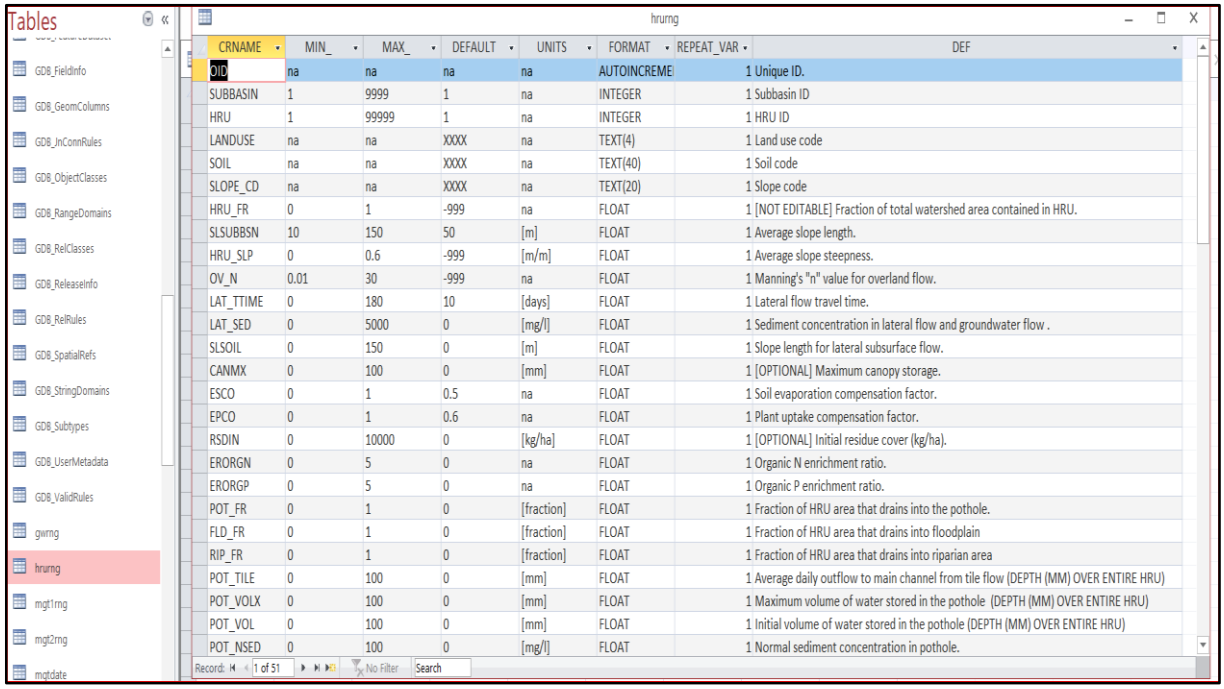

CRNAME	MIN_	MAX_	DEFAULT	UNITS	FORMAT	REPEAT_VAR	DEF
OID	na	na	na	na	AUTOINCREME	1	Unique ID.
SUBBASIN	1	9999	1	na	INTEGER	1	Subbasin ID
HRU	1	99999	1	na	INTEGER	1	HRU ID
LANDUSE	na	na	XXXX	na	TEXT(4)	1	Land use code
SOIL	na	na	XXXX	na	TEXT(40)	1	Soil code
SLOPE_CD	na	na	XXXX	na	TEXT(20)	1	Slope code
HRU_FR	0	1	-999	na	FLOAT	1	[NOT EDITABLE] Fraction of total watershed area contained in HRU.
SLSUBBSN	10	150	50	[m]	FLOAT	1	Average slope length.
HRU_SLP	0	0.6	-999	[m/m]	FLOAT	1	Average slope steepness.
OV_N	0.01	30	-999	na	FLOAT	1	Manning's "n" value for overland flow.
LAT_TTIME	0	180	10	[days]	FLOAT	1	Lateral flow travel time.
LAT_SED	0	5000	0	[mg/l]	FLOAT	1	Sediment concentration in lateral flow and groundwater flow .
SLSOIL	0	150	0	[m]	FLOAT	1	Slope length for lateral subsurface flow.
CANMX	0	100	0	[mm]	FLOAT	1	[OPTIONAL] Maximum canopy storage.
ESCO	0	1	0.5	na	FLOAT	1	Soil evaporation compensation factor.
EPCO	0	1	0.6	na	FLOAT	1	Plant uptake compensation factor.
RSDIN	0	10000	0	[kg/ha]	FLOAT	1	[OPTIONAL] Initial residue cover (kg/ha).
ERORGN	0	5	0	na	FLOAT	1	Organic N enrichment ratio.
ERORGP	0	5	0	na	FLOAT	1	Organic P enrichment ratio.
POT_FR	0	1	0	[fraction]	FLOAT	1	Fraction of HRU area that drains into the pothole.
FLD_FR	0	1	0	[fraction]	FLOAT	1	Fraction of HRU area that drains into floodplain
RIP_FR	0	1	0	[fraction]	FLOAT	1	Fraction of HRU area that drains into riparian area
POT_TILE	0	100	0	[mm]	FLOAT	1	Average daily outflow to main channel from tile flow (DEPTH (MM) OVER ENTIRE HRU)
POT_VOLX	0	100	0	[mm]	FLOAT	1	Maximum volume of water stored in the pothole (DEPTH (MM) OVER ENTIRE HRU)
POT_VOL	0	100	0	[mm]	FLOAT	1	Initial volume of water stored in the pothole (DEPTH (MM) OVER ENTIRE HRU)
POT_NSED	0	100	0	[mg/l]	FLOAT	1	Normal sediment concentration in pothole.

hrurng

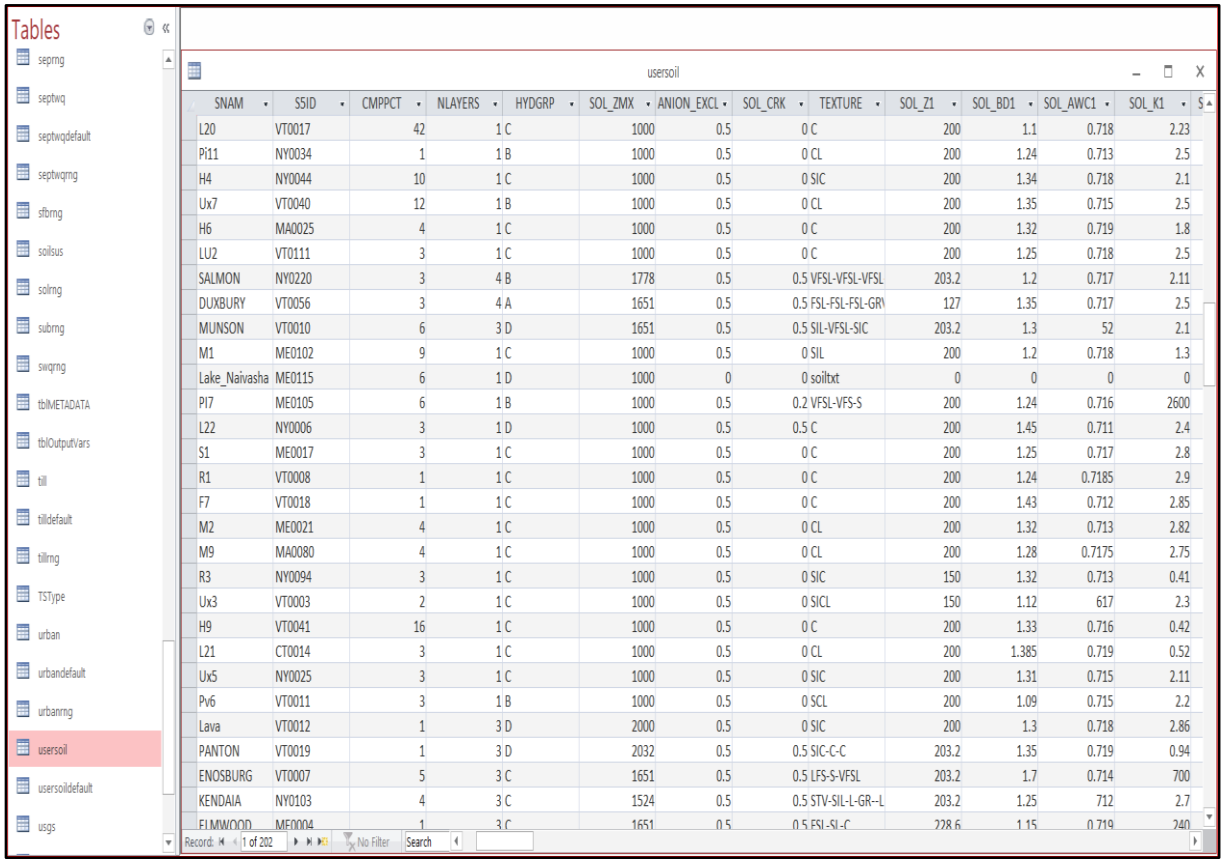

SNAM	S5ID	CMPPCT	NLAYERS	HYDGRP	SOL_ZMX	ANION_EXCL	SOL_CRK	TEXTURE	SOL_Z1	SOL_BD1	SOL_AWC1	SOL_K1
L20	VT0017	42	1	C	1000	0.5	0	C	200	1.1	0.718	2.23
Pi11	NY0034	1	1	B	1000	0.5	0	CL	200	1.24	0.713	2.5
H4	NY0044	10	1	C	1000	0.5	0	SIC	200	1.34	0.718	2.1
Ux7	VT0040	12	1	B	1000	0.5	0	CL	200	1.35	0.715	2.5
H6	MA0025	4	1	C	1000	0.5	0	C	200	1.32	0.719	1.8
LU2	VT0111	3	1	C	1000	0.5	0	C	200	1.25	0.718	2.5
SALMON	NY0220	3	4	B	1778	0.5	0.5	VFSL-VFSL-VFSL	203.2	1.2	0.717	2.11
DUXBURY	VT0056	3	4	A	1651	0.5	0.5	FSL-FSL-FSL-GR\	127	1.35	0.717	2.5
MUNSON	VT0010	6	3	D	1651	0.5	0.5	SIL-VFSL-SIC	203.2	1.3	52	2.1
M1	ME0102	9	1	C	1000	0.5	0	SIL	200	1.2	0.718	1.3
Lake_Naivasha	ME0115	6	1	D	1000	0	0	soiltxt	0	0	0	0
PI7	ME0105	6	1	B	1000	0.5	0.2	VFSL-VFS-S	200	1.24	0.716	2600
L22	NY0006	3	1	D	1000	0.5	0.5	C	200	1.45	0.711	2.4
S1	ME0017	3	1	C	1000	0.5	0	C	200	1.25	0.717	2.8
R1	VT0008	1	1	C	1000	0.5	0	C	200	1.24	0.7185	2.9
F7	VT0018	1	1	C	1000	0.5	0	C	200	1.43	0.712	2.85
M2	ME0021	4	1	C	1000	0.5	0	CL	200	1.32	0.713	2.82
M9	MA0080	4	1	C	1000	0.5	0	CL	200	1.28	0.7175	2.75
R3	NY0094	3	1	C	1000	0.5	0	SIC	150	1.32	0.713	0.41
Ux3	VT0003	2	1	C	1000	0.5	0	SICL	150	1.12	617	2.3
H9	VT0041	16	1	C	1000	0.5	0	C	200	1.33	0.716	0.42
L21	CT0014	3	1	C	1000	0.5	0	CL	200	1.385	0.719	0.52
Ux5	NY0025	3	1	C	1000	0.5	0	SIC	200	1.31	0.715	2.11
Pv6	VT0011	3	1	B	1000	0.5	0	SCL	200	1.09	0.715	2.2
Lava	VT0012	1	3	D	2000	0.5	0	SIC	200	1.3	0.718	2.86
PANTON	VT0019	1	3	D	2032	0.5	0.5	SIC-C-C	203.2	1.35	0.719	0.94
ENOSBURG	VT0007	5	3	C	1651	0.5	0.5	LFS-S-VFSL	203.2	1.7	0.714	700
KENDAIA	NY0103	4	3	C	1524	0.5	0.5	STV-SIL-L-GR--L	203.2	1.25	712	2.7
ELMWOOD	ME0004	1	3	C	1651	0.5	0.5	FSL-SL-C	228.6	1.15	0.719	240

usersoil

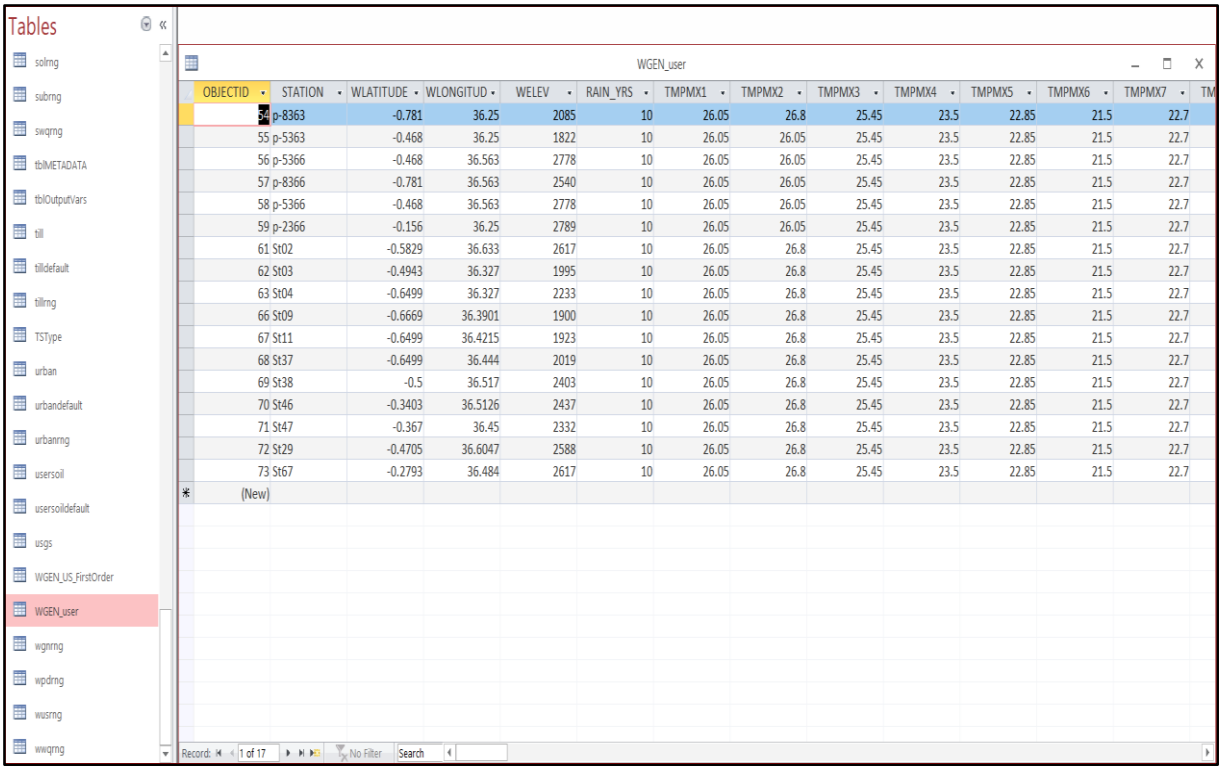

Tables

solrng
subrng
swqrng
tblMETADATA
tblOutputVars
till
tilldefault
tillrng
TSType
urban
urbandefault
urbanrng
usersoil
usersoildefault
usgs
WGEN_US_FirstOrder
WGEN_user
wgnrng
wpdrng
wusrng
wwqrng

WGEN_user

OBJECTID	STATION	WLATITUDE	WLONGITUD	WELEV	RAIN_YRS	TMPMX1	TMPMX2	TMPMX3	TMPMX4	TMPMX5	TMPMX6	TMPMX7	TM
54	p-8363	-0.781	36.25	2085	10	26.05	26.8	25.45	23.5	22.85	21.5	22.7	
55	p-5363	-0.468	36.25	1822	10	26.05	26.05	25.45	23.5	22.85	21.5	22.7	
56	p-5366	-0.468	36.563	2778	10	26.05	26.05	25.45	23.5	22.85	21.5	22.7	
57	p-8366	-0.781	36.563	2540	10	26.05	26.05	25.45	23.5	22.85	21.5	22.7	
58	p-5366	-0.468	36.563	2778	10	26.05	26.05	25.45	23.5	22.85	21.5	22.7	
59	p-2366	-0.156	36.25	2789	10	26.05	26.05	25.45	23.5	22.85	21.5	22.7	
61	St02	-0.5829	36.633	2617	10	26.05	26.8	25.45	23.5	22.85	21.5	22.7	
62	St03	-0.4943	36.327	1995	10	26.05	26.8	25.45	23.5	22.85	21.5	22.7	
63	St04	-0.6499	36.327	2233	10	26.05	26.8	25.45	23.5	22.85	21.5	22.7	
66	St09	-0.6669	36.3901	1900	10	26.05	26.8	25.45	23.5	22.85	21.5	22.7	
67	St11	-0.6499	36.4215	1923	10	26.05	26.8	25.45	23.5	22.85	21.5	22.7	
68	St37	-0.6499	36.444	2019	10	26.05	26.8	25.45	23.5	22.85	21.5	22.7	
69	St38	-0.5	36.517	2403	10	26.05	26.8	25.45	23.5	22.85	21.5	22.7	
70	St46	-0.3403	36.5126	2437	10	26.05	26.8	25.45	23.5	22.85	21.5	22.7	
71	St47	-0.367	36.45	2332	10	26.05	26.8	25.45	23.5	22.85	21.5	22.7	
72	St29	-0.4705	36.6047	2588	10	26.05	26.8	25.45	23.5	22.85	21.5	22.7	
73	St67	-0.2793	36.484	2617	10	26.05	26.8	25.45	23.5	22.85	21.5	22.7	
	(New)												

Record: 1 of 17 | No Filter | Search

WGEN-User

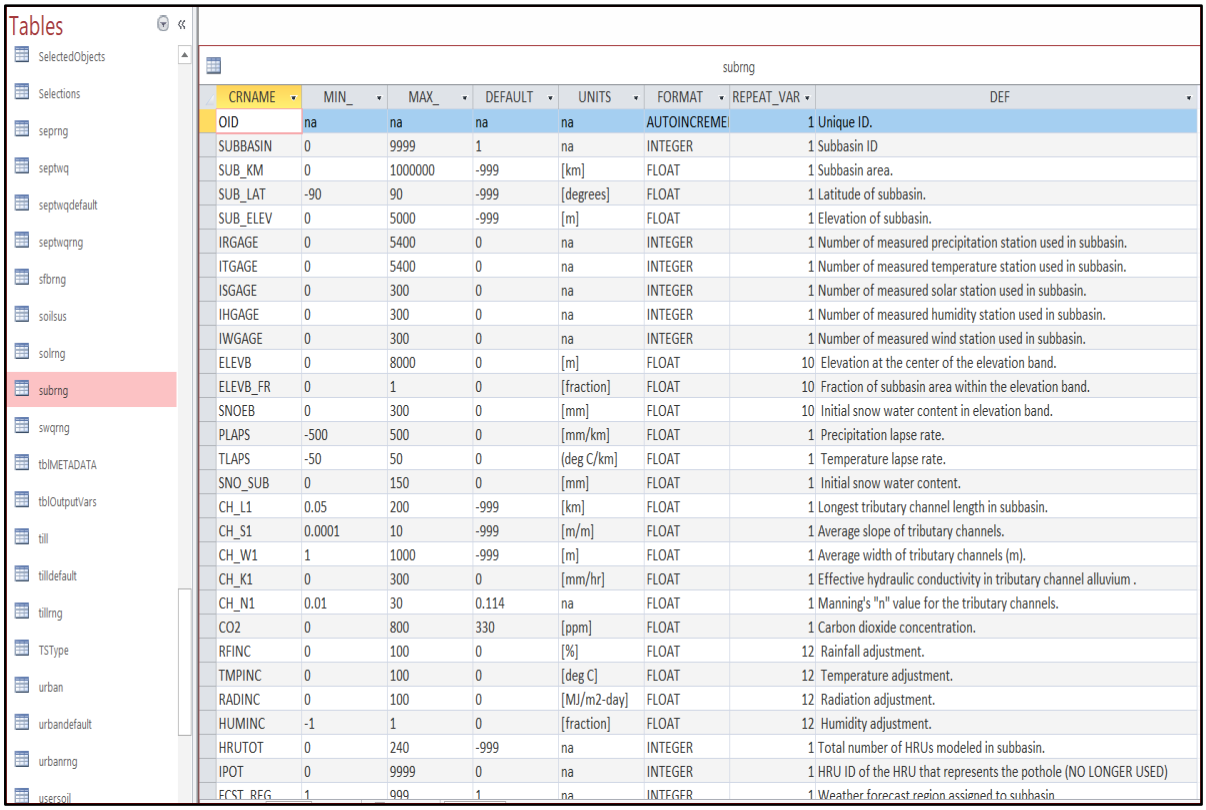

Tables

SelectedObjects
Selections
seprng
septwq
septwqdefault
septwqrng
sfbrng
soilsus
solrng
subrng
swqrng
tblMETADATA
tblOutputVars
till
tilldefault
tillrng
TSType
urban
urbandefault
urbanrng
usersoil

subrng

CRNAME	MIN_	MAX_	DEFAULT	UNITS	FORMAT	REPEAT_VAR	DEF
OID	na	na	na	na	AUTOINCREME	1	Unique ID.
SUBBASIN	0	9999	1	na	INTEGER	1	Subbasin ID
SUB_KM	0	1000000	-999	[km]	FLOAT	1	Subbasin area.
SUB_LAT	-90	90	-999	[degrees]	FLOAT	1	Latitude of subbasin.
SUB_ELEV	0	5000	-999	[m]	FLOAT	1	Elevation of subbasin.
IRGAGE	0	5400	0	na	INTEGER	1	Number of measured precipitation station used in subbasin.
ITGAGE	0	5400	0	na	INTEGER	1	Number of measured temperature station used in subbasin.
ISGAGE	0	300	0	na	INTEGER	1	Number of measured solar station used in subbasin.
IHGAGE	0	300	0	na	INTEGER	1	Number of measured humidity station used in subbasin.
IWGAGE	0	300	0	na	INTEGER	1	Number of measured wind station used in subbasin.
ELEVB	0	8000	0	[m]	FLOAT	10	Elevation at the center of the elevation band.
ELEVB_FR	0	1	0	[fraction]	FLOAT	10	Fraction of subbasin area within the elevation band.
SNOEB	0	300	0	[mm]	FLOAT	10	Initial snow water content in elevation band.
PLAPS	-500	500	0	[mm/km]	FLOAT	1	Precipitation lapse rate.
TLAPS	-50	50	0	[deg C/km]	FLOAT	1	Temperature lapse rate.
SNO_SUB	0	150	0	[mm]	FLOAT	1	Initial snow water content.
CH_L1	0.05	200	-999	[km]	FLOAT	1	Longest tributary channel length in subbasin.
CH_S1	0.0001	10	-999	[m/m]	FLOAT	1	Average slope of tributary channels.
CH_W1	1	1000	-999	[m]	FLOAT	1	Average width of tributary channels (m).
CH_K1	0	300	0	[mm/hr]	FLOAT	1	Effective hydraulic conductivity in tributary channel alluvium .
CH_N1	0.01	30	0.114	na	FLOAT	1	Manning's "n" value for the tributary channels.
CO2	0	800	330	[ppm]	FLOAT	1	Carbon dioxide concentration.
RFINC	0	100	0	[%]	FLOAT	12	Rainfall adjustment.
TMPINC	0	100	0	[deg C]	FLOAT	12	Temperature adjustment.
RADINC	0	100	0	[MJ/m2-day]	FLOAT	12	Radiation adjustment.
HUMINC	-1	1	0	[fraction]	FLOAT	12	Humidity adjustment.
HRUTOT	0	240	-999	na	INTEGER	1	Total number of HRUs modeled in subbasin.
IPOT	0	9999	0	na	INTEGER	1	HRU ID of the HRU that represents the pothole (NO LONGER USED)
FCST_REG	1	999	1	na	INTEGER	1	Weather forecast region assigned to subbasin

Subrng

Appendix 3: Model Outputs

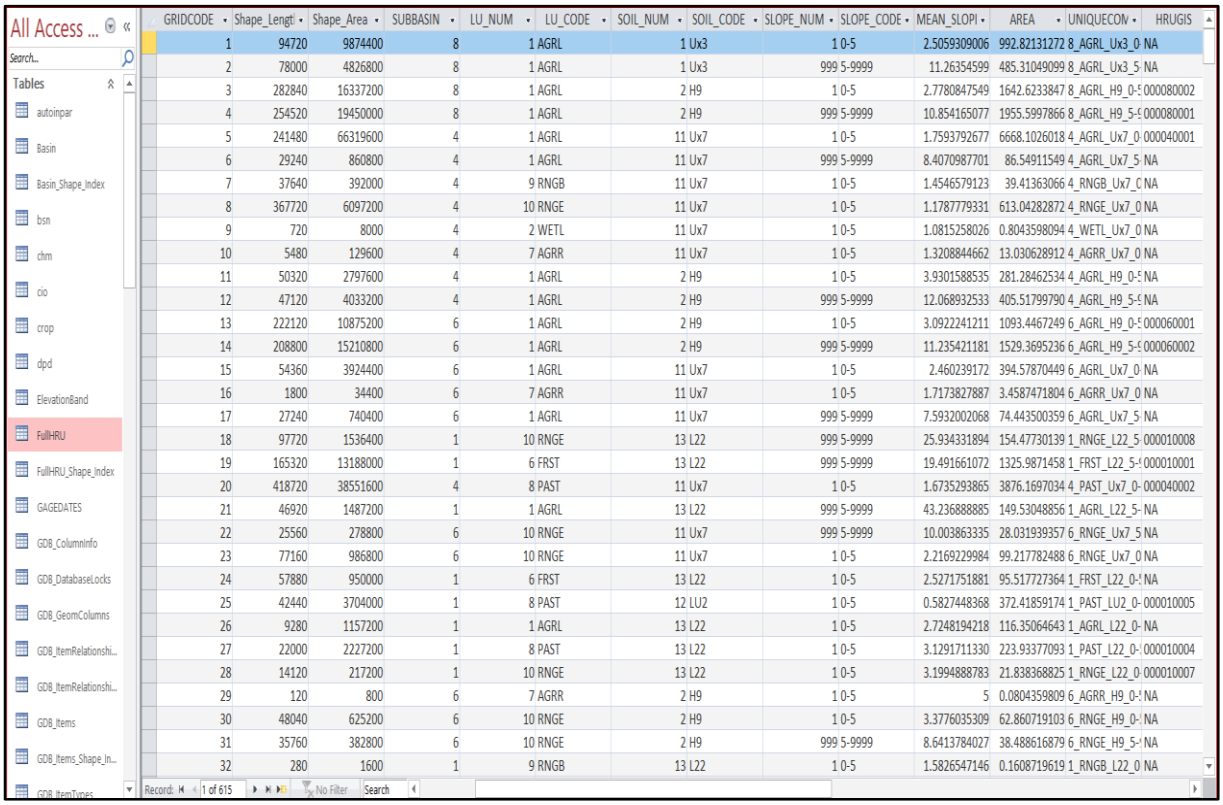

GRIDCODE	Shape_Lengt	Shape_Area	SUBBASIN	LU_NUM	LU_CODE	SOIL_NUM	SOIL_CODE	SLOPE_NUM	SLOPE_CODE	MEAN_SLOPI	AREA	UNIQUECON	HRUGIS
1	94720	9874400	8	1	AGRL	1	Ux3	1	0-5	2.5059309006	992.82131272	8_AGRL_Ux3_0	NA
2	78000	4826800	8	1	AGRL	1	Ux3	999	5-9999	11.26354599	485.31049099	8_AGRL_Ux3_5	NA
3	282840	16337200	8	1	AGRL	2	H9	1	0-5	2.7780847549	1642.6233847	8_AGRL_H9_0-5	000080002
4	254520	19450000	8	1	AGRL	2	H9	999	5-9999	10.854165077	1955.5997866	8_AGRL_H9_5-9	000080001
5	241480	66319600	4	1	AGRL	11	Ux7	1	0-5	1.7593792677	6668.1026018	4_AGRL_Ux7_0	000040001
6	29240	860800	4	1	AGRL	11	Ux7	999	5-9999	8.4070987701	86.54911549	4_AGRL_Ux7_5	NA
7	37640	392000	4	9	RNGB	11	Ux7	1	0-5	1.4546579123	39.41363066	4_RNGB_Ux7_0	NA
8	367720	6097200	4	10	RNGE	11	Ux7	1	0-5	1.1787779331	613.04282872	4_RNGE_Ux7_0	NA
9	720	8000	4	2	WETL	11	Ux7	1	0-5	1.0815258026	0.8043598094	4_WETL_Ux7_0	NA
10	5480	129600	4	7	AGRR	11	Ux7	1	0-5	1.3208844662	13.030628912	4_AGRR_Ux7_0	NA
11	50320	2797600	4	1	AGRL	2	H9	1	0-5	3.9301588535	281.28462534	4_AGRL_H9_0-5	NA
12	47120	4033200	4	1	AGRL	2	H9	999	5-9999	12.068932533	405.51799790	4_AGRL_H9_5-9	NA
13	222120	10875200	6	1	AGRL	2	H9	1	0-5	3.0922241211	1093.4467249	6_AGRL_H9_0-5	000060001
14	208800	15210800	6	1	AGRL	2	H9	999	5-9999	11.235421181	1529.3695236	6_AGRL_H9_5-9	000060002
15	54360	3924400	6	1	AGRL	11	Ux7	1	0-5	2.460239172	394.57870449	6_AGRL_Ux7_0	NA
16	1800	34400	6	7	AGRR	11	Ux7	1	0-5	1.7173827887	3.4587471804	6_AGRR_Ux7_0	NA
17	27240	740400	6	1	AGRL	11	Ux7	999	5-9999	7.5932002068	74.443500359	6_AGRL_Ux7_5	NA
18	97720	1536400	1	10	RNGE	13	L22	999	5-9999	25.934331894	154.47730139	1_RNGE_L22_5	000010008
19	165320	13188000	1	6	FRST	13	L22	999	5-9999	19.491661072	1325.9871458	1_FRST_L22_5-9	000010001
20	418720	38551600	4	8	PAST	11	Ux7	1	0-5	1.6735293865	3876.1697034	4_PAST_Ux7_0-	000040002
21	46920	1487200	1	1	AGRL	13	L22	999	5-9999	43.236888885	149.53048856	1_AGRL_L22_5-	NA
22	25560	278800	6	10	RNGE	11	Ux7	999	5-9999	10.003863335	28.031939357	6_RNGE_Ux7_5	NA
23	77160	986800	6	10	RNGE	11	Ux7	1	0-5	2.2169229984	99.217782488	6_RNGE_Ux7_0	NA
24	57880	950000	1	6	FRST	13	L22	1	0-5	2.5271751881	95.517727364	1_FRST_L22_0-5	NA
25	42440	3704000	1	8	PAST	12	LU2	1	0-5	0.5827448368	372.41859174	1_PAST_LU2_0-	000010005
26	9280	1157200	1	1	AGRL	13	L22	1	0-5	2.7248194218	116.35064643	1_AGRL_L22_0-	NA
27	22000	2227200	1	8	PAST	13	L22	1	0-5	3.1291711330	223.93377093	1_PAST_L22_0-	000010004
28	14120	217200	1	10	RNGE	13	L22	1	0-5	3.1994888783	21.838368825	1_RNGE_L22_0	000010007
29	120	800	6	7	AGRR	2	H9	1	0-5	5	0.0804359809	6_AGRR_H9_0-5	NA
30	48040	625200	6	10	RNGE	2	H9	1	0-5	3.3776035309	62.860719103	6_RNGE_H9_0-5	NA
31	35760	382800	6	10	RNGE	2	H9	999	5-9999	8.6413784027	38.488616879	6_RNGE_H9_5-9	NA
32	280	1600	1	9	RNGB	13	L22	1	0-5	1.5826547146	0.1608719619	1_RNGB_L22_0	NA

FullHRU

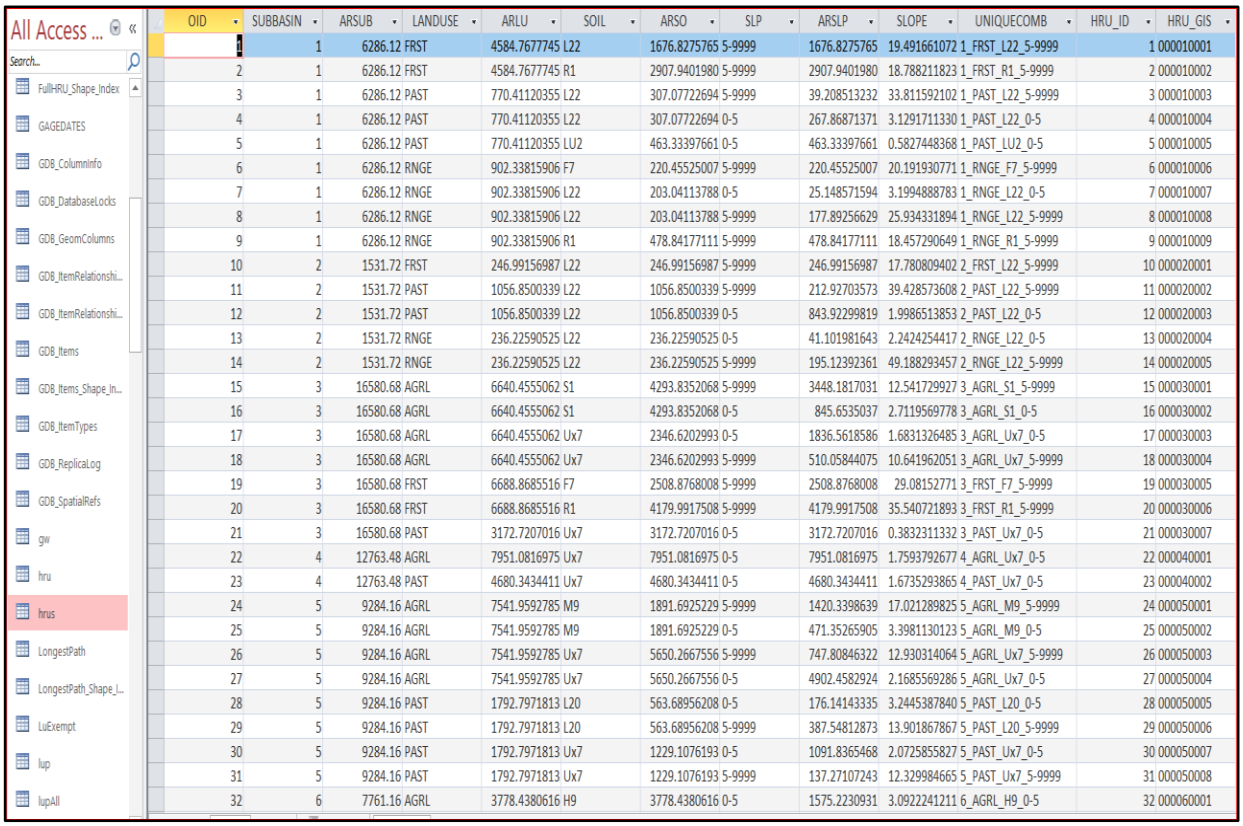

OID	SUBBASIN	ARSUB	LANDUSE	ARLU	SOIL	ARSO	SLP	ARSLP	SLOPE	UNIQUECOMB	HRU_ID	HRU_GIS
1	1	6286.12	FRST	4584.7677745	L22	1676.8275765	5-9999	1676.8275765	19.491661072	1_FRST_L22_5-9999	1	000010001
2	1	6286.12	FRST	4584.7677745	R1	2907.9401980	5-9999	2907.9401980	18.788211823	1_FRST_R1_5-9999	2	000010002
3	1	6286.12	PAST	770.41120355	L22	307.07722694	5-9999	39.208513232	33.811592102	1_PAST_L22_5-9999	3	000010003
4	1	6286.12	PAST	770.41120355	L22	307.07722694	0-5	267.86871371	3.1291711330	1_PAST_L22_0-5	4	000010004
5	1	6286.12	PAST	770.41120355	LU2	463.33397661	0-5	463.33397661	0.5827448368	1_PAST_LU2_0-5	5	000010005
6	1	6286.12	RNGE	902.33815906	F7	220.45525007	5-9999	220.45525007	20.191930771	1_RNGE_F7_5-9999	6	000010006
7	1	6286.12	RNGE	902.33815906	L22	203.04113788	0-5	25.148571594	3.1994888783	1_RNGE_L22_0-5	7	000010007
8	1	6286.12	RNGE	902.33815906	L22	203.04113788	5-9999	177.89256629	25.934331894	1_RNGE_L22_5-9999	8	000010008
9	1	6286.12	RNGE	902.33815906	R1	478.84177111	5-9999	478.84177111	18.457290649	1_RNGE_R1_5-9999	9	000010009
10	2	1531.72	FRST	246.99156987	L22	246.99156987	5-9999	246.99156987	17.780809402	2_FRST_L22_5-9999	10	000020001
11	2	1531.72	PAST	1056.8500339	L22	1056.8500339	5-9999	212.92703573	39.428573608	2_PAST_L22_5-9999	11	000020002
12	2	1531.72	PAST	1056.8500339	L22	1056.8500339	0-5	843.92299819	1.9986513853	2_PAST_L22_0-5	12	000020003
13	2	1531.72	RNGE	236.22590525	L22	236.22590525	0-5	41.101981643	2.2424254417	2_RNGE_L22_0-5	13	000020004
14	2	1531.72	RNGE	236.22590525	L22	236.22590525	5-9999	195.12392361	49.188293457	2_RNGE_L22_5-9999	14	000020005
15	3	16580.68	AGRL	6640.4555062	S1	4293.8352068	5-9999	3448.1817031	12.541729927	3_AGRL_S1_5-9999	15	000030001
16	3	16580.68	AGRL	6640.4555062	S1	4293.8352068	0-5	845.6535037	2.7119569778	3_AGRL_S1_0-5	16	000030002
17	3	16580.68	AGRL	6640.4555062	Ux7	2346.6202993	0-5	1836.5618586	1.6831326485	3_AGRL_Ux7_0-5	17	000030003
18	3	16580.68	AGRL	6640.4555062	Ux7	2346.6202993	5-9999	510.05844075	10.641962051	3_AGRL_Ux7_5-9999	18	000030004
19	3	16580.68	FRST	6688.8685516	F7	2508.8768008	5-9999	2508.8768008	29.08152771	3_FRST_F7_5-9999	19	000030005
20	3	16580.68	FRST	6688.8685516	R1	4179.9917508	5-9999	4179.9917508	35.540721893	3_FRST_R1_5-9999	20	000030006
21	3	16580.68	PAST	3172.7207016	Ux7	3172.7207016	0-5	3172.7207016	0.3832311332	3_PAST_Ux7_0-5	21	000030007
22	4	12763.48	AGRL	7951.0816975	Ux7	7951.0816975	0-5	7951.0816975	1.7593792677	4_AGRL_Ux7_0-5	22	000040001
23	4	12763.48	PAST	4680.3434411	Ux7	4680.3434411	0-5	4680.3434411	1.6735293865	4_PAST_Ux7_0-5	23	000040002
24	5	9284.16	AGRL	7541.9592785	M9	1891.6925229	5-9999	1420.3398639	17.021289825	5_AGRL_M9_5-9999	24	000050001
25	5	9284.16	AGRL	7541.9592785	M9	1891.6925229	0-5	471.35265905	3.3981130123	5_AGRL_M9_0-5	25	000050002
26	5	9284.16	AGRL	7541.9592785	Ux7	5650.2667556	5-9999	747.80846322	12.930314064	5_AGRL_Ux7_5-9999	26	000050003
27	5	9284.16	AGRL	7541.9592785	Ux7	5650.2667556	0-5	4902.4582924	2.1685569286	5_AGRL_Ux7_0-5	27	000050004
28	5	9284.16	PAST	1792.7971813	L20	563.68956208	0-5	176.14143335	3.2445387840	5_PAST_L20_0-5	28	000050005
29	5	9284.16	PAST	1792.7971813	L20	563.68956208	5-9999	387.54812873	13.901867867	5_PAST_L20_5-9999	29	000050006
30	5	9284.16	PAST	1792.7971813	Ux7	1229.1076193	0-5	1091.8365468	2.0725855827	5_PAST_Ux7_0-5	30	000050007
31	5	9284.16	PAST	1792.7971813	Ux7	1229.1076193	5-9999	137.27107243	12.329984665	5_PAST_Ux7_5-9999	31	000050008
32	6	7761.16	AGRL	3778.4380616	H9	3778.4380616	0-5	1575.2230931	3.0922241211	6_AGRL_H9_0-5	32	000060001

hrus

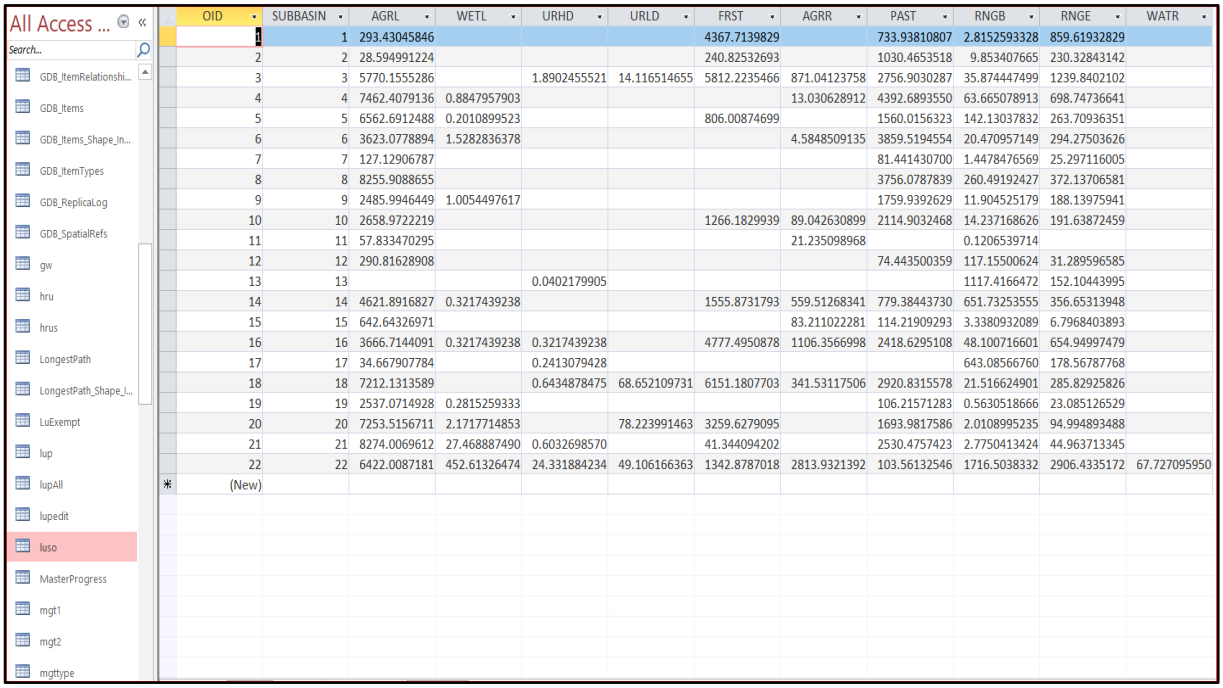

OID	SUBBASIN	AGRL	WETL	URHD	URLD	FRST	AGRR	PAST	RNGB	RNGE	WATR
1	1	293.43045846				4367.7139829		733.93810807	2.8152593328	859.61932829	
2	2	28.594991224				240.82532693		1030.4653518	9.853407665	230.32843142	
3	3	5770.1555286		1.8902455521	14.116514655	5812.2235466	871.04123758	2756.9030287	35.874447499	1239.8402102	
4	4	7462.4079136	0.8847957903				13.030628912	4392.6893550	63.665078913	698.74736641	
5	5	6562.6912488	0.2010899523			806.00874699		1560.0156323	142.13037832	263.70936351	
6	6	3623.0778894	1.5282836378				4.5848509135	3859.5194554	20.470957149	294.27503626	
7	7	127.12906787						81.441430700	1.4478476569	25.297116005	
8	8	8255.9088655						3756.0787839	260.49192427	372.13706581	
9	9	2485.9946449	1.0054497617					1759.9392629	11.904525179	188.13975941	
10	10	2658.9722219				1266.1829939	89.042630899	2114.9032468	14.237168626	191.63872459	
11	11	57.833470295					21.235098968		0.1206539714		
12	12	290.81628908						74.443500359	117.15500624	31.289596585	
13	13			0.0402179905					1117.4166472	152.10443995	
14	14	4621.8916827	0.3217439238			1555.8731793	559.51268341	779.38443730	651.73253555	356.65313948	
15	15	642.64326971					83.211022281	114.21909293	3.3380932089	6.7968403893	
16	16	3666.7144091	0.3217439238	0.3217439238		4777.4950878	1106.3566998	2418.6295108	48.100716601	654.94997479	
17	17	34.667907784		0.2413079428					643.08566760	178.56787768	
18	18	7212.1313589		0.6434878475	68.652109731	6151.1807703	341.53117506	2920.8315578	21.516624901	285.82925826	
19	19	2537.0714928	0.2815259333					106.21571283	0.5630518666	23.085126529	
20	20	7253.5156711	2.1717714853		78.223991463	3259.6279095		1693.9817586	2.0108995235	94.994893488	
21	21	8274.0069612	27.468887490	0.6032698570		41.344094202		2530.4757423	2.7750413424	44.963713345	
22	22	6422.0087181	452.61326474	24.331884234	49.106166363	1342.8787018	2813.9321392	103.56132546	1716.5038332	2906.4335172	67.727095950
(New)											

luso

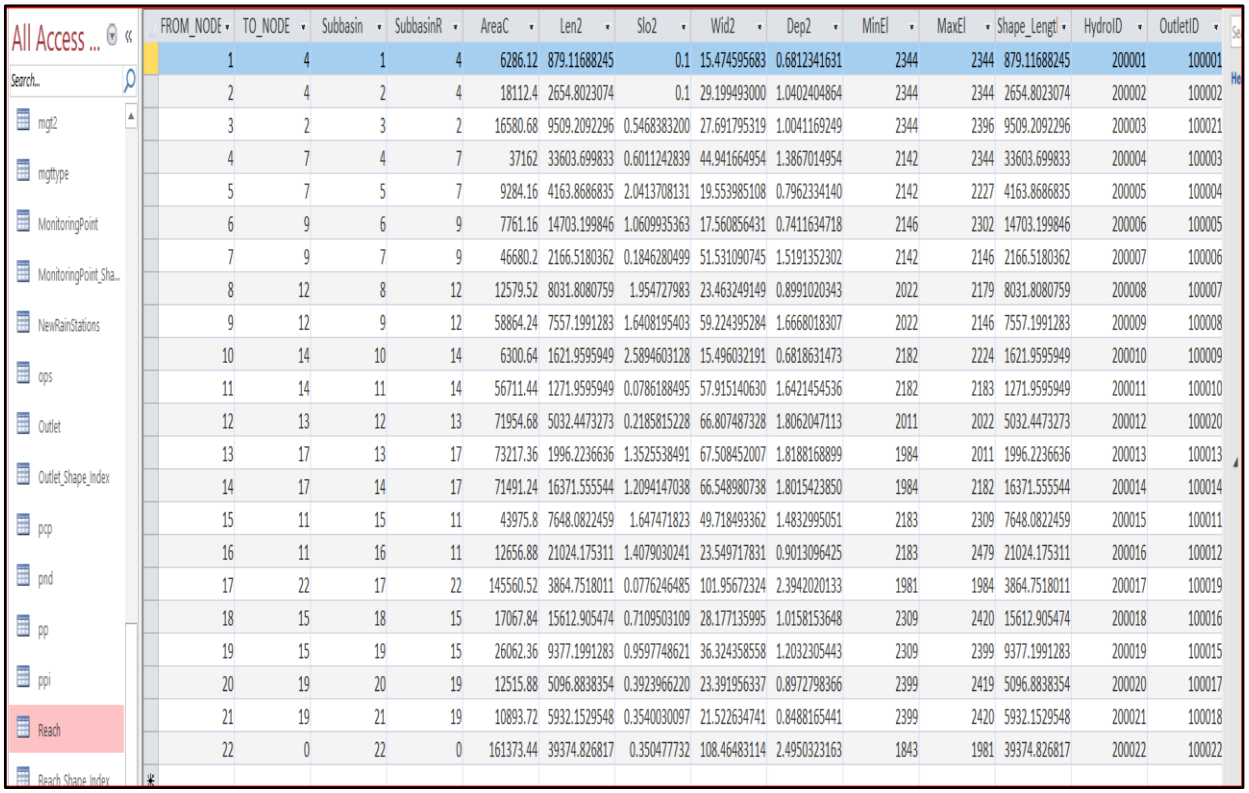

FROM_NODE	TO_NODE	Subbasin	SubbasinR	AreaC	Len2	Slo2	Wid2	Dep2	MinEl	MaxEl	Shape_Lengt	HydroID	OutletID
1	4	1	4	6286.12	879.11688245	0.1	15.474595683	0.6812341631	2344	2344	879.11688245	200001	100001
2	4	2	4	18112.4	2654.8023074	0.1	29.199493000	1.0402404864	2344	2344	2654.8023074	200002	100002
3	2	3	2	16580.68	9509.2092296	0.5468383200	27.691795319	1.0041169249	2344	2396	9509.2092296	200003	100021
4	7	4	7	37162	33603.699833	0.6011242839	44.941664954	1.3867014954	2142	2344	33603.699833	200004	100003
5	7	5	7	9284.16	4163.8686835	2.0413708131	19.553985108	0.7962334140	2142	2227	4163.8686835	200005	100004
6	9	6	9	7761.16	14703.199846	1.0609935363	17.560856431	0.7411634718	2146	2302	14703.199846	200006	100005
7	9	7	9	46680.2	2166.5180362	0.1846280499	51.531090745	1.5191352302	2142	2146	2166.5180362	200007	100006
8	12	8	12	12579.52	8031.8080759	1.954727983	23.463249149	0.8991020343	2022	2179	8031.8080759	200008	100007
9	12	9	12	58864.24	7557.1991283	1.6408195403	59.224395284	1.6668018307	2022	2146	7557.1991283	200009	100008
10	14	10	14	6300.64	1621.9595949	2.5894603128	15.496032191	0.6818631473	2182	2224	1621.9595949	200010	100009
11	14	11	14	56711.44	1271.9595949	0.0786188495	57.915140630	1.6421454536	2182	2183	1271.9595949	200011	100010
12	13	12	13	71954.68	5032.4473273	0.2185815228	66.807487328	1.8062047113	2011	2022	5032.4473273	200012	100020
13	17	13	17	73217.36	1996.2236636	1.3525538491	67.508452007	1.8188168899	1984	2011	1996.2236636	200013	100013
14	17	14	17	71491.24	16371.555544	1.2094147038	66.548980738	1.8015423850	1984	2182	16371.555544	200014	100014
15	11	15	11	43975.8	7648.0822459	1.647471823	49.718493362	1.4832995051	2183	2309	7648.0822459	200015	100011
16	11	16	11	12656.88	21024.175311	1.4079030241	23.549717831	0.9013096425	2183	2479	21024.175311	200016	100012
17	22	17	22	145560.52	3864.7518011	0.0776246485	101.95672324	2.3942020133	1981	1984	3864.7518011	200017	100019
18	15	18	15	17067.84	15612.905474	0.7109503109	28.177135995	1.0158153648	2309	2420	15612.905474	200018	100016
19	15	19	15	26062.36	9377.1991283	0.9597748621	36.324358558	1.2032305443	2309	2399	9377.1991283	200019	100015
20	19	20	19	12515.88	5096.8838354	0.3923966220	23.391956337	0.8972798366	2399	2419	5096.8838354	200020	100017
21	19	21	19	10893.72	5932.1529548	0.3540030097	21.522634741	0.8488165441	2399	2420	5932.1529548	200021	100018
22	0	22	0	161373.44	39374.826817	0.350477732	108.46483114	2.4950323163	1843	1981	39374.826817	200022	100022

Reach

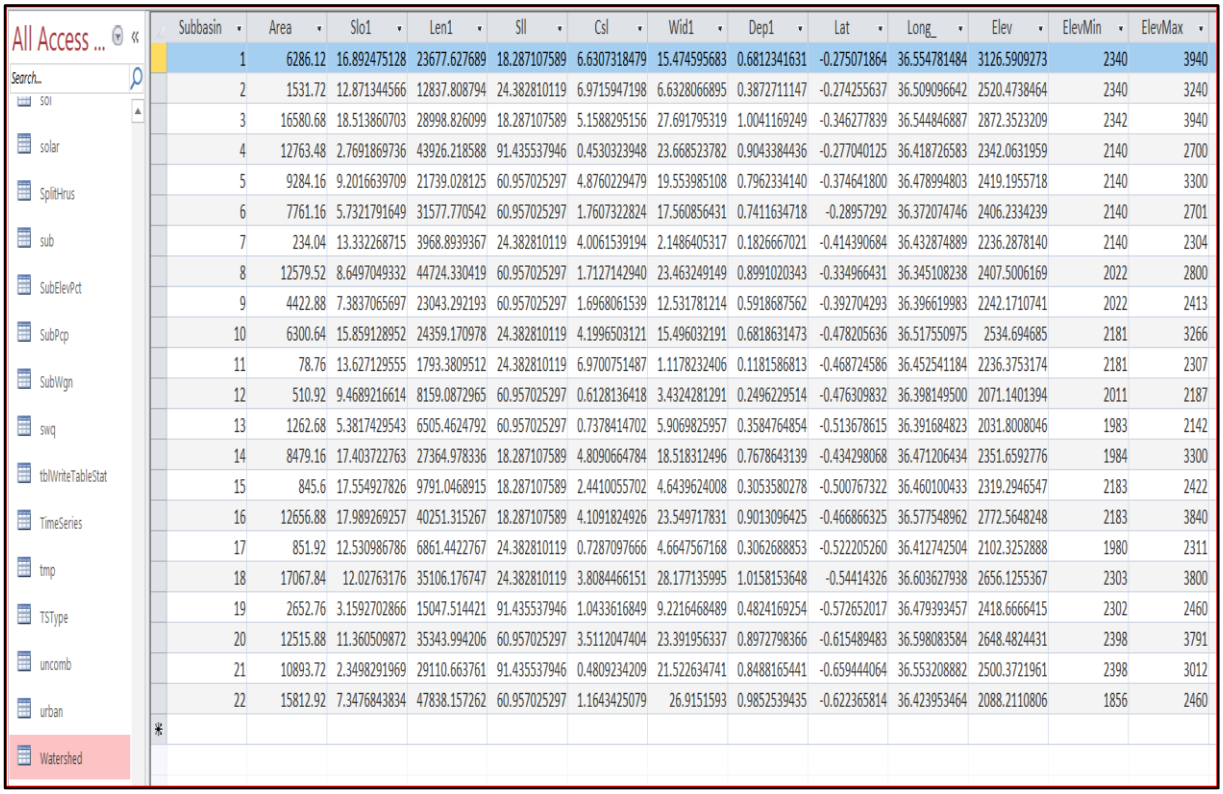

Subbasin	Area	Slo1	Len1	Sll	Csl	Wid1	Dep1	Lat	Long_	Elev	ElevMin	ElevMax
1	6286.12	16.892475128	23677.627689	18.287107589	6.6307318479	15.474595683	0.6812341631	-0.275071864	36.554781484	3126.5909273	2340	3940
2	1531.72	12.871344566	12837.808794	24.382810119	6.9715947198	6.6328066895	0.3872711147	-0.274255637	36.509096642	2520.4738464	2340	3240
3	16580.68	18.513860703	28998.826099	18.287107589	5.1588295156	27.691795319	1.0041169249	-0.346277839	36.544846887	2872.3523209	2342	3940
4	12763.48	2.7691869736	43926.218588	91.435537946	0.4530323948	23.668523782	0.9043384436	-0.277040125	36.418726583	2342.0631959	2140	2700
5	9284.16	9.2016639709	21739.028125	60.957025297	4.8760229479	19.553985108	0.7962334140	-0.374641800	36.478994803	2419.1955718	2140	3300
6	7761.16	5.7321791649	31577.770542	60.957025297	1.7607322824	17.560856431	0.7411634718	-0.28957292	36.372074746	2406.2334239	2140	2701
7	234.04	13.332268715	3968.8939367	24.382810119	4.0061539194	2.1486405317	0.1826667021	-0.414390684	36.432874889	2236.2878140	2140	2304
8	12579.52	8.6497049332	44724.330419	60.957025297	1.7127142940	23.463249149	0.8991020343	-0.334966431	36.345108238	2407.5006169	2022	2800
9	4422.88	7.3837065697	23043.292193	60.957025297	1.6968061539	12.531781214	0.5918687562	-0.392704293	36.396619983	2242.1710741	2022	2413
10	6300.64	15.859128952	24359.170978	24.382810119	4.1996503121	15.496032191	0.6818631473	-0.478205636	36.517550975	2534.694685	2181	3266
11	78.76	13.627129555	1793.3809512	24.382810119	6.9700751487	1.1178232406	0.1181586813	-0.468724586	36.452541184	2236.3753174	2181	2307
12	510.92	9.4689216614	8159.0872965	60.957025297	0.6128136418	3.4324281291	0.2496229514	-0.476309832	36.398149500	2071.1401394	2011	2187
13	1262.68	5.3817429543	6505.4624792	60.957025297	0.7378414702	5.9069825957	0.3584764854	-0.513678615	36.391684823	2031.8008046	1983	2142
14	8479.16	17.403722763	27364.978336	18.287107589	4.8090664784	18.518312496	0.7678643139	-0.434298068	36.471206434	2351.6592776	1984	3300
15	845.6	17.554927826	9791.0468915	18.287107589	2.4410055702	4.6439624008	0.3053580278	-0.500767322	36.460100433	2319.2946547	2183	2422
16	12656.88	17.989269257	40251.315267	18.287107589	4.1091824926	23.549717831	0.9013096425	-0.466866325	36.577548962	2772.5648248	2183	3840
17	851.92	12.530986786	6861.4422767	24.382810119	0.7287097666	4.6647567168	0.3062688853	-0.522205260	36.412742504	2102.3252888	1980	2311
18	17067.84	12.02763176	35106.176747	24.382810119	3.8084466151	28.177135995	1.0158153648	-0.54414326	36.603627938	2656.1255367	2303	3800
19	2652.76	3.1592702866	15047.514421	91.435537946	1.0433616849	9.2216468489	0.4824169254	-0.572652017	36.479393457	2418.6666415	2302	2460
20	12515.88	11.360509872	35343.994206	60.957025297	3.5112047404	23.391956337	0.8972798366	-0.615489483	36.598083584	2648.4824431	2398	3791
21	10893.72	2.3498291969	29110.663761	91.435537946	0.4809234209	21.522634741	0.8488165441	-0.659444064	36.553208882	2500.3721961	2398	3012
22	15812.92	7.3476843834	47838.157262	60.957025297	1.1643425079	26.9151593	0.9852539435	-0.622365814	36.423953464	2088.2110806	1856	2460

watershed

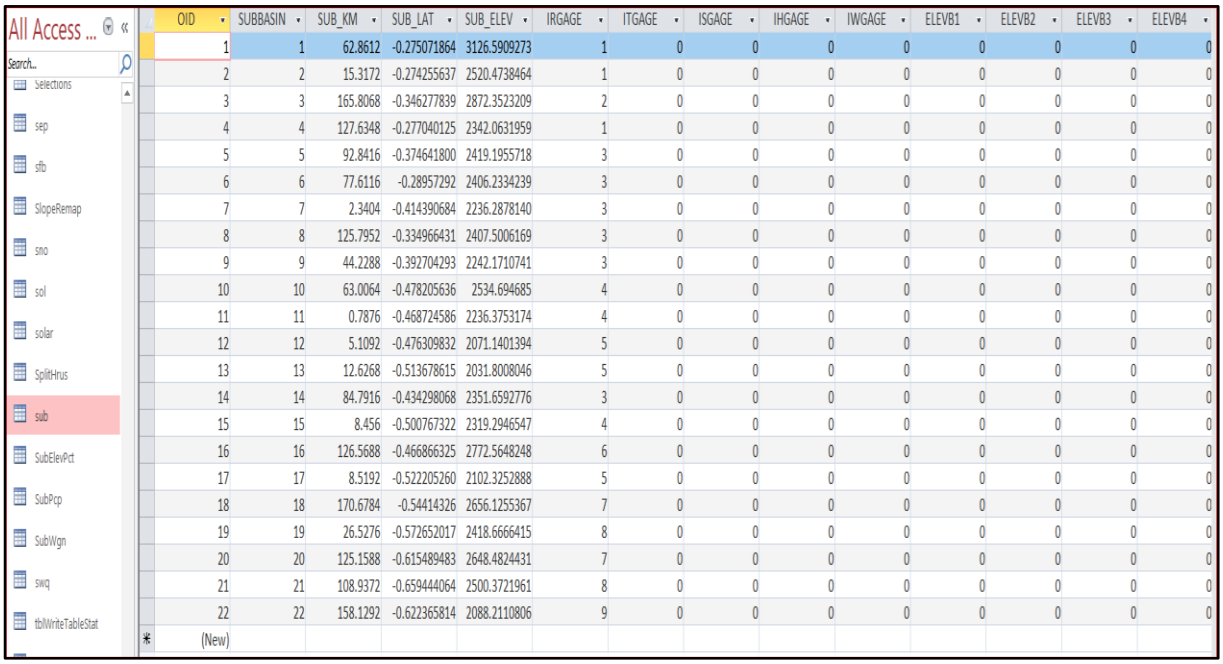

OID	SUBBASIN	SUB_KM	SUB_LAT	SUB_ELEV	IRGAGE	ITGAGE	ISGAGE	IHGAGE	IWGAGE	ELEVB1	ELEVB2	ELEVB3	ELEVB4
1	1	62.8612	-0.275071864	3126.5909273	1	0	0	0	0	0	0	0	0
2	2	15.3172	-0.274255637	2520.4738464	1	0	0	0	0	0	0	0	0
3	3	165.8068	-0.346277839	2872.3523209	2	0	0	0	0	0	0	0	0
4	4	127.6348	-0.277040125	2342.0631959	1	0	0	0	0	0	0	0	0
5	5	92.8416	-0.374641800	2419.1955718	3	0	0	0	0	0	0	0	0
6	6	77.6116	-0.28957292	2406.2334239	3	0	0	0	0	0	0	0	0
7	7	2.3404	-0.414390684	2236.2878140	3	0	0	0	0	0	0	0	0
8	8	125.7952	-0.334966431	2407.5006169	3	0	0	0	0	0	0	0	0
9	9	44.2288	-0.392704293	2242.1710741	3	0	0	0	0	0	0	0	0
10	10	63.0064	-0.478205636	2534.694685	4	0	0	0	0	0	0	0	0
11	11	0.7876	-0.468724586	2236.3753174	4	0	0	0	0	0	0	0	0
12	12	5.1092	-0.476309832	2071.1401394	5	0	0	0	0	0	0	0	0
13	13	12.6268	-0.513678615	2031.8008046	5	0	0	0	0	0	0	0	0
14	14	84.7916	-0.434298068	2351.6592776	3	0	0	0	0	0	0	0	0
15	15	8.456	-0.500767322	2319.2946547	4	0	0	0	0	0	0	0	0
16	16	126.5688	-0.466866325	2772.5648248	6	0	0	0	0	0	0	0	0
17	17	8.5192	-0.522205260	2102.3252888	5	0	0	0	0	0	0	0	0
18	18	170.6784	-0.54414326	2656.1255367	7	0	0	0	0	0	0	0	0
19	19	26.5276	-0.572652017	2418.6666415	8	0	0	0	0	0	0	0	0
20	20	125.1588	-0.615489483	2648.4824431	7	0	0	0	0	0	0	0	0
21	21	108.9372	-0.659444064	2500.3721961	8	0	0	0	0	0	0	0	0
22	22	158.1292	-0.622365814	2088.2110806	9	0	0	0	0	0	0	0	0
(New)													

sub

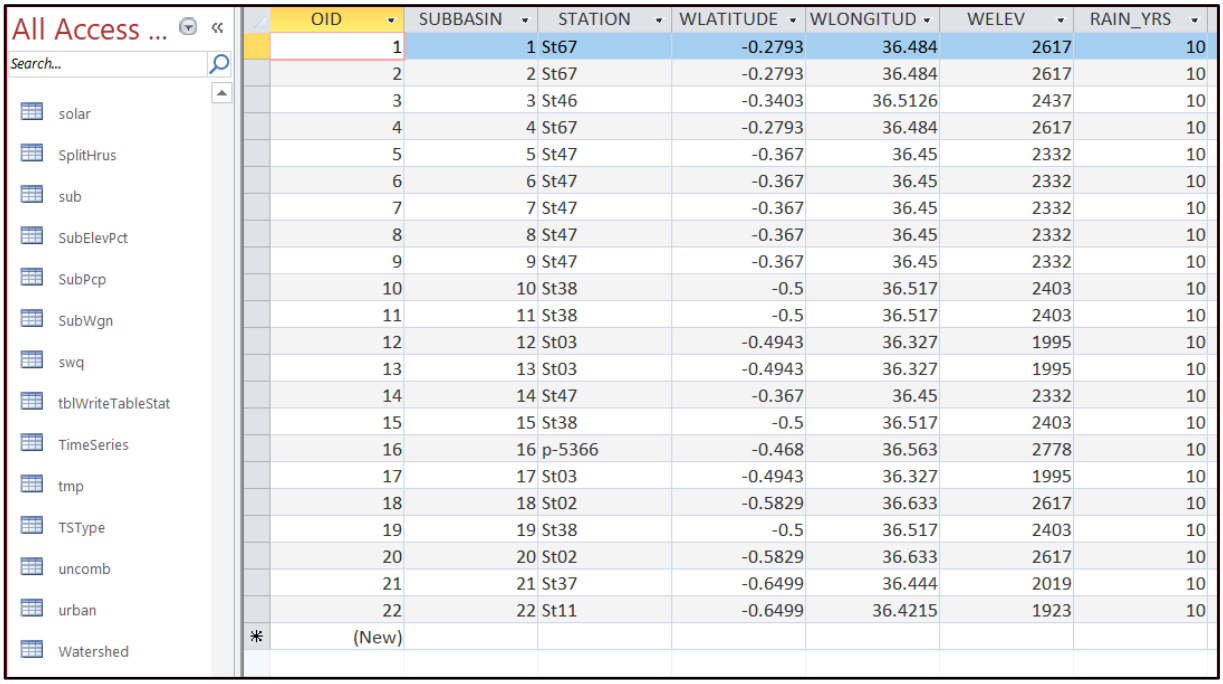

OID	SUBBASIN	STATION	WLATITUDE	WLONGITUD	WELEV	RAIN_YRS
1	1	St67	-0.2793	36.484	2617	10
2	2	St67	-0.2793	36.484	2617	10
3	3	St46	-0.3403	36.5126	2437	10
4	4	St67	-0.2793	36.484	2617	10
5	5	St47	-0.367	36.45	2332	10
6	6	St47	-0.367	36.45	2332	10
7	7	St47	-0.367	36.45	2332	10
8	8	St47	-0.367	36.45	2332	10
9	9	St47	-0.367	36.45	2332	10
10	10	St38	-0.5	36.517	2403	10
11	11	St38	-0.5	36.517	2403	10
12	12	St03	-0.4943	36.327	1995	10
13	13	St03	-0.4943	36.327	1995	10
14	14	St47	-0.367	36.45	2332	10
15	15	St38	-0.5	36.517	2403	10
16	16	p-5366	-0.468	36.563	2778	10
17	17	St03	-0.4943	36.327	1995	10
18	18	St02	-0.5829	36.633	2617	10
19	19	St38	-0.5	36.517	2403	10
20	20	St02	-0.5829	36.633	2617	10
21	21	St37	-0.6499	36.444	2019	10
22	22	St11	-0.6499	36.4215	1923	10
(New)						

wgn

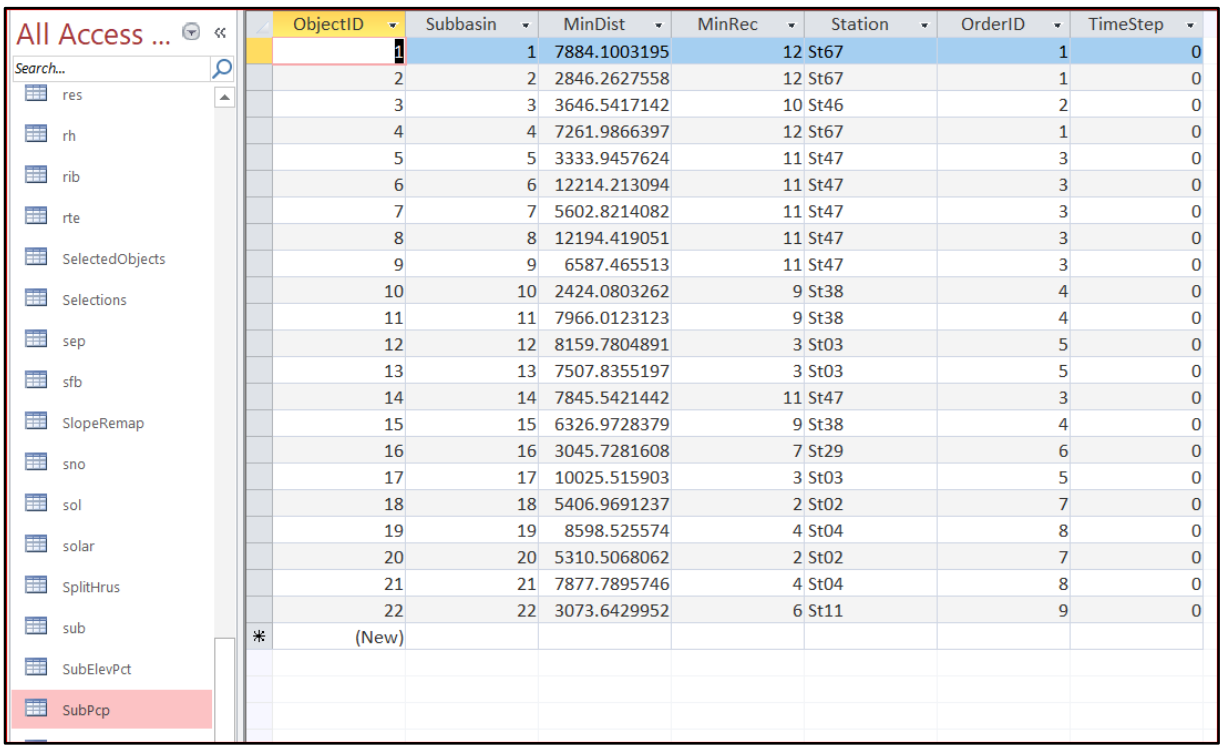

ObjectID	Subbasin	MinDist	MinRec	Station	OrderID	TimeStep
1	1	7884.1003195	12	St67	1	0
2	2	2846.2627558	12	St67	1	0
3	3	3646.5417142	10	St46	2	0
4	4	7261.9866397	12	St67	1	0
5	5	3333.9457624	11	St47	3	0
6	6	12214.213094	11	St47	3	0
7	7	5602.8214082	11	St47	3	0
8	8	12194.419051	11	St47	3	0
9	9	6587.465513	11	St47	3	0
10	10	2424.0803262	9	St38	4	0
11	11	7966.0123123	9	St38	4	0
12	12	8159.7804891	3	St03	5	0
13	13	7507.8355197	3	St03	5	0
14	14	7845.5421442	11	St47	3	0
15	15	6326.9728379	9	St38	4	0
16	16	3045.7281608	7	St29	6	0
17	17	10025.515903	3	St03	5	0
18	18	5406.9691237	2	St02	7	0
19	19	8598.525574	4	St04	8	0
20	20	5310.5068062	2	St02	7	0
21	21	7877.7895746	4	St04	8	0
22	22	3073.6429952	6	St11	9	0
(New)						

subPcp

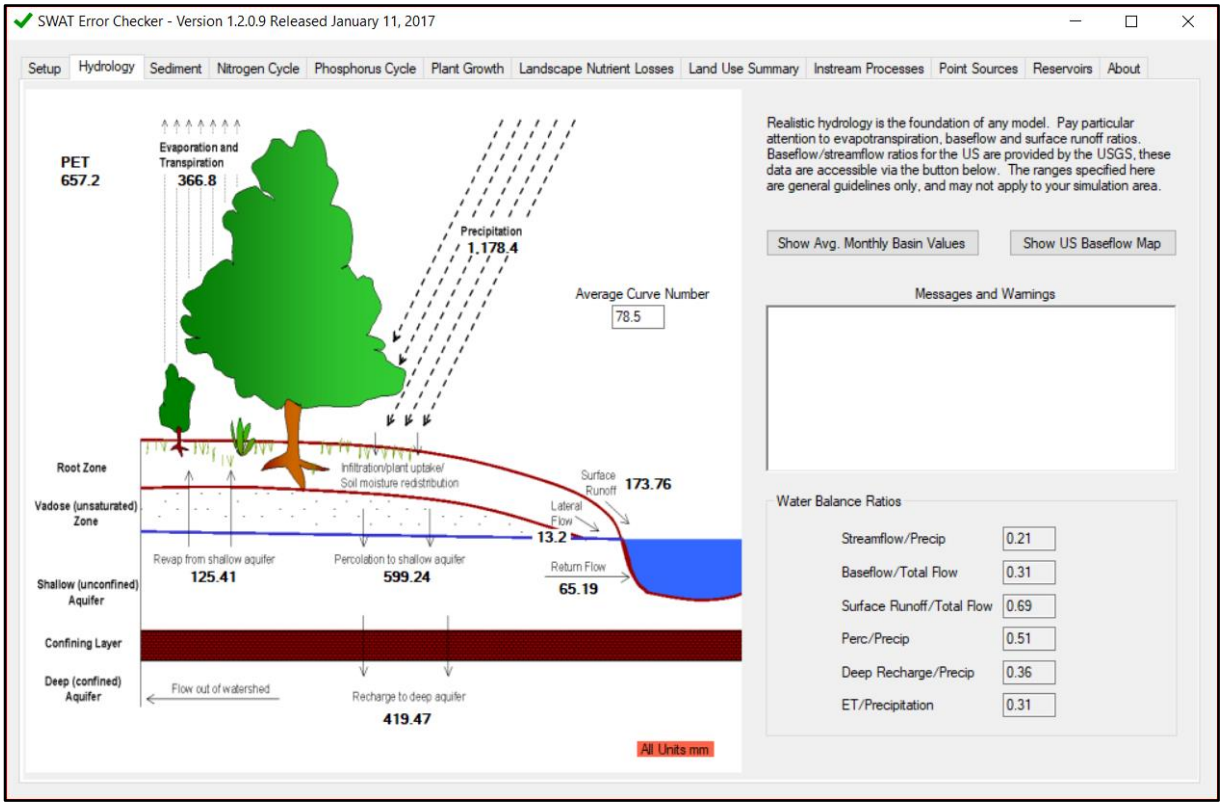

Waterbalance

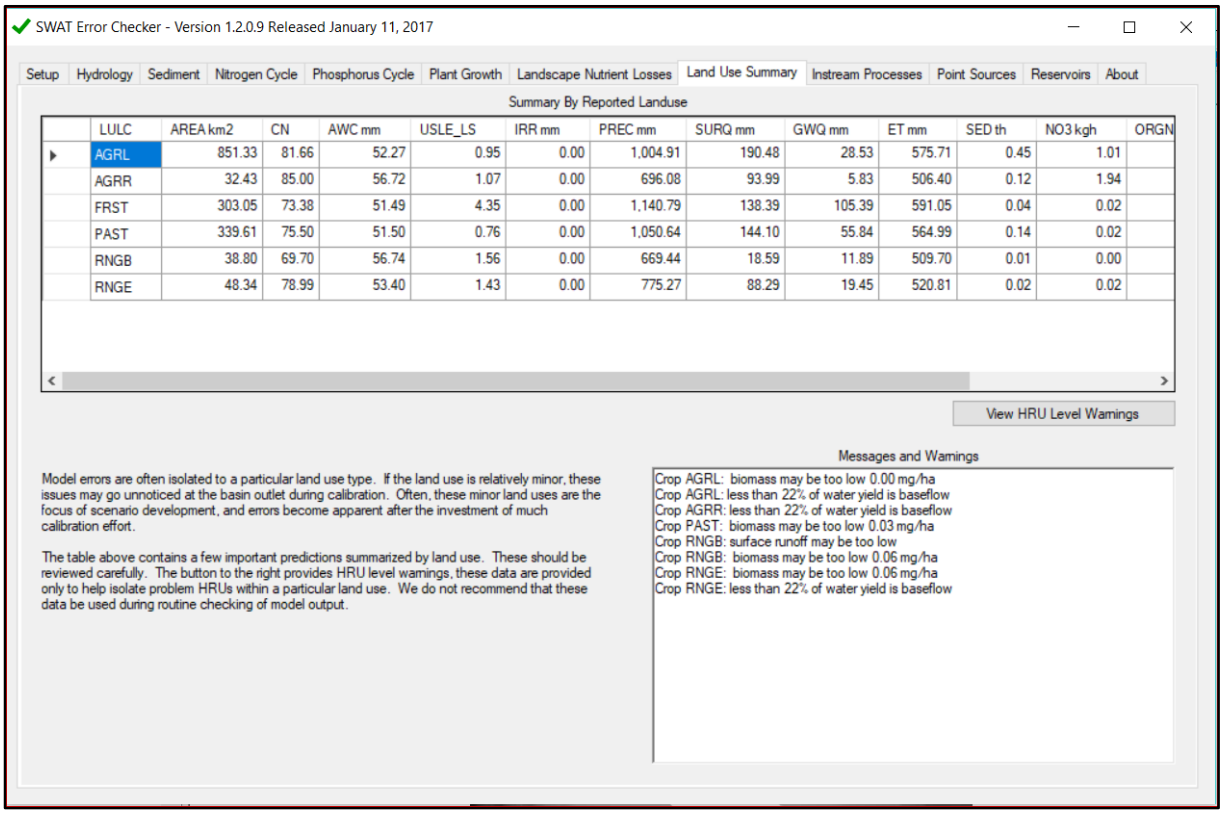

Land use summary

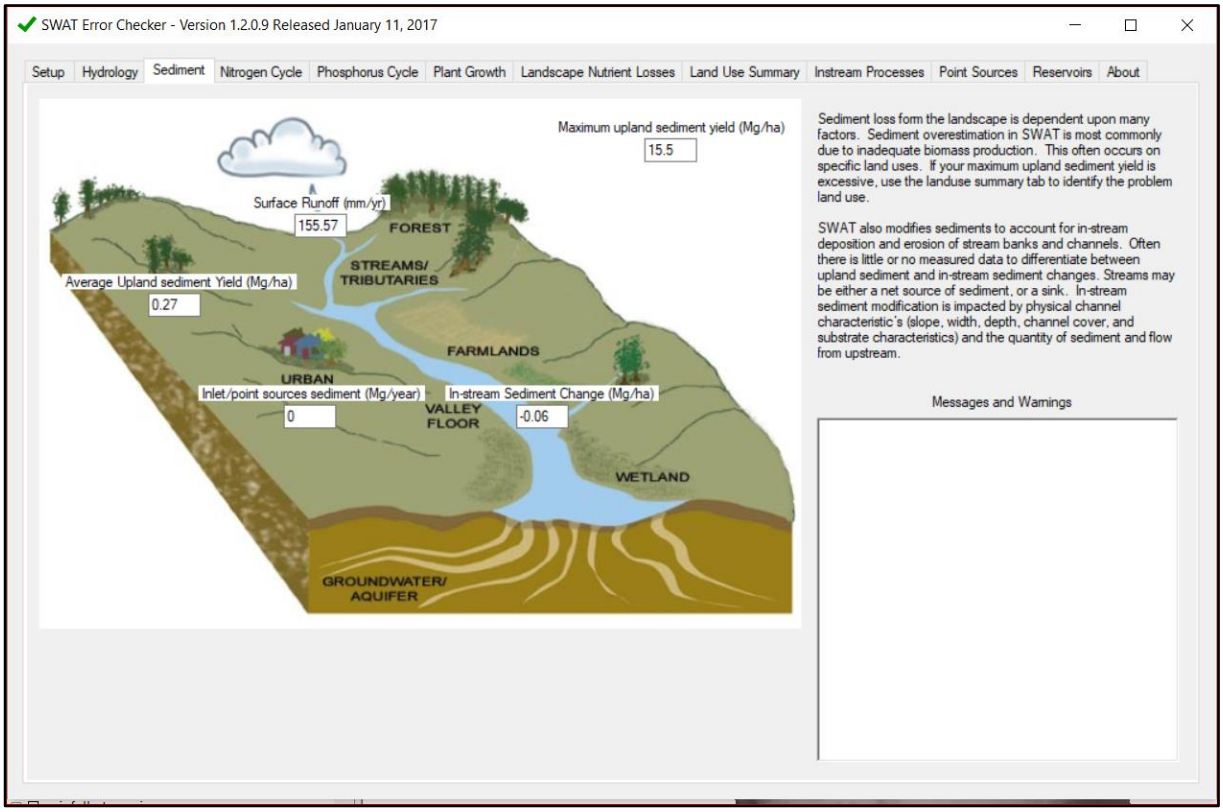

Sediment prdtn

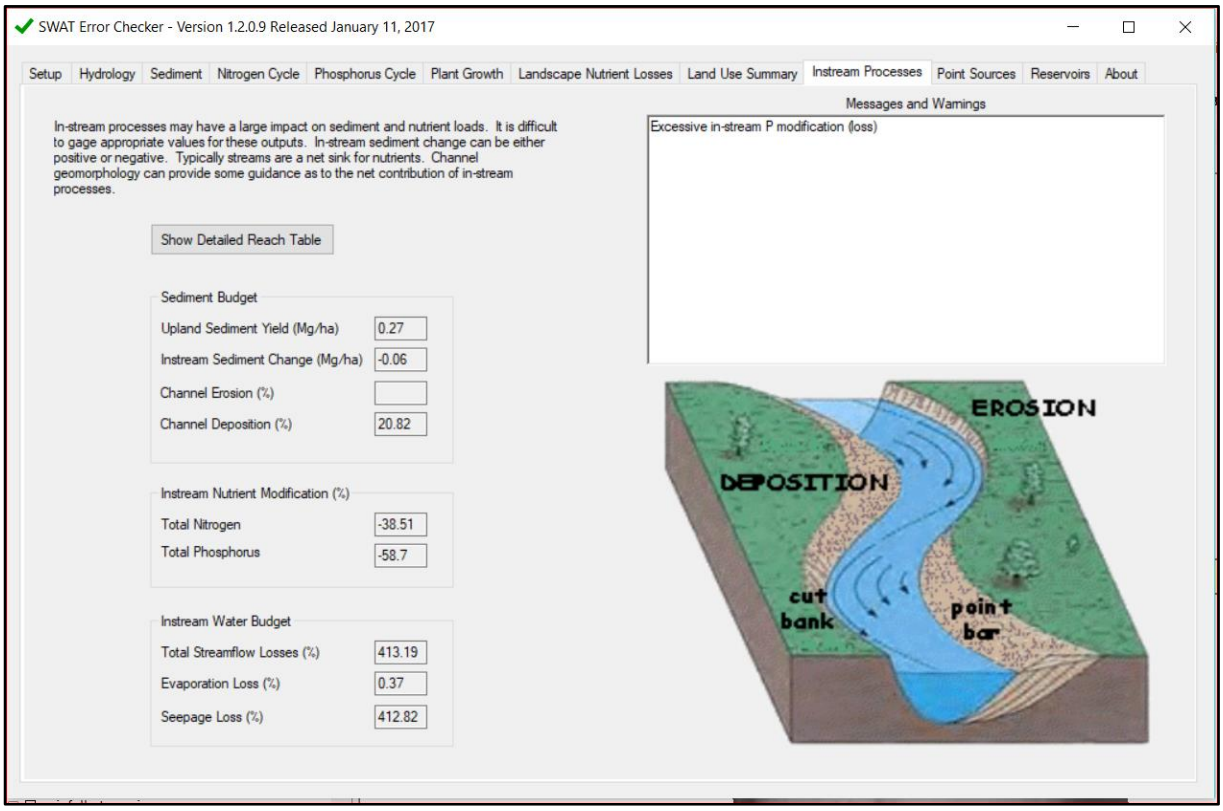

Instream processes

Appendix 4: Sub basins, Gauging stations and Rainfall stations in the watershed

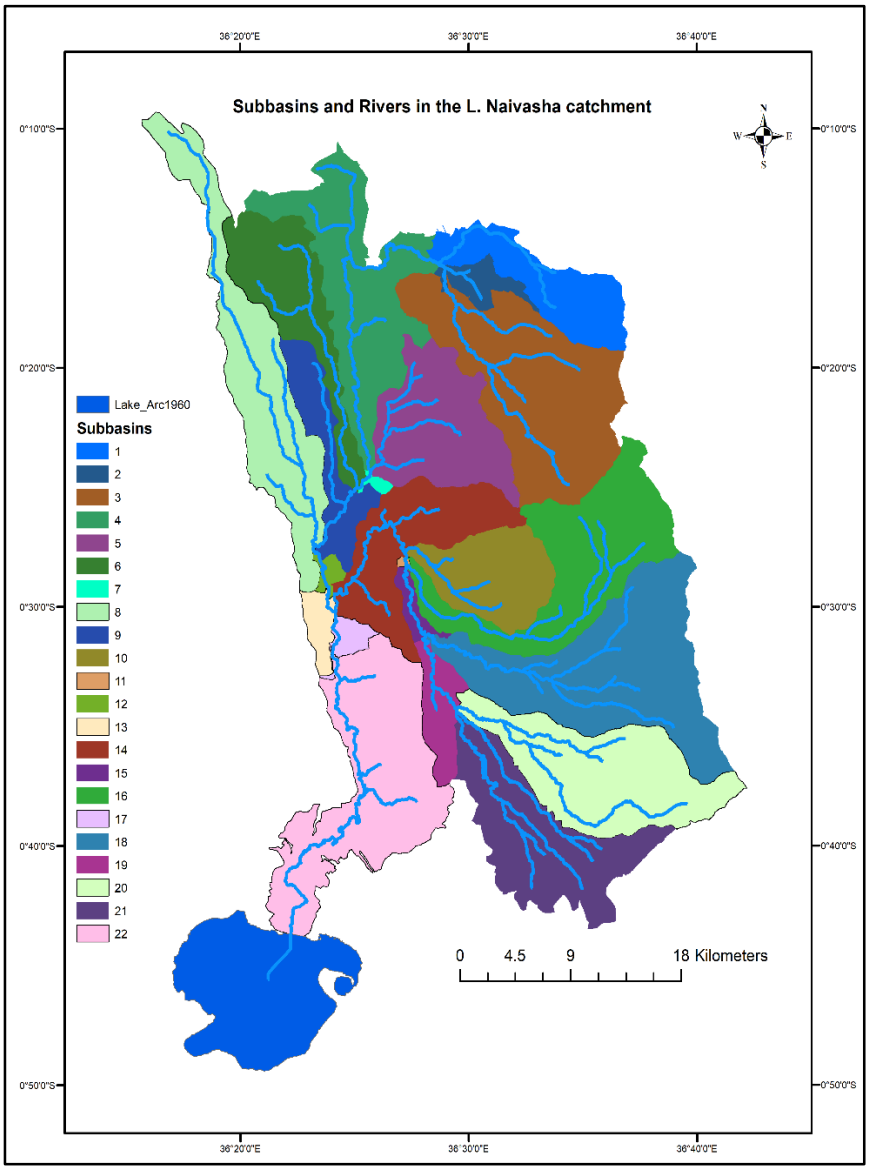

Sub basins and rivers

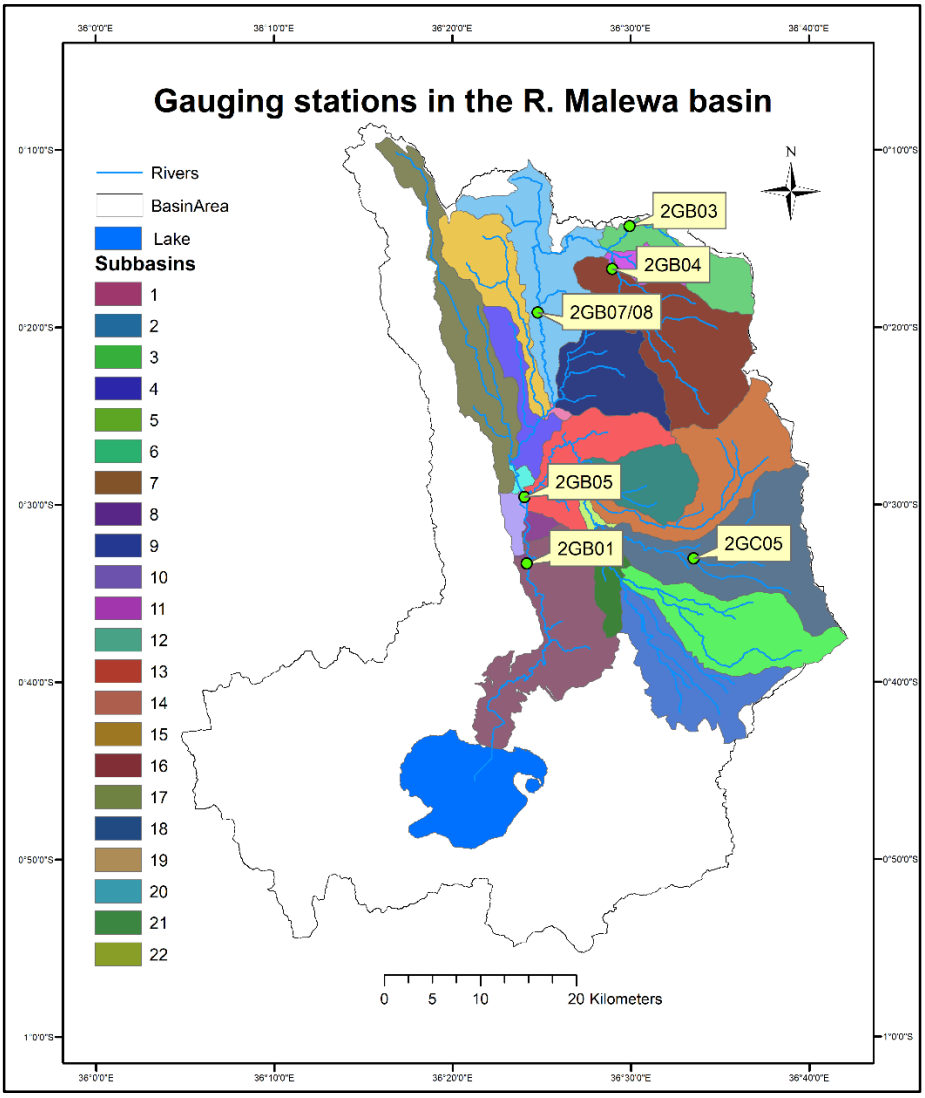

Gauging stations

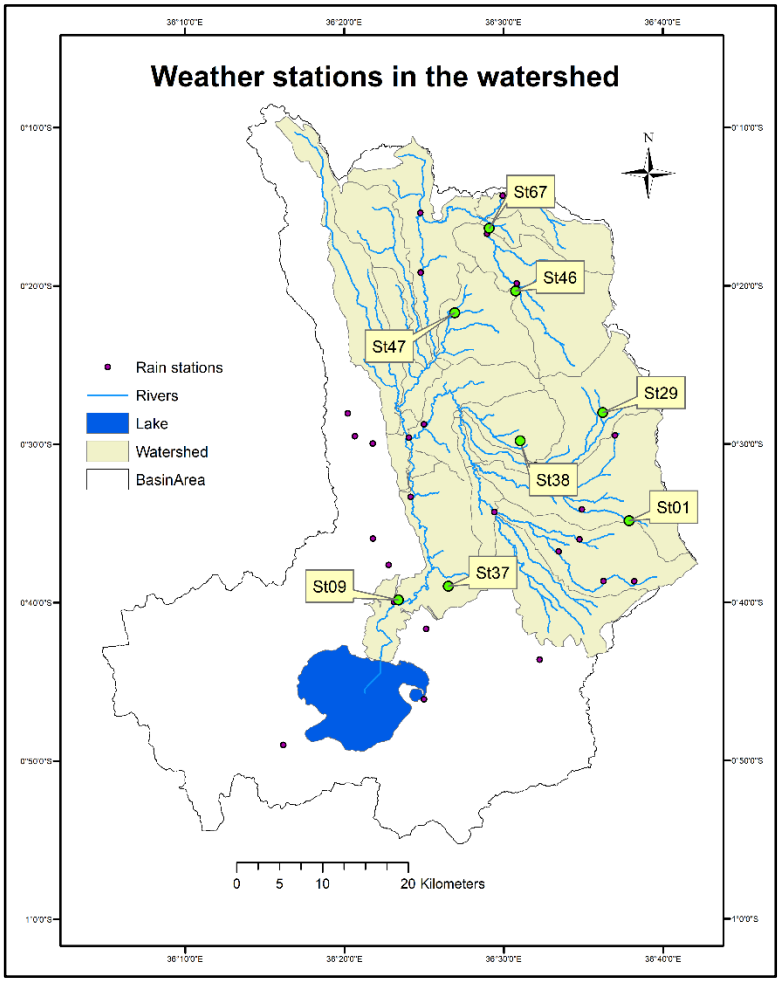

Weather stations